

**Surface Modification of Electrodes for Enzymatic Fuel Cell
Application**

Submitted by:

Rakesh Kumar M.Sc. (Hons)

**Thesis is submitted for the Ph.D Degree by Research of
The National University of Ireland**



National University of Ireland, Galway
Ollscoil na hÉireann, Gaillimh

Research was conducted in: School of Chemistry & Ryan
Institute, National University of
Ireland Galway.

Month and Year of Submission: November 2015

Supervisor of the Research: Professor Dónal Leech

Head of School: Professor Paul Murphy

Declaration

This thesis is the result of my own work carried out in the School of Chemistry & Ryan Institute, National University of Ireland Galway. The content of this dissertation are original and have not been submitted in whole or in part for consideration for any other degree or any other university.

Rakesh Kumar

November 2015

Acknowledgements

First and foremost, I would like to express my deep sense of gratitude to my supervisor Prof. Dónal Leech for giving me the opportunity to carry out this project and for all his advice, guidance, support and encouragement throughout the course of research.

I would like to express my gratitude to all who helped and assisted me throughout postgraduate studies.

To my friends in BERL group both past and present, for putting up with me.

To my parents, thank you for granting me a life of opportunity and for your unconditional support and encouragement to pursue my interests.

Finally, I would also like to thank my partner Kanwal Preet for being always the best and for her patience with me during the past months.

List of abbreviations

Γ_{os}	Osmium surface coverage
4-amp	4-aminomethyl pyridine
AuNP	Gold nanoparticle
BBD	Box-Behnken Design
Bpy	2,2'-bipyridine
C	Concentration
CMD	Carboxymethyl dextran
CV	Cyclic voltammetry
CNT	Carbon nanotube
CS	Chitosan
D	Diffusion co-efficient
DNA	Deoxyribonucleic acid
DMO	4,4'-dimethoxy
DoE	Design of experiment
DET	Direct electron transfer
EFC	Enzymatic fuel cell
EDC	N-(3-dimethylaminopropyl)-N'-ethylcarbodiimide
FAD	Flavin adenine dinucleotide
FADGDH	Flavin adenine dinucleotide-dependent glucose dehydrogenase
GOx	Glucose oxidase
MCO	Multicopper oxidase
MET	Mediated electron transport
MWCNT	Multiwalled carbon nanotube

MFC	Microbial fuel cell
NHS	N-hydroxysuccinimide
Os(bpy)-4AMP	$[\text{Os}(2,2'\text{-bipyridine})_2(4\text{-aminomethyl pyridine})\text{Cl}]^+$
Os(dmobpy)₂-4AMP	$[\text{Os}(4,4'\text{-dimethoxy-}2,2'\text{-bipyridine})_2(4\text{-aminomethyl pyridine})\text{Cl}]^+$
PVI	Poly vinyl imidazole
PBS	Phosphate buffer solution
PEM	Proton-exchange membrane
PEGDGE	Poly(ethylene glycol) diglycidyl ether
RSM	Response surface methodology
SHE	Standard hydrogen electrode
SWCNT	Single walled carbon nanotube
XPS	X-ray photoelectron spectroscopy

TABLE OF CONTENTS

DECLARATION.....	i
ACKNOWLEDGEMENTS.....	ii
LIST OF ABBREVIATIONS.....	iii
TABLE OF CONTENTS.....	v
ABSTRACT.....	viii
1. Introduction.....	1
1.1 Introduction.....	1
1.2 Fuel cells	2
1.3 Biofuel cells	4
1.3.1 Enzymatic fuel cells	5
1.3.1.1 Enzyme as a catalyst	7
1.3.1.2 Modified electrode	13
1.3.1.3 Addition of nanostructures to enzyme electrodes	17
1.3.1.4 Immobilisation strategie	19
1.3.1.5 Design of experiment (DoE) approach	22
1.4 Electrochemical principles and techniques	26
1.4.1 Faraday and charging currents.....	27
1.4.2 Modes of mass transfer	28
1.4.3 Solid electrode electrochemistry.....	28
1.5 Voltammetry	30
1.5.1 Cyclic voltammetry (CV)	30
1.6 Thesis proposition	33
1.7 References.....	36
2. Immobilisation of Alkylamine-Functionalised Osmium Redox Complex on Glassy Carbon using Electrochemical Oxidation	46
2.1 Abstract	47
2.2 Introduction	47

2.3 Experimental	49
2.3.1 Apparatus	50
2.4 Results and discussion	51
2.4.1 Electrochemically induced attachment of alkylamine functionalised redox complex to carbon surface	51
2.4.2 Characterization of redox complex modified surface	53
2.4.3 Bioelectrocatalysis for glucose oxidation	58
2.5 Conclusions	61
2.6 Acknowledgements	61
2.7 References	62
3. Coupling of Amine-Containing Osmium Complexes and Glucose Oxidase with Carboxylic Acid Polymer and Carbon Nanotube Matrix to Provide Enzyme Electrodes for Glucose Oxidation	65
3.1 Abstract	66
3.2 Introduction	67
3.3 Experimental.....	68
3.4 Results and discussion	70
3.5 Conclusions.....	80
3.6 Acknowledgements.....	81
3.7 References.....	82
4. A glucose anode for enzymatic fuel cells optimised for current production under physiological conditions using a design of experiments approach ...	84
4.1 Abstract	85
4.2 Introduction	86
4.3 Experimental.....	87
4.3.1 Materials.....	87
4.4 Results and discussion.....	89
4.4.1 Enzyme electrode electrochemistry	89
4.4.2 Response surface factorial design for the optimisation of EFC anode....	91
4.4.3 Model validation.....	96
4.4.4 Optimisation of enzyme electrode components	98

4.5 Conclusions.....	101
4.6 Acknowledgements.....	102
4.7 References.....	103
5. Immobilisation of redox complexes on electrode surfaces for application to biofuel cells.....	106
5.1 Introduction.....	106
5.2 Experimental	107
5.2.1 Materials and reagents.....	107
5.2.2 Methods.....	108
5.3 Results and discussion	108
5.3.1 Genipin cross-linked enzyme electrode	108
5.4 Conclusions.....	114
5.5 References.....	115
6. Conclusion	118
6.1 Conclusions	118
6.2 Future directions.....	120
6.3 References.....	123
Appendix.....	125

Abstract

The immobilisation chemistry of enzymes and redox complexes capable of shuttling electrons between enzymes and electrode surface can have an impact on the magnitude and stability of current response, with implications for application as biosensor and enzymatic biofuel cell development. Enzyme electrode prepared using co-immobilisation of redox mediators, multiwalled carbon nanotubes and polymer support using a chemical crosslinker provide 3-dimensional biofilms for an electrocatalytic response for substrate, such as sugar, important in biosensor and biofuel cell applications. The objective of this thesis was to investigate the interactions of redox complexes, enzyme and nanostructure on electrode surface for application to sensor and with view to developing a semi-or fully implantable, membrane-less enzymatic biofuel cell anode for energy generation. Furthermore, the optimisation of the electrochemical response of enzyme electrode was evaluated using a design of experiment approaches, in seeking to improve the current density under physiological conditions.

Chapter 2 reports a simple immobilisation strategy using electrochemically-induced grafting of osmium-based redox mediators onto carbon electrodes surface. The redox-active layer is produced by electrochemical oxidation of alkyl-amine functional group, distal to a ligand of the redox complex, to form reactive radicals that couple to carbon surfaces, with coupling characterized by XPS and voltammetry. The electrode surface modified by electrografting of an osmium complex was therefore examined for its ability to mediate electron transfer from glucose oxidase, in solution, as a result of glucose oxidation. The simple and efficient methodology for modifying carbon surfaces to obtain redox active monolayers offers many potential applications to biosensor and biofuel cell device development.

Chapter 3 reports on thicker bioelectrocatalytic films produced by the addition of nanostructured supports, and by cross-linking alkyl-amine functional groups, distal to a ligand of the redox complex, to the redox enzyme and functionalised polymers, with concomitant adsorption/grafting to the electrode surface. Co-immobilisation of enzyme, redox complex and polymer support using a chemical crosslinker, therefore,

provides a 3-dimensional biofilm for catalytic electro-oxidation of glucose. The chapter three focus on an investigation of the effect of the selection of polymers, possessing carboxylic acid functional groups, as chemical supports for immobilisation of mediators and enzymes at electrode surfaces. The electrochemical response was calculated for the enzyme electrode composed of glucose oxidase, multiwalled carbon nanotubes and a range of redox mediators and polymer supports, in seeking to improve the current density and stability of glucose-oxidising enzyme electrode under physiological conditions. Overall, a maximum current density of 3.4 mA cm^{-2} at $0.2 \text{ V vs. Ag/AgCl}$, in pH 7.4 phosphate buffers at $37 \text{ }^\circ\text{C}$, is achieved for oxidation of glucose, showing promise for application to glucose determination in blood and as an anode in a biofuel cell for power generation.

Chapter 4 reports on the design of experiment method to provide a more statistically relevant approach to optimise the amount of different components used to construct enzyme electrodes. The enzyme electrodes performance was evaluated and optimised under physiological conditions using design of experiment model. Based on the optimised amount of components, enzyme electrodes display improved current densities of $1.2 \pm 0.1 \text{ mA cm}^{-2}$ and $5.2 \pm 0.2 \text{ mA cm}^{-2}$ at $0.2 \text{ V vs. Ag/AgCl}$ in buffer containing 5 mM and 100 mM glucose, respectively. Design of experiment model was experimentally validated. The observed current density of enzyme electrodes in physiological conditions was consistent with the predicted values of the model. Therefore, design of experiment approach can be applied effectively and efficiently to improve the performance of enzyme electrodes for application to glucose oxidising enzymatic biofuel cell device.

Chapter 5, focus on the genipin based immobilisation procedure to fabricate enzymes and redox complexes on the electrode surfaces. The performance of enzyme electrode prepared by co-immobilisation of redox complexes and enzymes to chitosan matrix via genipin (a natural crosslinker) was evaluated for glucose oxidation. The genipin based crosslinking offer many biomedical applications for its ability to crosslink amine based biomaterials and exhibits lower cytotoxicity. The genipin crosslinked enzyme electrodes displayed current density of $0.74 \pm 0.08 \text{ mA cm}^{-2}$ at $0.45 \text{ V (vs. Ag/AgCl)}$ in $50 \text{ mM PBS (pH 7.4, } 37^\circ\text{C, } 150 \text{ rpm)}$ containing 100

mM glucose showing potential for incorporation a biocompatible technology in bioelectrochemical devices for *in vivo* applications.

Finally, Chapter 6 summarises the main research findings and provides some opinion on the future research direction to continue this work.

Chapter 1: Introduction

1.1 Introduction

There is an increased interest in development and deployment of implantable and semi-implantable devices in the field of medical diagnostics and bioelectronics over the past half-century. Over the last decade, the emergence of ultra-low-power bioelectronics has led to the development of highly energy-efficient and miniaturised devices for controlling and monitoring of various medical conditions [1-3]. Currently, lithium and alkaline electrolyte based batteries are used to power implantable and semi-implantable devices, such as insulin pumps, neurostimulators and pacemakers. These batteries provide electricity through an internal chemical reaction. Recent advancements in battery technology in terms of new nano-materials synthesis, has led to the increased stability and power densities of such devices [4-6]. Furthermore, modern technology has facilitated the improvement in battery devices particularly by shrinking battery size and enhancing lifetime [7]. These power devices such as cardiac pacemakers and are capable of continuous operation for approximately ten years. However, their replacement does require surgery and presents an absolute risk for the patient. The most common complications are internal bleeding, infection, haemorrhage and involuntary stimulation of nearby skeletal muscles by electrode [8-11]. Over 105,620 pacemaker implants are replaced each year due to battery depletion [12-14]. The lithium and alkaline electrolyte based battery technology used in medical devices, for example in pacemakers, is dependent on the use of corrosive or highly toxic components to humans. Therefore, batteries require protective membranes or casing to ensure isolation from the surrounding environment and from each other [1, 2, 15-18] limiting the degree of miniaturisation possible.

Development of medical devices that take advantage of fuel cells that derive their fuel and oxidant from the *in-vivo* environment would in principle allow for miniaturisation, as there is no longer a requirement to provide anode and cathode power generating capacity within the device, and for continuous power generation over periods. This would represent a step-change in medical device technology. Enzymatic fuel cells can be constructed to electrolyse ambient body fuels and

oxidants such as glucose and oxygen and convert the chemical energy into electric energy [19-21]. Such fuel cells use enzymes as a catalyst that work on a specific substrate such as glucose only, leading to ability to remove requirement of the membrane and casings to prevent cross-reactivity between anode and cathode, and therefore provide a route for further miniaturisation of a fuel cell. There are still challenges that need to be addressed for the successful application of enzymatic fuel cells, such as obtaining improved stability and increased power density.

1.2 Fuel cells

A fuel cell is an electrochemical device consisting of two compartments known as anode and cathode compartment. The fuel cell generates electricity from the oxidation of fuel at the anode and reduction of an oxidant at cathode [22]. The power (P_{CELL}) output of a fuel cell is a function of the rate of transfer of electrons through external circuit (I_{CELL}) and the cell voltage (V_{CELL}), as shown in equation 1.1. Ideally, V_{CELL} is the difference between the formal potential of the fuel in the anode and oxidant in the cathode compartments. The reversible potential difference of the cell is equal to the potential difference between the anode and cathode, minus irreversible losses or overpotential (η) in volts which reflect the influence of slow kinetics of heterogeneous electron transfer, ohmic resistance and concentration gradients. The flow of charge through an external circuit from the anode to cathode (I_{CELL}) depends on the electrode size and rate of the reaction occurring in the fuel cell.

$$P_{\text{CELL}} = V_{\text{CELL}} \times I_{\text{CELL}} \quad (1.1)$$

$$V_{\text{CELL}} = (E^{\theta'}_{\text{cathode}} - E^{\theta}_{\text{anode}}) - \eta \quad (1.2)$$

Figure 1.1 shows an example of the anodic and cathodic half reactions taking place within the hydrogen-oxygen proton-exchange membrane (PEM) fuel cell with the electrochemical reactions given in equation 1.3 and 1.4.

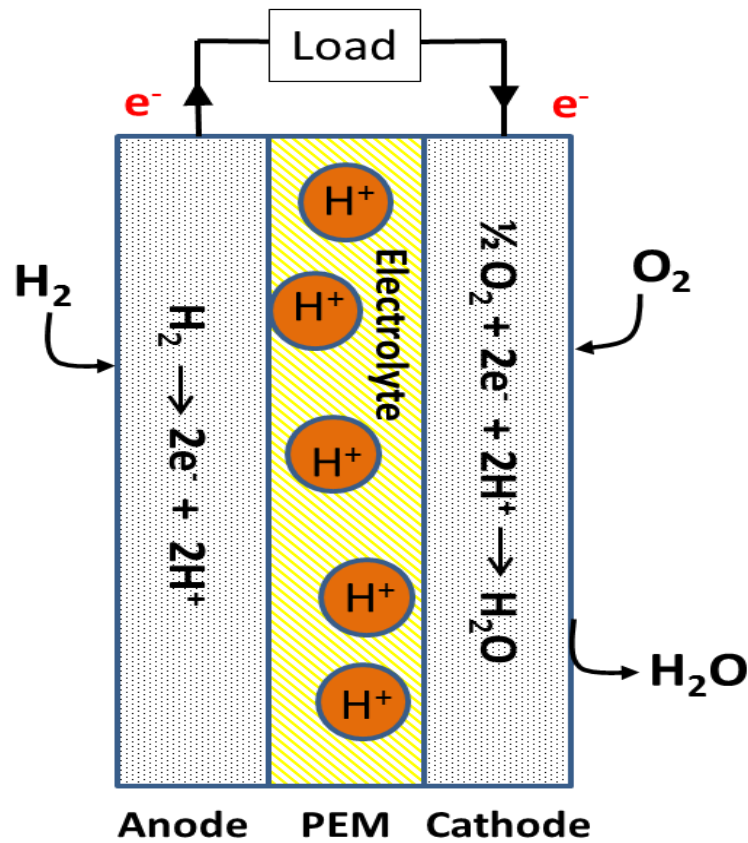
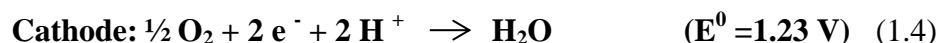


Figure 1.1: Simplified schematic of a hydrogen-oxygen fuel cell.

The catalyst used in the anode is typically of platinum metal and converts hydrogen gas into protons and electrons. The protons migrate towards the cathode via a proton exchange membrane, maintaining the separation of catholyte and anolyte, and electrons are shunted through the external circuit creating the electron flow. At the cathode oxygen is catalytically combined, using a platinum metal catalyst, with the protons and electrons and water is formed [7, 23] as shown in reaction 1.4. The standard potential difference between the anode and cathode of this fuel cell is 1.23 V [22].



The platinum catalyst used in the fuel cell is non-selective, therefore necessitating the use of a membrane and casing to prevent migration and reaction of the fuel and

oxidant at opposing electrodes. The platinum catalyst employed as an electrode material is typically highly effective but expensive and prone to deactivation through surface poisoning [19, 23].

1.3 Biofuel cells

Biofuel cells are electrochemical devices capable of transforming chemical energy into electrical energy *via* bioelectrochemical reactions [24, 25]. Biofuel cell devices are built from two parent technologies: fuel cell and biotechnology. Like conventional fuel cells, conversion of biochemical energy is achieved by oxidation of a fuel at anode which generates protons and electrons, coupled with reduction of an oxidant at cathode which uses these electrons and protons [17, 26]. Unlike the traditional fuel cell, biofuel cells use enzymes or microbes as catalyst replacing the precious metal catalysts. Based on the types of biocatalyst used for the reaction, biofuel cells can be categorised into two types: microbial and enzymatic. Microbial fuel cells use living microbes as a catalyst to generate electrical power, whereas enzymatic fuel cell use enzymes extracted from organisms for the electrochemical reactions. In both cases (i.e. microbial fuel cells or enzymatic fuel cells), the biocatalysts can be free in solution or confined to the electrode surface.

Microbial fuel cells (MFCs) are biofuel cells that generate power from organic substrates (frequently derived from waste) as a fuel using whole living organisms, such as algae or bacteria, as a catalyst. A typical MFC consists of anode and cathode compartments separated by an ion exchange membrane and connected to an external circuit. At the anode, fuel is oxidised by the mixed or pure culture of microbial organisms, generating electrons and protons. The electrons are transferred to the cathode through an external circuit, and cations migrate through a membrane. The electrons and protons are consumed in the cathode compartment, combining with oxygen to form water [16, 27-31]. MFCs will not be discussed further as this thesis focuses on research aimed at improving power and stability of enzymatic fuel cell electrodes.

1.3.1 Enzymatic fuel cells (EFCs)

In the early 1960's Clark and Lyons coined the term "enzyme electrode", for an electrode constructed using the enzyme glucose oxidase, to oxidise glucose, immobilised in close proximity to a platinum or Clark electrode used to measure oxygen concentration that is depleted during the enzyme reaction, and thus report on glucose concentration [25, 32-34]. A couple of years later the first enzyme based biofuel cell was reported using glucose oxidase as anodic catalyst and glucose as the fuel [24]. Many improvements have been made since that time and enzymatic fuel cells have received increased attention following the discovery and development of new redox enzymes, electrode materials, nanostructures and enabling technologies to immobilise enzymes at electrodes [24, 35-37]. In contrast to a traditional fuel cell, an EFC uses enzymes as a catalyst enabling the cell to work under mild conditions and utilise more complex renewable sources than hydrogen as a fuel. Also, enzymes immobilised on non-catalytic base electrode surfaces of anode and cathode confers substrate specificity on the electrode. This eliminates the need for the protective case or membrane as required for conventional fuel cells to prevent reactant cross-over, which allows for the miniaturisation of the cell [26, 38]. In the early 1990s there was renewed interest in the field of enzymatic fuel cells and an upsurge in research was driven by advances in biosensor design, material science and enzyme electrochemistry [39-43]. The most commonly described enzymatic fuel cell prototype consists of a glucose oxidising anode and an O₂ reducing cathode [1, 2, 16, 20, 44-46], although other enzymatic fuel cells based on H₂/O₂ [47], glucose/H₂O₂ [48], fructose/O₂ [49], and alcohol/O₂ [50] have been reported previously.

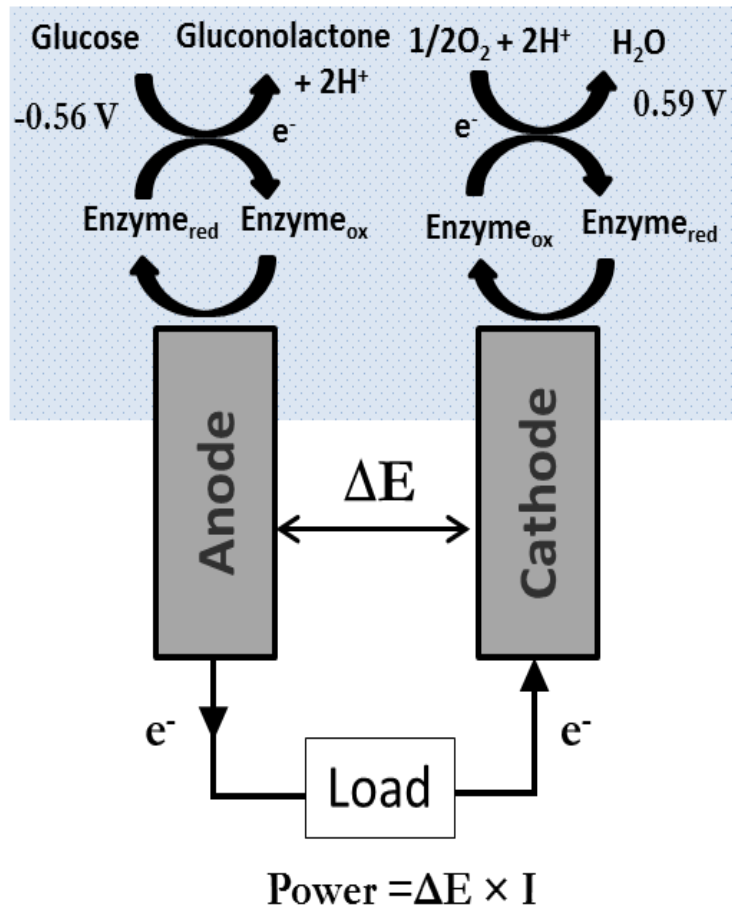
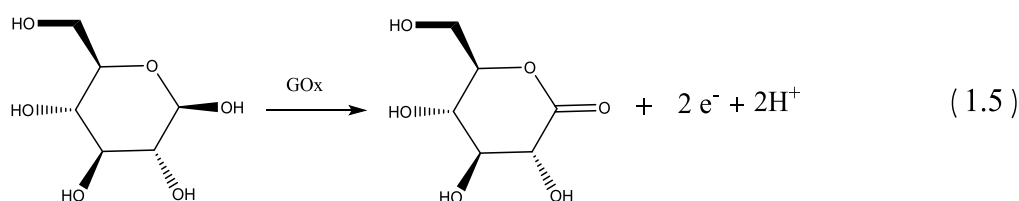
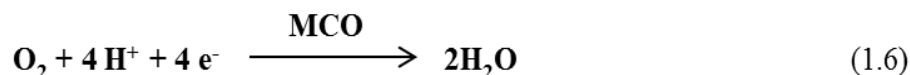


Figure 1.2: Operating principle of a fully enzymatic glucose/oxygen biofuel cell, with potential quoted vs. Ag/AgCl at pH 7.4 (Figure adapted from [45]).

The electrochemical reactions in such an EFC consist of two separate reactions (Figure 1.2): an oxidation half-cell reaction at anode and reduction half-cell reaction at cathode. The β -D-glucose is catalytically split into β -D-gluconolactone at the anode (scheme 1.1) producing ions, which travel through the electrolyte to the cathode and electrons travel via external circuit from the anode to the cathode. At cathode compartment, the reduction half-reaction occurs where oxygen is catalytically reduced by an enzyme and combines with protons to form water (scheme 1.2). The power output of the cell is the product of the cell voltage (ΔE) and the cell current (I).



Scheme 1.1: Oxidation of β -D-glucose to β -D-gluconolactone catalysed by glucose oxidase.



Scheme 1.2: Reduction of dioxygen to water catalysed by multicopper oxidase (MCO).

Low power densities and a short operational lifetime of the biocatalyst are the main hurdles to prototype development and operation for EFCs. For EFCs to compete with the lithium ion batteries, an operational lifetime of greater than five years may be required: this will be difficult to achieve. Implanted power sources can be located remotely from the operational devices. An alternative approach may therefore be used where the enzyme electrodes are printed onto a disposable patch that connects to an implanted miniature electrical component to provide power from glucose oxidation and oxygen reduction in body fluids, that could regularly be replaced [51, 52]. Therefore, for EFCs to be considered a realistic possibility to use as an *in vivo* (or semi-implanted) power source it is critical that they operate effectively under physiological conditions (pH 7.4, 37 °C, 5 mM glucose, 150 mM NaCl).

1.3.1.1 Enzyme as a catalyst

Enzymes are biological molecules that have many advantages over the traditional metal catalyst used in a fuel cell. Enzymes, like all catalysts, speed up reactions by lowering activation energy. Enzymes, due to their 3-dimensional protection of the active site by their protein structure, can be specific in nature, catalysing conversion of only selected chemical reactions to product allowing removal of separating membrane between anodic and cathodic reactions. Consequently, it is possible to miniaturise EFCs for *in vivo* power generation applications. Another significant advantage of enzymes over metal based catalysts is their ability to work efficiently

under moderate operating temperature and mild conditions, such as physiological pH. The most commonly described EFC prototype in the literature consists of glucose oxidising enzymes immobilised on the anode connected to an O₂ reducing enzyme such as bilirubin oxidase immobilised on the cathode [1, 21, 45, 46]. Enzymes are renewable and relatively inexpensive to produce which has led to extensive research on them as biocatalysts for fuel cells. The studies performed within this thesis have focused on enzyme electrodes using glucose as fuel, due to the high concentration (5-8 mM) available in the blood in the context of enzymatic anode for biofuel cells with *in vivo* applications. Chapter 3, 4 and 5 report on preparation, immobilisation and optimisation of a glucose oxidase (GOx) based enzyme electrode as a bioanode for EFC applications, necessitating an introduction to the properties of this enzyme.

Glucose Oxidase

Glucose oxidase (GOx) was discovered by Muller (1928) in *Aspergillus niger* extracts [53, 54]. It is a dimeric protein that specifically oxidises β-D-glucose to gluconolactone which further hydrolyses to gluconic acid. GOx consists of two equal subunits with a molecular mass of 80 kDa each, encoded by the same gene [54]. GOx requires a cofactor, flavin adenine dinucleotide (FAD) (Figure 1.4) to function as a biocatalyst. Figure 1.3 shows a crystal structure of one of the GOx monomers. The FAD active site of the enzyme functions as an initial electron acceptor and is reduced to FADH₂ upon oxidation of glucose as shown in equations 1.7 and 1.8. Finally, FADH₂ is oxidised by oxygen, or an artificial electron acceptor (mediator) which replaces oxygen, in the electron transfer mechanism.

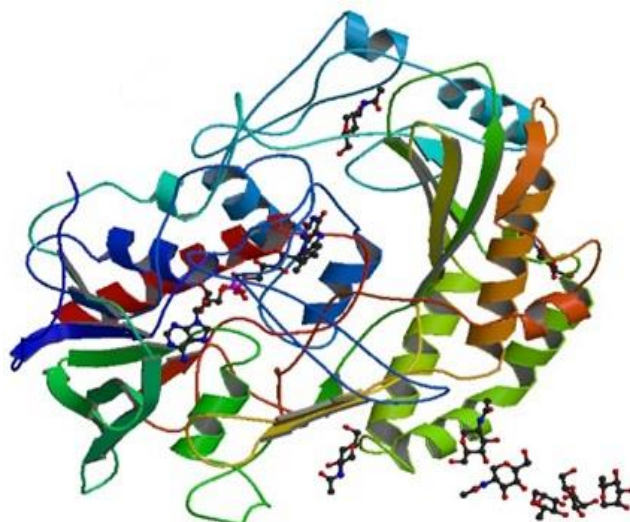


Figure 1.3: Crystal structure of the *Aspergillus niger* glucose oxidase (PDB ID: 1GAL) [55].

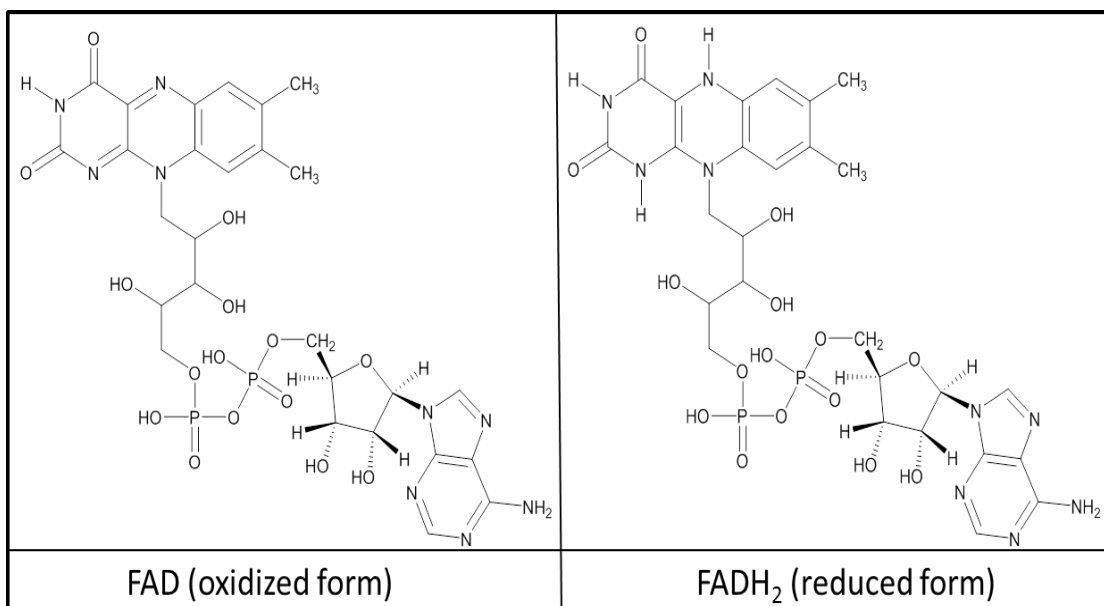
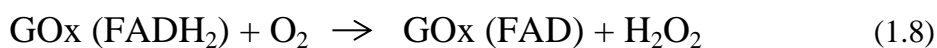


Figure 1.4: Chemical structure of the FAD/FADH₂ active site of glucose oxidase.



The GOx enzyme displays a high thermo-stability and enthalpy of denaturation [54]. It is stable for two and eight years at 0 °C and -15 °C respectively, however in solution stability depends on the pH. It is more stable at around pH 5 [53, 56]. The catalytic properties of GOx form the basis of assaying body fluids, such as blood,

urine and tears for glucose [53, 57, 58]. GOx catalyses the oxidation of glucose to β -gluconolactone, producing hydrogen peroxide when oxygen is the electron acceptor: this is a toxic product and could affect the bioactive material. Nonetheless, due to its stability, substrate specificity and commercial availability, GOx is extensively used in diagnostic tests as biosensors [57] and biofuel cells for *in vivo* or *ex vivo* power generation [19, 20, 53, 59, 60].

Although the FAD site is deeply buried within the enzyme, there have been two reported approaches to extract electrons from the site instead of permitting oxygen act as electron acceptor: direct electron transfer (DET) and mediated electron transfer (MET) to the solid electrode surface [19, 20, 61]. In the case of DET, the active centre of the enzyme is reportedly directly connected to the electrode surface. For example, Mano and co-workers report on direct electron transfer from the active site of de-glycosylated GOx immobilised on a vitreous carbon electrode. The cyclic voltammogram exhibits a redox couple at -0.49 V vs. Ag/AgCl attributed to the FAD/FADH₂ redox process. The glucose oxidising current density of 235 $\mu\text{A cm}^{-2}$ at -0.2 V vs. Ag/AgCl is observed in 20 mM PBS (pH7.4) solution containing 45 mM glucose [62]. Others have reported DET for GOx when immobilised on nanocomposite electrode materials [44, 63, 64]. However, DET as a mechanism for a catalytic current generation in GOx is not conclusive. Recent reports show that regardless of electrode matrix DET between the active site of GOx and nanostructured electrodes is difficult to attain [65, 66]. Despite the apparent simplicity of DET, catalytic current generated may be hindered due to the large distance of the FAD active site of the enzyme to the surface of the electrode. The correct orientation of enzyme at the electrode surface, that is difficult to control, further hampers catalytic current capture, as does blockage of access of substrate to the active site in the presence of the electrode. Moreover, the current density achieved by DET is lower when compared to MET, as a maximum monolayer coverage of enzyme at electrode surface is attainable.

For most enzymes, including GOx, it is necessary to use an electron transfer mediator as a replacement for oxygen or DET to shuttle electrons between the electrodes and active site in the enzyme. Mediators are artificial co-substrates that can participate in the redox reaction with the enzyme and effect transfer of electrons [20]. Mediator redox potential plays a significant role in the operational cell voltage

of an EFC. Therefore, tailoring the design of such mediators is critical. Ideally the mediator potential should be slightly positive in the case of anode and negative in the case of cathode compared to the redox potential of the enzyme active site for thermodynamically favourable conditions [67, 68]. In the event of redox mediation, the redox potential of mediators are reported to require an approximately 50 mV potential downhill from the redox potential of enzyme [69, 70]. Cass *et al.* [71] first reported that ferrocene acts as a mediator to detect glucose close to the redox potential of ferrocene, ~ 0.35 V vs Ag/AgCl, when co-immobilised with GOx on graphite electrodes. Forrow *et al.* [72] reported on the structure influence of ferrocenium derivatives on GOx mediation in solution. Bu *et al.* [73] reported on the preparation and electrocatalytic characterisation of ferrocene containing polyacrylamide based redox gel as the electron shuttle redox hydrogel for biosensor applications. Likewise, Hodak *et al.* [74] reported on the redox mediation of electrostatically deposited GOx in the self-assembled structure of cationic poly(allylamine) modified by ferrocene on an alkanethiol-modified gold surface. Subsequently a glucose oxidation current density of 2 mA cm^{-2} at 0.13 V vs. Ag/AgCl in pH 7.4 buffer containing 100 mM glucose was obtained by crosslinking GOx with a dimethylferrocene-modified poly(ethyleneimine) polymer on electrodes [75].

However, ferrocene based mediators are unstable in the oxidised form in aqueous solution and are not readily soluble in their reduced form, resulting in difficulties with enzyme electrode preparation and the MET process [20]. Zakeeruddin *et al.* [68] reported several decades ago on the use of a range of (4,4'-substituted-2,2'-bipyridine) complexes of iron, ruthenium, and osmium as mediators for GOx and other redox proteins. Osmium-based redox complexes have been found to be excellent electron transfer mediators due to their relative stability in both oxidised and reduced states and their fast electron exchange rate compared to other metal based mediators [38, 76, 77]. Apart from stability to redox cycling and rapid self-exchange rate constant, their redox potential can be easily tuned through chemical modification of the ligands attached to the osmium metal centre [42, 68, 76, 78]. Polyvinyl imidazole (PVI) bound osmium polypyridyl series of redox polymers have been widely used in mediated enzyme electrodes for application as biosensor and EFC electrodes for power generation. However, a difficulty with the use of PVI as

the polymer backbone for the preparation of redox polymers is the lack of commercial availability of PVI. Also, the laboratory-scale synthesis of PVI requires bulk free radical polymerisation [79] which results in broad molecular weight distribution that affects the physical properties of redox polymers such as solubility and density. Recently, Allen *et. al.* [80] reported on controlled radical polymerisation of *N*-vinylimidazole to produce mono-disperse homo-polymer that provides a route for the improvement on this issue. In addition, osmium redox complex loading on the PVI backbone by ligand substitution is also difficult to control and replicate, leading to batch-to-batch variation in enzyme electrode performance using these redox polymers [20, 60, 81].

Tetherable ligand-based osmium polypyridyl complexes (Figure 1.5) have been employed in research and development of mediated enzyme electrodes for a wide range of applications as biosensors and EFC electrodes and forms the basis of the study reported in this thesis. The starting osmium [Os(N-N)₂Cl₂] complexes can be prepared according to literature methods [82, 83], where N-N represents a bidentate, mostly bipyridine-based, ligand. Osmium polypyridyl redox complexes have been found to be effective mediators due to their stability to Os(II/III) transition states and rapid self-exchange constants [38, 76, 77]. The corresponding redox potentials can also be tuned to what is required through substitution of the electron withdrawing or electron accepting groups in the 4 and 4' positions of the bipyridine ligand attached to osmium metal centres. The functional groups present in these complexes also means that they can be easily anchored to the surface of electrodes or to the backbone of several different polymers. Therefore, a library of osmium based metal complexes having different redox potential could be created and potentially used as mediator for a variety of different enzymes.

In chapter 2, we report on direct grafting of osmium based redox complex containing an alkylamine ligand distal to the metal co-ordinate site, to glassy carbon surface by simple electro-oxidation methodology. The direct electro-oxidation of an alkylamine functional group of a redox complex provides a simple route to prepare redox active layer on surfaces and the average surface coverage of attached redox layer is close to that predicted for a closed packed monolayer of complex. However, a glucose oxidation current density of only 7 $\mu\text{A cm}^{-2}$ is obtained from the redox modified electrode in phosphate buffered saline (37 °C, pH 7.4, 150 mM NaCl with 100 mM

glucose containing glucose oxidase (9U). This is due to the low amount of osmium redox centres at the surface to wire with biocatalyst. Therefore, in order to enhance the glucose oxidation current density for application as an anode in EFC, an alternative approach is used to form multiple layers of osmium complex and biocatalyst on the electrode surfaces. Redox complexes and biocatalysts possessing amine functionality can be coupled to carboxylic acid functional groups of polymers via carbodiimide reagent, which offers greater versatility in preparation of multilayered films, as described in Chapter 3.

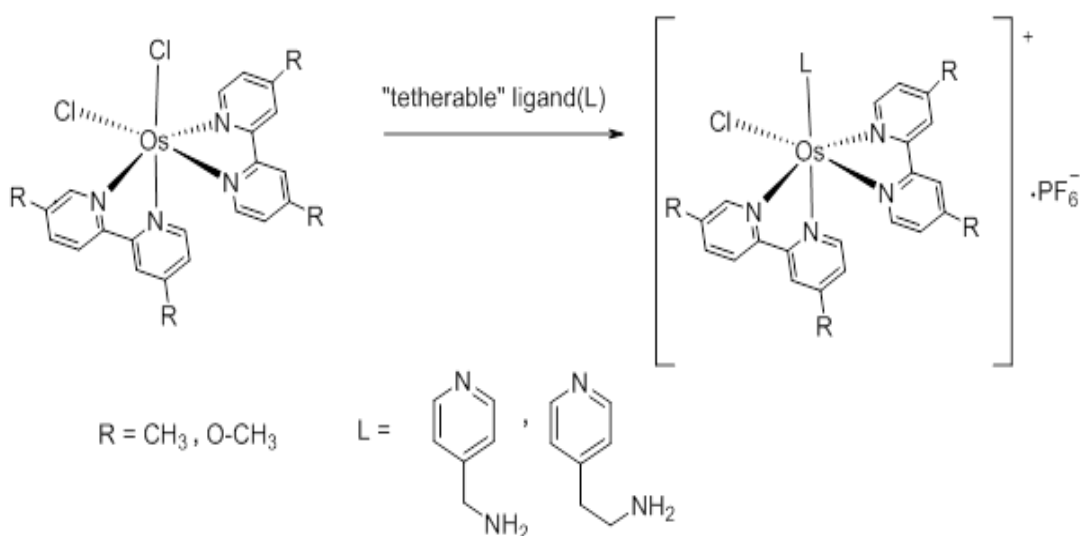


Figure 1.5: Structure of the “starting complex” $[\text{Os}(\text{2,2}'\text{-bipyridine})_2\text{Cl}_2]$ and tetherable osmium redox complexes formed by ligand substitution reaction [59, 68].

1.3.1.2 Modified electrode

Modification of the electrode surface with redox layers is important to many technological applications such as biosensors, molecular electronics, biofuel cell devices and electrocatalysis [84, 85]. Modified electrodes represent an important class of integrated systems which have the ability to exert control over the nature of an electrode via immobilisation of redox complexes onto the surfaces. Probing and understanding the redox properties of electroactive centres within an organised monolayer has received considerable attention over the past three decades [86, 87]. In redox active monolayers both the nature of the chemical functional groups and

their topology can be controlled thus providing a platform to probe how overall electron transfer occurs through the interface. Deliberate surface attachment offers a means of introducing different states of known energy and molecular nature into the band gap with electrochemical kinetic implications [88]. Redox active molecules attached to electrode surfaces can be applied in electrocatalysis. The attached molecules may act as a fast electron transfer mediator for a substrate dissolved in contacting solution [89-92]. The modified electrode can be prepared using different methods ranging from simple chemisorption to electrosynthesis of polymer films at an electrode surface [93]. Overviews of the different types of modified electrodes are shown in Table 1.1.

Table 1.1. An overview of types of modified electrodes

Method	Description	Examples	Ref.
Chemisorption	Based on the interaction between molecules and surface in which electron density is shared by the adsorbed molecules and the surface.	-Alkenes and alkynes irreversibly chemisorbed on metal surfaces. -Adsorption of aromatic molecules on platinum and carbon surfaces. -Use of thiol, sulphide and disulphides as adsorption agents from homogenous solution for the modification of the gold surface. These films have been called “self-assembled” monolayers.	[94, 95] [96, 97] [98-100]
Covalent Bond Formation	Forming covalent bonds between a functional group of modifier and electrode material.	-Coupling to functional groups –OH, –COOH or –NH ₂ formed on the surface of electrode material. This chemistry has been used to attach a number of functional groups to SiO ₂ , RuO ₂ , TiO ₂ , Pt, and Au and other electrode surfaces. -Aryl diazonium salt reduction -Coupling of organosilanes to the surface. -Covalent bonding of alkenes, alkynes and amine to the surface.	[36, 90] [85, 101] [102] [103] [85-87, 91]
Langmuir-Blodgett method	Chemical films strongly adsorbed on the electrode.	Langmuir-Blodgett formed via adsorption of highly ordered monolayer films at air/water interface. This method entails the use of a molecule with a polar “head group” and hydrophobic “tails”.	[104-107]

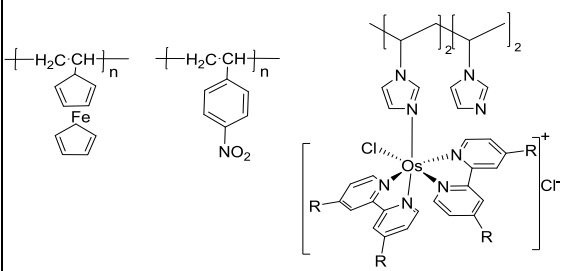
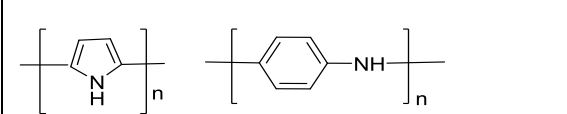
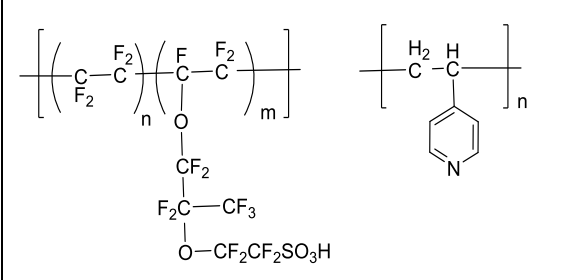
Polymer film coating	<p>Modified electrodes prepared by coating surfaces with polymer films or through direct electro polymerisation onto the electrode surface.</p>	<p>-Redox polymers that contain electroactive functionalities either within polymer chain or in side groups.</p> <p>-polyvinylferrocene, osmium and ruthenium bipyridyl complexes bound to polymers.</p>  <p>-Electronically conductive polymers</p> <p>Polymer chains in this family of material are themselves electroactive and are prepared chemically in the presence of the catalyst or grown electrochemically on the electrode surface.</p> <p>Polypyrrole, polythiophene, polyaniline, etc.</p>  <p>-Ion exchange polymers</p> <p>These polymers are not electroactive themselves but can be used to incorporate electroactive ions.</p> 	<p>[35, 108]</p> <p>[38, 39, 76, 82]</p> <p>[5, 109]</p> <p>[110, 111]</p>
-----------------------------	---	--	--

Table 1.1. An overview of types of modified electrodes – cont.

Method	Description	Examples	Ref.
Composite electrode surfaces	A composite electrode has a surface that consists of conductor regions separated by an insulator. It mainly consists of inorganic microcrystalline structure materials.	A variety of composite materials have been used as electrodes for electroanalysis. For example, clays, zeolites, graphene and inorganic material used to coat electrode surfaces.	[41, 112-114]

A range of electrochemical sensors has been developed that operate on the basis of oxidation and reduction of the analyte mostly catalysed by immobilised molecules at electrode surfaces [38, 86, 115]. Biological molecules are integrated with electronic elements to provide a device for biosensing or the conversion of the biocatalytic process into electrical power [2, 57]. The mediated electrocatalysis by enzymes is of special interest in biological sensing mainly due to catalytic activity for a specific analyte. Their utilisation in enzyme based electrodes allows for increased sensitivity, selectivity and detection limits of analyte at lower overpotential in many applications ranging from industry, environmental and energy application areas [20, 116, 117]. Furthermore, the addition of nanoparticles to redox enzyme containing biofilms on electrodes may contribute to improved current and signal stability, and is therefore an active area of research for both biosensors [45, 57, 124, 127, 128] and EFC applications [46, 63, 124, 126, 130, 179].

1.3.1.3 Addition of nanostructures to enzyme electrodes

Carbon nanotubes (CNTs) consist of hollow cylindrical tubes made entirely of carbon with high aspect ratio (length/diameter) [118, 119]. There are two basic types of CNTs: single-wall carbon nanotubes (SWCNTs) and multi-wall carbon nanotubes

(MWCNTs) (Figure 1.6). SWCNTs are of fundamental cylindrical structure of covalently bonded carbon atoms. MWCNTs are made of coaxial cylinder structure having interlayer spacing close to the interlayer distance in graphite [120]. Different forms of CNT besides single walled have been synthesised, for example multiwalled CNTs, double-walled CNTs [121], bamboo CNTs [122] and herringbone CNTs [123]. CNT based electrodes are often employed as the basic material for construction of high-performance capacitors for electrochemical storage of energy [124, 125].

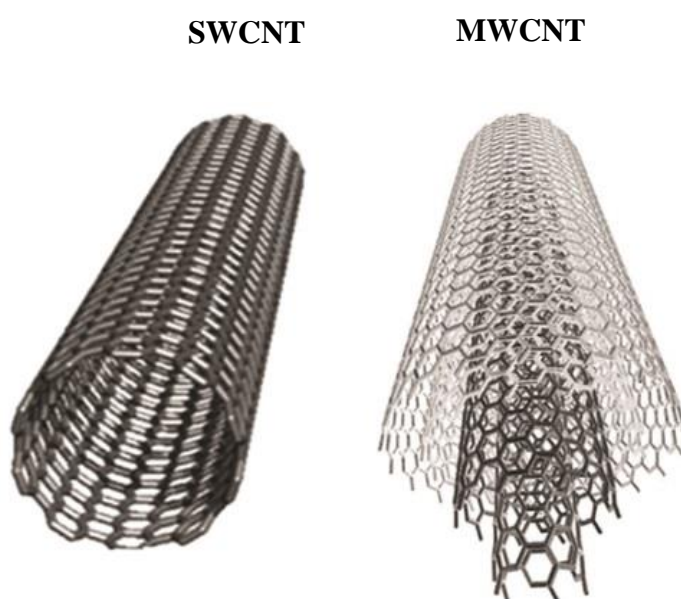


Figure 1.6 Single-wall carbon nanotube (SWCNT) and multi-wall carbon nanotube (MWCNT) (Figure adapted from [120])

Recent applications of CNTs to EFCs have shown potential for improved performance due to provision of highly conductive, mechanically strong, high surface area and chemically stable electrodes [124, 126, 127]. The addition of nanomaterials to an enzyme electrode matrix may result in improved surface area or electrical connections and provide signal stability and is therefore a promising area of research for both biosensor and EFC applications [118, 124, 126, 128, 129]. For example, recent studies on the addition of multiwalled carbon nanotubes to enzymatic electrodes based on either GOx or a flavin adenine dinucleotide-dependent glucose dehydrogenase (FADGDH) and redox polymer demonstrate

improved operational stability of glucose oxidation response with greater retention of activity of enzyme on the surface compared to films prepared without CNTs [60, 130, 131]. CNT based electrochemical sensors have been developed to detect neurotransmitters [132-137], proteins [138-141], glucose [20, 59, 60, 126, 130, 142, 143] and DNA [144-147]. Thus, incorporation of CNTs is an interesting approach to improve the biocatalytic signal and stability of enzyme electrodes, forming the basis for the investigation reported on in chapter 3 and 4 of this thesis.

The inclusion of other nanoparticles such as gold nanoparticles (AuNP) to catalytic films has also been reported to provide direct electron transfer between immobilised biocatalyst to the surface of electrode, displaying increased current and stability compared to planar electrodes [148-151]. For example, bilirubin oxidase based enzyme electrodes containing AuNP provide a current density of 5.2 mA cm^{-2} for oxygen reduction at a 4000 rpm electrode rotation rate and retained 90% of initial current after 48 h of continuous operation [152]. A power density of 0.87 mW cm^{-2} at 0.3 V is reported from the carbon paper-based bilirubin oxidase/AuNP electrode when connected to a fructose dehydrogenase anode to form an EFC [152]. Moreover, Zebda *et al.* reported a current density of 4.4 mA cm^{-2} for a biocathode obtained by immobilising laccase on carbon nanotube electrodes [51].

1.3.1.4 Immobilisation strategies

A major obstacle towards miniaturisation of biofuel cell devices is the leaching of enzymes and redox mediators from the surface. The immobilisation methodology used to retain the biocatalyst on electrode surfaces can have an impact on the magnitude and stability of output response, with implications for application as biosensors and fuel cell enzyme electrodes. The effective immobilisation of enzyme at the electrode is necessary to develop a favourable environment for maintaining enzyme activity and thereby extending stability. It can be achieved by either chemical methods such as covalent binding or by physical methods via adsorption, entrapment, encapsulation and crosslinking [153-157] as summarised in Table.1.2.

Table 1.2: Different immobilisation methods used to construct enzyme electrodes

Method	Description	Examples
Adsorption	Biocatalyst dissolved in solution and the solid support is placed in contact with the enzyme solution for fixed period.	Enzyme immobilised via physical adsorption [38, 42, 158, 159], Electrostatic [160] or layer by layer deposition [161, 162] on the surface of the electrode.
Entrapment	Biocatalyst immobilised within 3D matrix such as electro-polymerised film, polymer matrix, silica gel, carbon paste, or polydimethylsiloxane.	Enzyme immobilised in polypyrrole [163-165] or polyaniline matrix [166, 167], silica sol-gel [168, 169], poly(ethyleneimine) microcapsules [170] or carbon paste electrode [43, 171].
Covalent	Biocatalyst coupled to the surface through a functional group to an activated support. Thiol containing enzymes directly self-assembled on a gold surface.	Enzyme via carbodiimide coupling (EDC/NHS) [115, 172, 173] or thiol groups [174, 175] or by introducing functional groups through site directed mutagenesis [176, 177]
Cross-linking	Immobilisation of the enzyme by cross-linking with glutaraldehyde or other bi-functional agents.	Enzyme crosslinked with each other or functional inert support. Example glutaraldehyde based crosslinking [157, 178-181] or poly(ethylene glycol) diglycidyl ether [20, 21, 38, 59, 76, 182] based cross-linker.

Different immobilisation procedures, as shown in Table 1.2, have been used to increase not only the active lifetime but also the stability of these biocatalytic films at electrode surfaces. For example, Gregg and Heller [42] developed a technique using poly(ethylene glycol) diglycidyl ether (PEGDGE) as a cross-linker to create a redox hydrogel to entrap enzyme and mediators in films. The redox hydrogel form a three-dimensional network that connects the enzyme redox centre to the electrode surface via diffusional electron transport or self-exchange within, the redox complexes in the hydrogel, irrespective of the orientation of the enzyme active site in films. The crosslinked hydrogel is permeable to substrate or product through the polymer matrix and allows for charge transport through self-exchange “diffusion” of electrons. Ohara *et al.* [76] reported on enzyme electrodes formed by co-immobilising osmium based redox polymer and GOx on electrode surfaces using PEGDGE, for sensing glucose levels.

One of the greatest challenges at present is to extend the operational lifetime of enzyme electrodes. Coupling of the enzyme to polymer support is a traditional chemical immobilisation method used to develop enzymatic biosensors [84, 155]. The biocatalysts are bonded to the surface of electrodes or support through functional groups that are not essential for their catalytic activity. Bifunctional reagents such as glutaraldehyde or coupling chemicals such as carbodiimides are used to couple enzymes to the electrode/support. The support can be either an inorganic material or polymer [156, 157]. The water-soluble carbodiimide reagent N-(3-dimethylaminopropyl)-N'-ethylcarbodiimide (EDC) couples carboxyl groups to amino functions. This is frequently used with an N-hydroxysuccinimide reagent, used to stabilise the activated ester formed as an intermediate from the carboxylic acid by EDC, to increase the coupling efficiency, in a scheme as shown in Figure 1.7. The EDC/NHS coupling procedure is widely used to develop enzymatic sensors [40, 183-186].

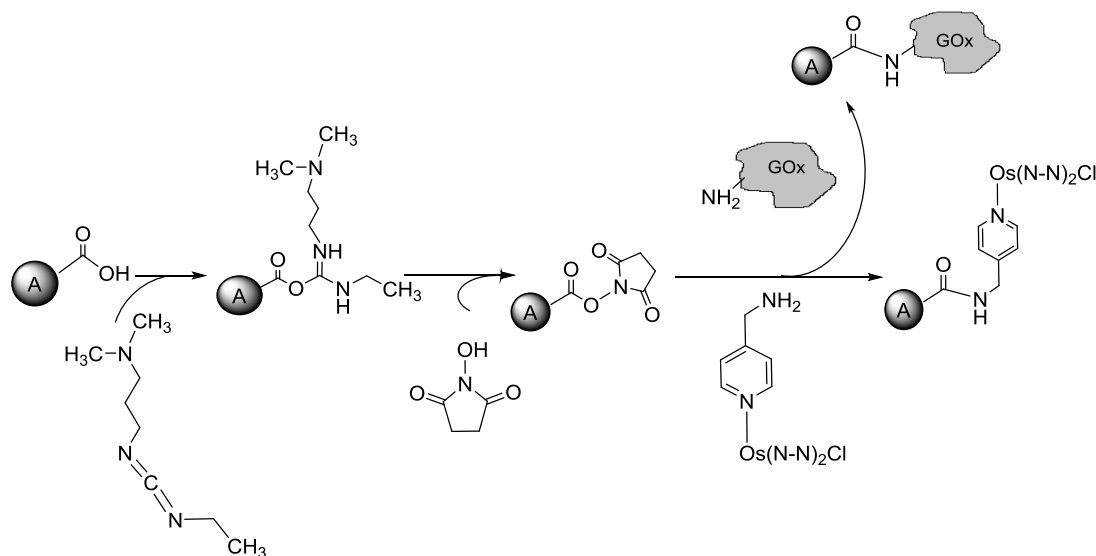


Figure 1.7: Immobilisation techniques on polymer bearing carboxylic functional group, as chemical support with amine-containing osmium redox complexes and enzyme (GOx) by EDC/NHS coupling (A= carboxylic acid functionalised polymer).

The use of an EDC/NHS coupling technique to crosslink enzyme and redox mediators in a polymer matrix, together with nanostructured CNT support, is reported in chapters 3 and 4. Those chapters in the thesis examine the effect of the selection of polymers possessing carboxylic acid functional groups as a chemical support for immobilisation of redox complexes and enzymes in three-dimensional films at electrode surfaces.

1.3.1.5 Design of experiment (DoE) approach

Design of experiment (DoE) is a structured, organised method for determining the relationships among factors affecting a process and its output. In general, the design of the experiment is a statistical design of any experiment where variation is present. DoE is widely used in research as well as industrial settings. The primary goal of scientific research is usually to determine the statistical significance of an effect that a particular factor exerts on the dependent variable of interest [187, 188].

The typical approach of changing variables one factor at a time employed by researchers is based on a trial-and-error method. This technique, though very informative is a lengthy process for incremental system improvement and extremely

time-consuming. DoE is a systematic approach which considers all variables simultaneously leading to more effective improvements [189]. Rather than adopt an optimisation approach based on alteration of one factor at a time for experiment or process, a DoE approach will take many steps, as described below:

Definition of DoE project: DoE begins with determining the objective of an experiment and selecting the process factors for the study.

The response variable (Output): Selection of the response variable (y) that easily and accurately measured the performance.

Factors, level and ranges: It is desirable to identify all the important factors that may significantly influence the response variable. There are two kinds of factors, continuous and discrete. The number of levels or range of each factor depends on types of experiment considered. The levels of experimental factors provide more information of the experiment. The selection of an extended range of a factor also requires additional experimental runs to finish the experiment.

Experimental design: Experimental design will depend on the number of factors, the number of levels in each factor and a total number of experimental runs.

Perform the experiment: This step will involve the raw data collection from the DoE designed experiment.

Analysis of data: Different statistical methods are used to analyse the data. For example estimating the regression coefficients in the model; identifying the relative importance of each factor by numerical score using analysis of variance (ANOVA) method; predicting and validating the accuracy of model; graphical or numerical optimising of parameters for desired response. Once the data analysis is completed, the conclusions about the experiment can be drawn. The verification of the concluded information can be done using experimental runs [189, 190].

Response Surface Methodology (RSM) can be used to detail and optimise various process parameters. RSM is based on the combination of statistical and optimisation methods that can be used in many applications in design and improvement of product and processes. RSM provides information about interaction and response of interconnected factors over a wide range of values. The input variables for the experiment are called factors (X) and the measured outcome of the experiment are called responses (Y). The initial step of the DoE approach is to define each factor and the range over which each factor varies [188]. Figure 1.8 shows a model of a typical

process. The process explains a system, either a chemical reaction or manufacturing process, with all associated variables that changes the input into an output that has one or more predicted response. The variable of a process is either controllable or uncontrollable.

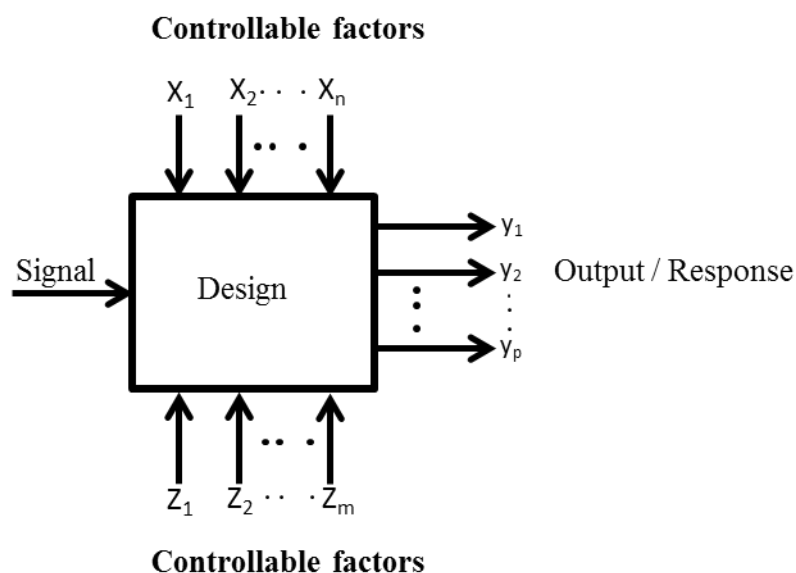


Figure 1.8: A model/design of process and system [187].

Previously, RSM of DoE has been used for optimisation of various chemical, biological and physical processes [191-193], but not as yet been applied extensively to optimise enzyme electrode preparation for application to EFCs.. Rather than adopt an optimisation approach based on alteration of one factor at a time, a design-of-experiment (DoE) approach can be used to determine optimal enzyme electrode performance. For example, recently Babanova *et al.* [194] reported on a DoE approach for optimisation of the performance of an air-breathing bilirubin oxidase-based EFC cathode. Given the number of different components, and the range of amounts and methods used to prepare enzyme electrodes for biofuel cell application, a comprehensive study is required on optimisation of each component used in enzyme electrode preparation steps to identify the interaction or dependency of these components on the performance of enzyme electrodes. Therefore, in chapter 4 a DoE approach is employed to optimise the amount of different components used in the construction of an EFC anode. The evaluation of enzyme electrodes prepared by co-immobilisation of different amounts of carboxymethylated dextran, multiwalled

carbon nanotubes, GOx and redox complexes is tested under pseudo-physiological conditions. Moreover, the DoE model generated from the experimental data can be validated using confirmatory experiments.

The response surface can be expressed as follows if all variables are assumed to be measurable,

$$y = f(x_1, x_2, x_3 \dots x_k) \quad (1.9)$$

Where y is the response of the system and x_i are the factors. The main aim is to optimise the response variable assuming those independent variables are continuous and controlled by experiments with negligible error. Therefore, a suitable approximation for a functional relationship between variable and response surface is required. RSM design layouts can be used to generate sufficient experimental design to fit second order models. Most commonly used response surface designs are the central composite design, Box-Behnken design and D-optimal design [187, 190].

Box-Behnken Design (BBD) is rotatable second order design based on a three-level factorial design and used to evaluate the main and interaction effects of components. In a three level DoE, three values for each component called levels are used for evaluating three to sixteen parameter ranges. Box-Behnken design requires an experiment number according to $N = 2k(k-1) + C_0$, [191] where k is the number of factors, and C_0 is the number of central points. The Box-Behnken design is a spherical, revolving design viewed as a cube (Figure 1.9). It consists of a central point and middle points of the edges. Figure 1.9 provides a graphical sketch of the experimental layout of a Box-Behnken design with three factors. The mathematical relationship between the predicted response and variables can be presented by a second-degree quadratic equation [191].

$$y = b_0 + b_1x_1 + b_2x_2 + b_3x_3 + b_4x_4 + b_{11}x_1^2 + b_{22}x_2^2 + b_{33}x_3^2 + b_{44}x_4^2 + b_{12}x_1x_2 + b_{13}x_1x_3 + b_{14}x_1x_4 + b_{23}x_2x_3 + b_{24}x_2x_4 + b_{34}x_3x_4 \quad (1.10)$$

where y is the predicted value, x_1, x_2, x_3 and x_4 are the factors, b_0 is the constant coefficient (intercept), b_1, b_2, b_3, b_4 and $b_{12}, b_{13}, b_{14}, b_{23}, b_{24}, b_{34}$ are linear and cross product coefficients, respectively, and the quadratic coefficients are b_{11}, b_{22}, b_{33} and b_{44} .

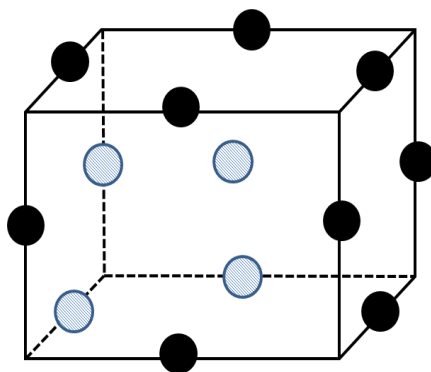


Figure 1.9: Example of a Box-Behnken experimental design for $k = 3$.

A quadratic polynomial equation is fitted to evaluate the effect of each factor on the response. On the basis of this equation, design model provides a tool for improvement of experimental outcome by finding the best combination of component value within the test set. The main advantages of the Box-Behnken design are the use of 3-levels for each factor and the need for fewer numbers of experimental runs [187, 189, 192, 193].

Electroanalytical methodologies are used to characterise the systems under investigation. A brief introduction to some of the basic principles and methodologies utilised is therefore presented in the following sections.

1.4 Electrochemical principles and techniques

Electrochemistry is an interdisciplinary branch of chemistry which is concerned with charge separation phenomena at mostly metal-liquid interfaces driven by the electrochemical potential of an electrode. In a redox reaction, the electrons are transferred from one reactant to another. The reactant is oxidised when it loses the electrons, or it is reduced when it gains electrons [195, 196]. At an electrode, the electron is transferred between reactant and electrode. The electrochemical reactions that involve the transfer of charge at solution/electrode interface are classed as a heterogeneous process [24, 195]. The rate of the electrochemical reaction is determined by a number of steps, involving transport of electroactive species to the

electrode surface and charge transfer at the interface [22]. Consider a simple electrochemical reaction of the type:



Where Ox is the oxidised species and Red is the reduced species. In general, redox reactions involve the following steps:

- Diffusion of Ox from the bulk solution to the electrode's surface;
- Transfer of electrons at the electrode surface;
- Chemical reactions preceding (homogeneous or heterogeneous process);
- Diffusion of Red species from the electrode surface into the bulk solution;
- Other surface reactions, such as adsorption or desorption etc. [197].

In addition, the overall electrochemical reaction can involve homogeneous chemical reactions or heterogeneous processes, such as adsorption or desorption of reactants or products, that may be coupled to the electrode reaction. The overall rate of electrode reaction will be determined by the slowest of all of these reactions involved in that process, which is called the rate determining step [22, 93, 97, 158, 196].

1.4.1 Faradaic and charging currents

The observed current in an electrochemical reaction involves two different processes at the electrode surface. The electron transfer process across the electrode solution interface gives rise to a faradaic current which results from either oxidation or reduction of electroactive species [197]. The flow of current as a result of chemical reactions is proportional to the amount of electricity passed. At peak current, the magnitude of the faradaic current is usually limited by mass transfer processes and/or electrochemical techniques being used. The second electrode process gives rise to charging (or capacitive) current, and results from the changing structure of the electrode/solution interface with changing potential. The interface has been shown experimentally to behave like a capacitor with the interfacial region being called the electrical double layer [77, 93, 158] and has a significant influence on the behaviour of colloids and other surface in contact with solution [94]. Capacitors have advantages in applications where a large amount of power is needed for short time [94, 197]. In voltammetric and amperometric studies, only faradaic current is of

analytical interest. Many methods are currently available which can be used to discriminate against the charging current [22, 197].

1.4.2 Modes of mass transfer

Different types of mass transfer processes occur during electrolysis.

Convection involves the mass transfer to/from the electrode due to gross physical movement (flowing, stirring, vibrating) and density gradients. This mode of mass transfer is commonly utilised in rotating disk voltammetry and stripping voltammetry techniques. Elimination of convective mass transfer is achieved in quiescent solutions [22, 93].

Migration involves the movement of a charged species under the influence of an electric field. The minimisation of the migrational type of mass transport of species in solution can be accomplished by the addition of an excess of electrolyte provided the electrolyte ions cannot be oxidised or reduced in the potential window of interest. Total charge within the analyte solution can be carried practically by the ions, leading to negligible migration currents in the system [93, 197].

Diffusion is a spontaneous movement of particles due to a concentration gradient. Molecules move from the region of higher concentrations to regions of lower concentrations. Diffusional flux, J , can be calculated from Fick's first law [22, 93, 198].

$$J = -D \frac{dC}{dx} \quad (1.11)$$

Where D is the diffusion coefficient ($\text{cm}^2 \text{s}^{-1}$), C is the concentration and x is the distance from the surface. The concentration gradient is often called the driving force in the diffusional process. The minus sign in the equation means that diffusion is down the concentration gradient. The flux is the number of molecules entering a unit area of the imaginary plane in a unit time and has units of $\text{mol cm}^{-2}\text{s}^{-1}$ [22, 197].

1.4.3 Solid electrode electrochemistry

Generally, the electrode/solution system has four different components: the

electrode; the double layer, which made up of several layers containing solvent molecules and specifically adsorbed ions or molecules; the diffusion layer; and bulk solution [199, 200].

Electrode

A working electrode serves as a transducer to the excitation signal where the reaction of interest is occurring. The most commonly used working electrode materials are gold, silver or platinum, mercury and carbon. The working electrode is used with an auxiliary electrode and reference electrode in a three electrode setup. The main factors to be considered for the selection of working material are:

- The material should exhibit fast, reproducible redox behaviour with the analyte.
- The material should exhibit a wide potential window in a given electrolyte solution.
- The cost of material, ease of surface renewal following a measurement and toxicity [201].

Reference electrode

For electroanalytical applications, it is important that the half-cell potential of one electrode be known and remains constant to the composition of the testing solution. Hence, the reference electrode is employed in a three electrode setup with working and auxiliary electrodes. Several electrode systems meet this requirement but the most common reference electrode system used is a Ag/AgCl electrode in a known excess of chloride ions. The silver chloride-coated silver electrode is usually immersed in a 3 M solution of sodium chloride. The solution is contained in a tube that is sealed at the end with porous plug to facilitate ionic contact with the sample solution.

The half-cell can be represented as:



And the half reaction of the cell is



At 25 °C, the potential of the electrode is 0.199 V vs. the Standard Hydrogen Electrode (SHE). These reference electrodes develop a potential proportional to chloride concentration that remains constant. To obtain the best measurement of

working electrode potential, the reference electrode should be placed as close as possible to the working electrodes.

Counter Electrode

The counter electrode, also known as the auxiliary electrode, acts as a source or sink of electrons in the electrochemical circuit formed with working electrode. Concentration polarisation and overpotential can both occur at the working and auxiliary electrodes [22]. The surface area of the counter electrode should be more than the working electrode to avoid current limitation through the counter electrode, rather than the working electrode [197].

1.5 Voltammetry

Voltammetry is based on the current measurement in an electrochemical cell in response to a variation in potential across the cell. This technique is widely used in analytical, inorganic, physical and biological chemistry to investigate the rate of reaction, surface process and mechanism of electron transfer, etc. There are many different ways of applying potential [197, 199, 200]. A brief introduction to the basic principles, and primary technique used, cyclic voltammetry, is, therefore, merited.

1.5.1 Cyclic voltammetry (CV)

Cyclic voltammetry is the most widely used technique to study the electrochemical reaction mechanism and in acquiring qualitative information about the response. Cyclic voltammetry involves applying a linearly varying electrode potential, cycled between two limits, (E_{initial} and E_{final}) [22, 93], to the working electrode, versus a reference electrode, between two limits, at a particular rate and measuring the resulting current that develops in an electrochemical cell [22, 93].

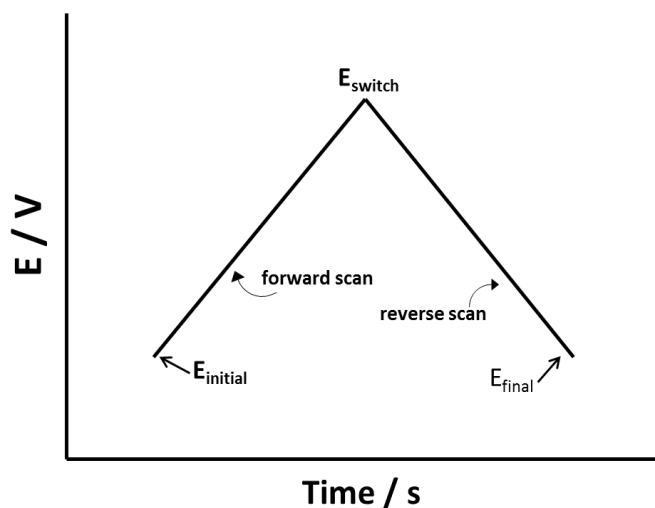


Figure 1.10: Triangular excitation signal (Potential vs. Time) for cyclic voltammetry (Figure adapted from [200]).

The applied potential is adjusted in order to observe oxidation or reduction of species [158]. The initial potential scan may be either negative or positive depending on the sample composition. Single or multiple scans may be used and the potential ramp can also be varied. A typical cyclic voltammogram for a solution species with the diagnostic features given in the diagram is shown in Figure 1.11.

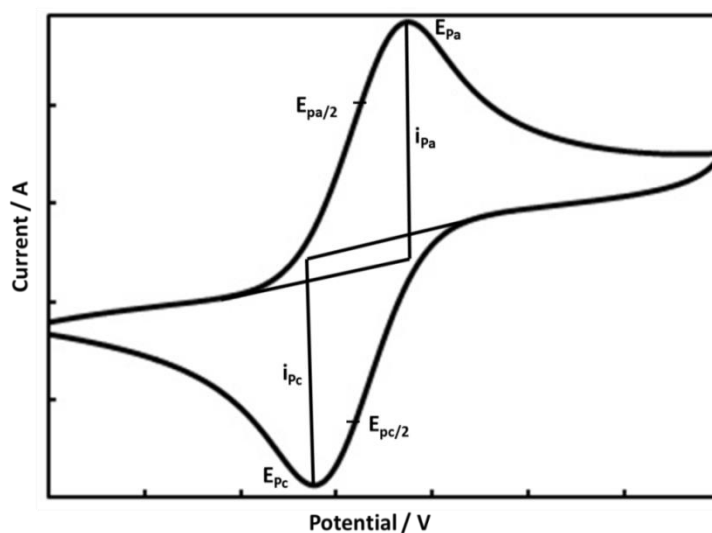


Figure 1.11: Diagnostic features of a cyclic voltammogram. E_{pa} , E_{pa} , and i_{pc} represent the anodic and cathodic peak potentials and currents respectively. $E_{pa/2}$ and $E_{pc/2}$ represent the anodic and cathodic half peak potentials respectively.

The relevant parameters in a cyclic voltammogram include the anodic (E_{pa}) and cathodic (E_{pc}) peak potentials and the anodic (i_{pa}) and cathodic (i_{pc}) peak currents. The peak current measured depends on the both the rate of mass transfer and electron transfer reaction.

For a reversible redox system, quantitative information is determined from the Randles-Sevcik equation [197, 202].

$$i_p = 0.4463 \cdot n \cdot F \sqrt{\frac{nF}{RT}} \cdot A \cdot D^{1/2} \cdot C \cdot \nu^{1/2} \quad (1.14)$$

Where i_p is the peak current, n is the number of electrons being transferred, A is the electrode area (cm^2), D is the diffusion coefficient ($\text{cm}^2 \text{s}^{-1}$), ν is the scan rate (Vs^{-1}) and C is the bulk solution concentration of electroactive species (mol cm^{-3}) [202, 203].

In the reversible system, the equilibrium ratio for the redox reaction is determined by the approximate Nernst equation (1.15). Here the electron transfer reaction at the electrode surface is rapid enough to maintain the concentrations of oxidised and reduced species in equilibrium.

$$E = E^{o'} - \frac{0.059}{n} \text{Log} \frac{[red]}{[ox]} \quad (1.15)$$

Where E is the electrode potential relative to $E^{o'}$, the formal potential, n is the number of electrons in the half reaction. Under these conditions the separation of potential between the current peaks is:

$$\Delta E = E_{pa} - E_{pc} = 59/n \text{ mV} \quad (1.16)$$

The position of peak potentials does not alter as a function of voltage scan rate.

For an irreversible reaction, the peaks obtained in a cyclic voltammogram are widely separated and reduced in size due to the sluggish electron exchange [202]. The voltage applied will not result in the generation of concentrations at electrode surface as predicted by Nernst equation. Therefore, the equilibria are not established rapidly

due to slow kinetics of reaction in comparison to the voltage scan rate. For a quasi-reversible reaction, the peak potentials alter as a function of voltage scan rate.

1.6 Thesis proposition

The aim of this thesis is to investigate the integration of redox complexes, enzymes and nanostructures to provide an improved biocatalytic electrode for use in an enzymatic fuel cell and for application to biosensing. Modification of electrode surfaces with redox layers is of interest to many application areas. Various methods have been reported for modification of electrode surfaces such as self-assembled monolayers using thiol chemistry on gold or covalent modification via reduction of aryldiazonium salts on carbon and selected metal surfaces [84, 87]. However, several drawbacks are associated with these approaches such as thermal instability, UV photo-oxidation or the difficulty in synthesis and isolation of the diazonium salt, which is not always straightforward [116]. The covalent attachment of alkylamines to carbon and metallic surface using an electro-oxidation method has been reviewed previously [15, 90, 101] and proven to be an excellent method for surface modifications. Therefore, we initially demonstrate formation of a redox-active layer on a carbon surface using this simple approach a layer of osmium redox complexes that are capable of mediating electron transfer to/from enzymatic system on electrode.

Chapter 2 will demonstrate a simple electrochemical oxidation method to immobilise osmium redox complexes bearing an amine functional group distal to the metal coordination site on carbon electrodes. The electrochemical oxidation of the amine can form radicals that couple to carbon surfaces, with coupling characterised by X-ray spectroscopy and cyclic voltammetry. The bioelectrocatalytic activity of the redox-active layer on the electrode surface is evaluated by oxidation of glucose in a buffer solution containing glucose oxidase. Use of this chemical coupling methodology can provide a simple route for covalent modification of an electrode surface with a variety of redox complexes. The redox active surface could have applications in a broad range of biosensor and biofuel cell devices. However, the modified electrode displays low current response attributed to the low surface coverage of the electron

shuttling redox complexes. For efficient electrocatalysis to occur the redox complexes and catalysts must be present in high concentration at the electrode surface. This can be done via formation of multilayer films on the electrode surface using a nanostructured support and polymer matrix into which electroactive biomaterials can be entrapped or coupled. Thus, the concept of multilayer formation of redox complexes and catalysts using such a matrix on surface of electrodes is investigated as described in chapter 3.

Chapter 3 reports on formation of thicker films on electrodes by addition of nanostructured supports, and by cross-linking alkylamine functional groups, distal to a ligand of the redox complex, to redox enzyme and functionalised polymers, with concomitant adsorption/grafting to the electrode surface. Initially, carboxymethyl dextran and polyacrylic acid polymers bearing carboxylic acid functional groups as chemical supports are investigated for the immobilisation of amine-containing osmium redox complexes and enzymes on the electrode surface. Lowering the redox potential of mediators (required to improve cell voltage in an EFC using glucose oxidation at the anode) is achieved by substitution of groups in the 4 and 4' position of the bipyridine ligand, by synthesis of complexes using 4,4'-dimethoxy-2,2'-bipyridine as a ligand instead of 2,2'-bipyridine. After synthesis of low redox potential based mediators, enzyme electrodes are prepared using co-immobilisation of carboxymethyl dextran, multiwalled carbon nanotubes and $[\text{Os}(4,4'\text{-dimethoxy-2,2'\text{-bipyridine}})_2(4\text{-aminomethyl pyridine})\text{Cl}]\text{PF}_6$, thus producing current densities of $0.83 \pm 0.21 \text{ mA cm}^{-2}$ in 5 mM glucose and $3.4 \pm 0.7 \text{ mA cm}^{-2}$ in saturated glucose solution in phosphate buffer saline at applied potential of 0.2 V vs Ag/AgCl. The co-immobilisation of enzymes and redox complexes to polymer support matrix is achieved using a chemical crosslinker (EDC/NHS) which therefore provides a 3-dimensional biofilm for electrocatalysis showing promise for application as glucose oxidising anodes for EFC and biosensors. Given the number of different components and the range of amounts and method used to prepare these enzyme electrodes, a comprehensive study is required on the optimisation of each component used in enzyme electrode preparation to identify the interaction or dependency of the performance of enzyme electrodes on these components. A traditional approach based on varying one factor at a time is tedious and cannot probe how each factor

interacts with each other. Therefore, a design of experiment approach is used to determine optimal enzyme electrode performance as described in chapter 4.

Chapter 4 focuses on the optimisation of the electrochemical response of these enzyme electrodes using a design of experiment approach, in seeking to improve further the current density under physiological conditions. The design of experiment model is validated and experimental results found to be consistent with the predicted values. Overall, a maximum current density of $1.2 \pm 0.1 \text{ mA cm}^{-2}$ or $5.2 \pm 0.2 \text{ mA cm}^{-2}$ at 0.2 V vs. Ag/AgCl, in pH 7.4 phosphate buffer at 37 °C containing 5 mM or 100 mM glucose, respectively, is achieved for oxidation of glucose using such biofilms incorporating multiwalled nanotubes, showing promise for application as an anode in a biofuel cell for electric power generation.

Furthermore, Chapter 5 examines the suitability of genipin-based immobilisation technique for the fabrication of enzyme electrodes. Genipin has attracted interest for biomedical applications because it can be used to crosslink cellular tissue and biomaterial and exhibits lower cytotoxicity than conventional cross-linkers [204, 205]. Therefore, there is a potential for incorporation of more biocompatible technology in EFC preparation for *in vivo* applications. The performance of enzyme electrodes prepared by co-immobilisation of redox complexes and enzymes via genipin as a crosslinker is evaluated for glucose oxidation. The enzyme electrode displays a current density of $0.74 \pm 0.08 \text{ mA cm}^{-2}$ at 0.45 V (vs. Ag/AgCl) in 50 mM phosphate buffer saline (pH 7.4, 37°C, 150 rpm) containing 100 mM glucose showing promise as a new biocompatible anode for EFC applications.

Chapter 6 summarises the research advances made during this Ph.D., and provides some opinions on the future research directions. An appendix is included providing a complete list of my co-authored publications as well as a list of the oral and poster presentations I have made over the course of my Ph.D. studies.

1.7 References

- [1] A. Heller, *Physical Chemistry Chemical Physics*, 6 (2004) 209-216.
- [2] S. Calabrese Barton, J. Gallaway, P. Atanassov, *Chemical Reviews*, 104 (2004) 4867-4886.
- [3] S.M. Kurtz, J.A. Ochoa, E. Lau, Y. Shkolnikov, B.B. Pavri, D. Frisch, A.J. Greenspon, *Pacing Clin Electrophysiol*, 33 (2010) 705-711.
- [4] C.A. Vincent, *Solid State Ionics*, 134 (2000) 159-167.
- [5] B. Wessling, *Polymers*, 2 (2010) 786-798.
- [6] J.C. Forgie, S. El Khakani, D.D. MacNeil, D. Rochefort, *Physical Chemistry Chemical Physics*, 15 (2013) 7713-7721.
- [7] A.F. Sammells, *Journal of Chemical Education*, 60 (1983) 320.
- [8] M.E. DeBakey, A.M. Gotto, *The new living heart*, Adams Media Corp., Holbrook, Mass., 1997.
- [9] M.S. Link, N.A. Estes, 3rd, J.J. Griffin, P.J. Wang, J.D. Maloney, J.B. Kirchhoffer, G.F. Mitchell, J. Orav, L. Goldman, G.A. Lamas, *J Interv Card Electrophysiol*, 2 (1998) 175-179.
- [10] G. Gregoratos, M.D. Cheitlin, A. Conill, A.E. Epstein, C. Fellows, T.B. Ferguson, R.A. Freedman, M.A. Hlatky, G.V. Naccarelli, S. Saksena, R.C. Schlant, M.J. Silka, *Circulation*, 97 (1998) 1325-1335.
- [11] R.J. Schilling, *Heart*, 87 (2002) 276-278.
- [12] C.M. Tracy, A.E. Epstein, D. Darbar, J.P. DiMarco, S.B. Dunbar, N.A. Estes, 3rd, T.B. Ferguson, Jr., S.C. Hammill, P.E. Karasik, M.S. Link, J.E. Marine, M.H. Schoenfeld, A.J. Shanker, M.J. Silka, L.W. Stevenson, W.G. Stevenson, P.D. Varosy, K.A. Ellenbogen, R.A. Freedman, L.S. Gettes, A.M. Gillinov, G. Gregoratos, D.L. Hayes, R.L. Page, M.O. Sweeney, *Circulation*, 126 (2012) 1784-1800.
- [13] A.C. Ruwald, C. Schuger, A.J. Moss, V. Kutlyifa, B. Olshansky, H. Greenberg, D.S. Cannom, N.A. Estes, M.H. Ruwald, D.T. Huang, H. Klein, S. McNitt, C.A. Beck, R. Goldstein, M.W. Brown, J. Kautzner, M. Shoda, D. Wilber, W. Zareba, J.P. Daubert, *Circ Arrhythm Electrophysiol*, 7 (2014) 785-792.
- [14] H.G. Mond, A. Proclemer, *Pacing Clin Electrophysiol*, 34 (2011) 1013-1027.
- [15] B.I. Rapoport, J.T. Kedzierski, R. Sarpeshkar, *PLoS ONE*, 7 (2012) e38436.
- [16] F. Davis, S.P.J. Higson, *Biosensors and Bioelectronics*, 22 (2007) 1224-1235.
- [17] J. Kim, H. Jia, P. Wang, *Biotechnol Adv*, 24 (2006) 296-308.

- [18] H. Endo, Y. Yonemori, K. Hibi, H. Ren, T. Hayashi, W. Tsugawa, K. Sode, *Biosensors and Bioelectronics*, 24 (2009) 1417-1423.
- [19] D. Leech, P. Kavanagh, W. Schuhmann, *Electrochimica Acta*, 84 (2012) 223-234.
- [20] P. Kavanagh, D. Leech, *Physical Chemistry Chemical Physics*, 15 (2013) 4859-4869.
- [21] N. Mano, A. Heller, *Journal of The Electrochemical Society*, 150 (2003) A1136-A1138.
- [22] D.C. Harris, *Quantitative Chemical Analysis*, Freeman, New York,, 2007.
- [23] A. Morozan, B. Joussetme, S. Palacin, *Energy & Environmental Science*, 4 (2011) 1238-1254.
- [24] A.T. Yahiro, S.M. Lee, D.O. Kimble, *Biochim Biophys Acta*, 88 (1964) 375-383.
- [25] S. Setford, J. Newman, *Enzyme Biosensors*, in: J. Barredo (Ed.) *Microbial Enzymes and Biotransformations*, vol. 17, Humana Press, 2005, pp. 29-60.
- [26] F. Davis, S.P. Higson, *Biosens Bioelectron*, 22 (2007) 1224-1235.
- [27] R. Allen, H.P. Bennetto, *Applied Biochemistry and Biotechnology*, 39-40 (1993) 27-40.
- [28] T. Catal, P. Kavanagh, V. O'Flaherty, D. Leech, *Journal of Power Sources*, 196 (2011) 2676-2681.
- [29] M.A. Moqsud, K. Omine, N. Yasufuku, M. Hyodo, Y. Nakata, *Waste Management*, 33 (2013) 2465-2469.
- [30] M. Zhou, J. Yang, H. Wang, T. Jin, D.J. Hassett, T. Gu, Chapter 9 - *Bioelectrochemistry of Microbial Fuel Cells and their Potential Applications in Bioenergy*, in: V.K. Gupta, M.G.T.P. Kubicek, J.S. Xu (Eds.) *Bioenergy Research: Advances and Applications*, Elsevier, Amsterdam, 2014, pp. 131-152.
- [31] D.R. Lovley, *Current Opinion in Biotechnology*, 19 (2008) 564-571.
- [32] L.C. Clark, Jr., C. Lyons, *Ann N Y Acad Sci*, 102 (1962) 29-45.
- [33] L.C. Clark, Jr., *Surg Forum*, 11 (1960) 143-144.
- [34] L.C. Clark, Jr., *Biosensors and Bioelectronics*, 8 (1993) 3-7.
- [35] A. Merz, A.J. Bard, *Journal of the American Chemical Society*, 100 (1978) 3222-3223.
- [36] R.W. Murray, *Accounts of Chemical Research*, 13 (1980) 135-141.
- [37] G. Inzelt, *Electrochimica Acta*, 34 (1989) 83-91.
- [38] E.J. Calvo, C. Danilowicz, L. Diaz, *Journal of the Chemical Society, Faraday Transactions*, 89 (1993) 377-384.
- [39] R.J. Forster, J.G. Vos, *Macromolecules*, 23 (1990) 4372-4377.
- [40] S. Lofas, B. Johnsson, *Journal of the Chemical Society, Chemical Communications*, (1990) 1526-1528.
- [41] D.R. Rolison, *Chemical Reviews*, 90 (1990) 867-878.

- [42] B.A. Gregg, A. Heller, *The Journal of Physical Chemistry*, 95 (1991) 5970-5975.
- [43] S. Yabuki, F. Mizutani, T. Katsura, *Biosensors and Bioelectronics*, 7 (1992) 695-700.
- [44] A. Ramanavicius, A. Kausaite, A. Ramanaviciene, *Biosensors and Bioelectronics*, 20 (2005) 1962-1967.
- [45] D. MacAodha, P.Ó. Conghaile, B. Egan, P. Kavanagh, D. Leech, *ChemPhysChem*, 14 (2013) 2302-2307.
- [46] P. Ó Conghaile, D. MacAodha, B. Egan, P. Kavanagh, D. Leech, *Journal of The Electrochemical Society*, 160 (2013) G3165-G3170.
- [47] S. Tsujimura, M. Fujita, H. Tatsumi, K. Kano, T. Ikeda, *Physical Chemistry Chemical Physics*, 3 (2001) 1331-1335.
- [48] A. Pizzariello, M. Stred'ansky, S. Miertuš, *Bioelectrochemistry*, 56 (2002) 99-105.
- [49] Y. Kamitaka, S. Tsujimura, N. Setoyama, T. Kajino, K. Kano, *Physical Chemistry Chemical Physics*, 9 (2007) 1793-1801.
- [50] N.L. Akers, C.M. Moore, S.D. Minter, *Electrochimica Acta*, 50 (2005) 2521-2525.
- [51] A. Zebda, S. Cosnier, J.P. Alcaraz, M. Holzinger, A. Le Goff, C. Gondran, F. Boucher, F. Giroud, K. Gorgy, H. Lamraoui, P. Cinquin, *Sci. Rep.*, 3 (2013).
- [52] M. Falk, C.W. Narváez Villarrubia, S. Babanova, P. Atanassov, S. Shleev, *ChemPhysChem*, 14 (2013) 2045-2058.
- [53] C.M. Wong, K.H. Wong, X.D. Chen, *Appl Microbiol Biotechnol*, 78 (2008) 927-938.
- [54] R. Wilson, A.P.F. Turner, *Biosensors and Bioelectronics*, 7 (1992) 165-185.
- [55] H.J. Hecht, H.M. Kalisz, J. Hendle, R.D. Schmid, D. Schomburg, *J Mol Biol*, 229 (1993) 153-172.
- [56] H.N. Bhatti, M. Madeeha, M. Asgher, N. Batool, *Canadian Journal of Microbiology*, 52 (2006) 519-524.
- [57] J. Wang, *Electroanalysis*, 13 (2001) 983-988.
- [58] Q. Yan, B. Peng, G. Su, B.E. Cohan, T.C. Major, M.E. Meyerhoff, *Analytical Chemistry*, 83 (2011) 8341-8346.
- [59] P. Ó Conghaile, S. Kamireddy, D. MacAodha, P. Kavanagh, D. Leech, *Anal Bioanal Chem*, 405 (2013) 3807-3812.
- [60] D. MacAodha, M.L. Ferrer, P.O. Conghaile, P. Kavanagh, D. Leech, *Physical Chemistry Chemical Physics*, 14 (2012) 14667-14672.
- [61] J.E. Frew, H.A.O. Hill, *European Journal of Biochemistry*, 172 (1988) 261-269.
- [62] O. Courjean, F. Gao, N. Mano, *Angewandte Chemie International Edition*, 48 (2009) 5897-5899.

- [63] D. Ivnitski, B. Branch, P. Atanassov, C. Apblett, *Electrochemistry Communications*, 8 (2006) 1204-1210.
- [64] A.L. Ghindilis, P. Atanasov, E. Wilkins, *Electroanalysis*, 9 (1997) 661-674.
- [65] M. Wooten, S. Karra, M. Zhang, W. Gorski, *Analytical Chemistry*, 86 (2013) 752-757.
- [66] J.M. Goran, S.M. Mantilla, K.J. Stevenson, *Analytical Chemistry*, 85 (2013) 1571-1581.
- [67] E. Katz, I. Willner, A.B. Kotlyar, *Journal of Electroanalytical Chemistry*, 479 (1999) 64-68.
- [68] S.M. Zakeeruddin, D.M. Fraser, M.K. Nazeeruddin, M. Grätzel, *Journal of Electroanalytical Chemistry*, 337 (1992) 253-283.
- [69] A. Heller, *AIChE Journal*, 51 (2005) 1054-1066.
- [70] T. Chen, S.C. Barton, G. Binyamin, Z. Gao, Y. Zhang, H.-H. Kim, A. Heller, *Journal of the American Chemical Society*, 123 (2001) 8630-8631.
- [71] A.E.G. Cass, G. Davis, G.D. Francis, H.A.O. Hill, W.J. Aston, I.J. Higgins, E.V. Plotkin, L.D.L. Scott, A.P.F. Turner, *Analytical Chemistry*, 56 (1984) 667-671.
- [72] N.J. Forrow, G.S. Sanghera, S.J. Walters, *Journal of the Chemical Society, Dalton Transactions*, (2002) 3187-3194.
- [73] H.-z. Bu, S.R. Mikkelsen, A.M. English, *Analytical Chemistry*, 67 (1995) 4071-4076.
- [74] J. Hodak, R. Etchenique, E.J. Calvo, K. Singhal, P.N. Bartlett, *Langmuir*, 13 (1997) 2708-2716.
- [75] M.T. Meredith, D.-Y. Kao, D. Hickey, D.W. Schmidtke, D.T. Glatzhofer, *Journal of The Electrochemical Society*, 158 (2011) B166-B174.
- [76] T.J. Ohara, R. Rajagopalan, A. Heller, *Analytical Chemistry*, 65 (1993) 3512-3517.
- [77] R.J. Forster, J.G. Vos, *Electrochimica Acta*, 37 (1992) 159-167.
- [78] P. Kavanagh, D. Leech, *Tetrahedron Letters*, 45 (2004) 121-123.
- [79] B.B. Dambatta, J.R. Ebdon, *European Polymer Journal*, 22 (1986) 783-786.
- [80] M.H. Allen, S.T. Hemp, A.E. Smith, T.E. Long, *Macromolecules*, 45 (2012) 3669-3676.
- [81] J.W. Gallaway, S.A. Calabrese Barton, *Journal of Electroanalytical Chemistry*, 626 (2009) 149-155.
- [82] E.M. Kober, J.V. Caspar, B.P. Sullivan, T.J. Meyer, *Inorganic Chemistry*, 27 (1988) 4587-4598.
- [83] A.B.P. Lever, *Inorganic Chemistry*, 29 (1990) 1271-1285.
- [84] S. Boland, F. Barrière, D. Leech, *Langmuir*, 24 (2008) 6351-6358.
- [85] M.A. Ghanem, J.-M. Chretien, A. Pinczewska, J.D. Kilburn, P.N. Bartlett, *Journal of Materials Chemistry*, 18 (2008) 4917-4927.

- [86] A.J. Downard, *Electroanalysis*, 12 (2000) 1085-1096.
- [87] X. Li, Y. Wan, C. Sun, *Journal of Electroanalytical Chemistry*, 569 (2004) 79-87.
- [88] T.P. Silverstein, *Journal of Chemical Education*, 89 (2012) 1159-1167.
- [89] R.W. Murray, A.G. Ewing, R.A. Durst, *Analytical Chemistry*, 59 (1987) 379A-390A.
- [90] M. Delamar, R. Hitmi, J. Pinson, J.M. Saveant, *Journal of the American Chemical Society*, 114 (1992) 5883-5884.
- [91] R.S. Deinhammer, M. Ho, J.W. Anderegg, M.D. Porter, *Langmuir*, 10 (1994) 1306-1313.
- [92] R.J. Forster, J.G. Vos, *Langmuir*, 10 (1994) 4330-4338.
- [93] P. Kissinger, W.R. Heineman, *Laboratory Techniques in Electroanalytical Chemistry*, 2 ed., Marcel Dekker, Inc., 1996.
- [94] E. Gileadi, *Adsorption in Electrochemistry*, in: E. Gileadi (Ed.) *Electrosorption*, Springer US, 1967, pp. 1-18.
- [95] R.F. Lane, A.T. Hubbard, *The Journal of Physical Chemistry*, 77 (1973) 1401-1410.
- [96] M.P. Soriaga, A.T. Hubbard, *Journal of the American Chemical Society*, 104 (1982) 3937-3945.
- [97] A.P. Brown, F.C. Anson, *Analytical Chemistry*, 49 (1977) 1589-1595.
- [98] A. Ulman, *Chemical Reviews*, 96 (1996) 1533-1554.
- [99] L. Strong, G.M. Whitesides, *Langmuir*, 4 (1988) 546-558.
- [100] K. Uosaki, Y. Sato, H. Kita, *Langmuir*, 7 (1991) 1510-1514.
- [101] J. Pinson, F. Podvorica, *Chemical Society Reviews*, 34 (2005) 429-439.
- [102] G. Shul, C.A.C. Ruiz, D. Rochefort, P.A. Brooksby, D. Bélanger, *Electrochimica Acta*, 106 (2013) 378-385.
- [103] L. Netzer, J. Sagiv, *Journal of the American Chemical Society*, 105 (1983) 674-676.
- [104] I.R. Peterson, *Journal of Physics D: Applied Physics*, 23 (1990) 379.
- [105] G.G. Roberts, *Contemporary Physics*, 25 (1984) 109-128.
- [106] M.C. Petty, *Endeavour*, 7 (1983) 65-69.
- [107] J. Zasadzinski, R. Viswanathan, L. Madsen, J. Garnæs, D. Schwartz, *Science*, 263 (1994) 1726-1733.
- [108] M.R. Van de Mark, L.L. Miller, *Journal of the American Chemical Society*, 100 (1978) 3223-3225.
- [109] U. Lange, N.V. Roznyatovskaya, V.M. Mirsky, *Analytica Chimica Acta*, 614 (2008) 1-26.
- [110] M.N. Szentirmay, C.R. Martin, *Analytical Chemistry*, 56 (1984) 1898-1902.
- [111] N. Oyama, F.C. Anson, *Journal of the American Chemical Society*, 101 (1979) 739-741.
- [112] A. Fitch, *Clays and Clay Minerals*, 38 (1990) 391-400.

- [113] K. Itaya, I. Uchida, V.D. Neff, *Accounts of Chemical Research*, 19 (1986) 162-168.
- [114] D.E. Tallman, S.L. Petersen, *Electroanalysis*, 2 (1990) 499-510.
- [115] H.M. Wu, R. Olier, N. Jaffrezic-Renault, P. Clechet, A. Nyamsi, C. Martelet, *Electrochimica Acta*, 39 (1994) 327-331.
- [116] M.H. Schoenfisch, J.E. Pemberton, *Journal of the American Chemical Society*, 120 (1998) 4502-4513.
- [117] K. Habermüller, A. Ramanavicius, V. Laurinavicius, W. Schuhmann, *Electroanalysis*, 12 (2000) 1383-1389.
- [118] S.K. Vashist, D. Zheng, K. Al-Rubeaan, J.H.T. Luong, F.-S. Sheu, *Biotechnology Advances*, 29 (2011) 169-188.
- [119] R. Hirlekar, M. Yamagar, H. Garse, M. Vij, V. Kadam, *Asian Journal of Pharmaceutical and Clinical Research*, 2 (2009) 17-27.
- [120] V. Choudhary, A. Gupta, *Polymer/Carbon Nanotube Nanocomposites*, 2011.
- [121] S. Bandow, M. Takizawa, K. Hirahara, M. Yudasaka, S. Iijima, *Chemical Physics Letters*, 337 (2001) 48-54.
- [122] Y. Saito, T. Yoshikawa, *Journal of Crystal Growth*, 134 (1993) 154-156.
- [123] N.A. Kiselev, J. Sloan, D.N. Zakharov, E.F. Kukovitskii, J.L. Hutchison, J. Hammer, A.S. Kotosonov, *Carbon*, 36 (1998) 1149-1157.
- [124] S. Cosnier, M. Holzinger, A. Le Goff, *Frontiers in Bioengineering and Biotechnology*, 2 (2014) 45.
- [125] H. Pan, J. Li, Y. Feng, *Nanoscale Research Letters*, 5 (2010) 654-668.
- [126] M. Holzinger, A. Le Goff, S. Cosnier, *Electrochimica Acta*, 82 (2012) 179-190.
- [127] Y. Yan, W. Zheng, L. Su, L. Mao, *Advanced Materials*, 18 (2006) 2639-2643.
- [128] N. Liu, Q. Zhang, M. Chan-Park, C. Li, P. Chen, *Carbon Nanotubes for Electrochemical and Electronic Biosensing Applications*, in: D. Shi (Ed.) *NanoScience in Biomedicine*, Springer Berlin Heidelberg, 2009, pp. 205-246.
- [129] Y.-M. Yan, I. Baravik, O. Yehezkeli, I. Willner, *The Journal of Physical Chemistry C*, 112 (2008) 17883-17888.
- [130] I. Osadebe, D. Leech, *ChemElectroChem*, 1 (2014) 1988-1993.
- [131] Y. Lin, W. Yantasee, J. Wang, *Front Biosci*, 10 (2005) 492-505.
- [132] M. Mazloum-Ardakani, H. Beitollahi, B. Ganjipour, H. Naeimi, M. Nejati, *Bioelectrochemistry*, 75 (2009) 1-8.
- [133] D. Zheng, J. Ye, W. Zhang, *Electroanalysis*, 20 (2008) 1811-1818.

- [134] M.C. Rodríguez, J. Sandoval, L. Galicia, S. Gutiérrez, G.A. Rivas, *Sensors and Actuators B: Chemical*, 134 (2008) 559-565.
- [135] H. Beitollahi, H. Karimi-Maleh, H. Khabazzadeh, *Analytical Chemistry*, 80 (2008) 9848-9851.
- [136] Y. Li, Y. Umasankar, S.-M. Chen, *Analytical Biochemistry*, 388 (2009) 288-295.
- [137] A. Liu, I. Honma, H. Zhou, *Biosensors and Bioelectronics*, 23 (2007) 74-80.
- [138] S. Dong, S. Zhang, L. Chi, P. He, Q. Wang, Y. Fang, *Analytical Biochemistry*, 381 (2008) 199-204.
- [139] L. Meng, J. Jin, G. Yang, T. Lu, H. Zhang, C. Cai, *Analytical Chemistry*, 81 (2009) 7271-7280.
- [140] S. Fei, J. Chen, S. Yao, G. Deng, D. He, Y. Kuang, *Analytical Biochemistry*, 339 (2005) 29-35.
- [141] P. Hu, A. Fasoli, J. Park, Y. Choi, P. Estrela, S.L. Maeng, W.I. Milne, A.C. Ferrari, *Journal of Applied Physics*, 104 (2008) 074310.
- [142] J. Lin, C. He, L. Zhang, S. Zhang, *Analytical Biochemistry*, 384 (2009) 130-135.
- [143] Y.T. Wang, L. Yu, Z.Q. Zhu, J. Zhang, J.Z. Zhu, C. Fan, *Sensors and Actuators B: Chemical*, 136 (2009) 332-337.
- [144] F. Berti, L. Lozzi, I. Palchetti, S. Santucci, G. Marrazza, *Electrochimica Acta*, 54 (2009) 5035-5041.
- [145] J. Li, Q. Liu, Y. Liu, S. Liu, S. Yao, *Analytical Biochemistry*, 346 (2005) 107-114.
- [146] X. Zhang, K. Jiao, S. Liu, Y. Hu, *Analytical Chemistry*, 81 (2009) 6006-6012.
- [147] E. Yapaslan, A. Caliskan, H. Karadeniz, A. Erdem, *Materials Science and Engineering: B*, 169 (2010) 169-173.
- [148] L. Wang, E. Wang, *Electrochemistry Communications*, 6 (2004) 49-54.
- [149] X. Wang, M. Falk, R. Ortiz, H. Matsumura, J. Bobacka, R. Ludwig, M. Bergelin, L. Gorton, S. Shleev, *Biosensors and Bioelectronics*, 31 (2012) 219-225.
- [150] V. Andoralov, M. Falk, D.B. Suyatin, M. Granmo, J. Sotres, R. Ludwig, V.O. Popov, J. Schouenborg, Z. Blum, S. Shleev, *Sci. Rep.*, 3 (2013).
- [151] M. Falk, Z. Blum, S. Shleev, *Electrochimica Acta*, 82 (2012) 191-202.
- [152] K. Murata, K. Kajiya, N. Nakamura, H. Ohno, *Energy & Environmental Science*, 2 (2009) 1280-1285.
- [153] J. Shim, G.-Y. Kim, S.-H. Moon, *Journal of Electroanalytical Chemistry*, 653 (2011) 14-20.

- [154] M. Pellissier, F. Barrière, A.J. Downard, D. Leech, *Electrochemistry Communications*, 10 (2008) 835-838.
- [155] S. Boland, P. Jenkins, P. Kavanagh, D. Leech, *Journal of Electroanalytical Chemistry*, 626 (2009) 111-115.
- [156] U.T. Bornscheuer, *Angewandte Chemie International Edition*, 42 (2003) 3336-3337.
- [157] A. Sassolas, L.J. Blum, B.D. Leca-Bouvier, *Biotechnology Advances*, 30 (2012) 489-511.
- [158] D. Leech, *The Development and Characterisation of Some Novel Amperometric Sensors*, in, Dublin City University, PhD Thesis, 1991.
- [159] R. Singhal, A. Gambhir, M.K. Pandey, S. Annapoorni, B.D. Malhotra, *Biosensors and Bioelectronics*, 17 (2002) 697-703.
- [160] S.-N. Liu, Y.-J. Yin, C.-X. Cai, *Chinese Journal of Chemistry*, 25 (2007) 439-447.
- [161] S.A. Miscoria, G.D. Barrera, G.A. Rivas, *Sensors and Actuators B: Chemical*, 115 (2006) 205-211.
- [162] S. Rengaraj, V. Mani, P. Kavanagh, J. Rusling, D. Leech, *Chemical Communications*, 47 (2011) 11861-11863.
- [163] Y.M. Uang, T.C. Chou, *Biosensors and Bioelectronics*, 19 (2003) 141-147.
- [164] J. Njagi, S. Andreescu, *Biosensors and Bioelectronics*, 23 (2007) 168-175.
- [165] L. Zhu, R. Yang, J. Zhai, C. Tian, *Biosensors and Bioelectronics*, 23 (2007) 528-535.
- [166] A. Eftekhari, *Synthetic Metals*, 145 (2004) 211-216.
- [167] D. Shan, S. Wang, Y. He, H. Xue, *Materials Science and Engineering: C*, 28 (2008) 213-217.
- [168] A. Salimi, R.G. Compton, R. Hallaj, *Analytical Biochemistry*, 333 (2004) 49-56.
- [169] S. Liu, Y. Sun, *Biosensors and Bioelectronics*, 22 (2007) 905-911.
- [170] D. Rochefort, L. Kouisni, K. Gendron, *Journal of Electroanalytical Chemistry*, 617 (2008) 53-63.
- [171] M.D. Rubianes, G.A. Rivas, *Electrochemistry Communications*, 5 (2003) 689-694.
- [172] Rajesh, V. Bisht, W. Takashima, K. Kaneto, *Biomaterials*, 26 (2005) 3683-3690.
- [173] Rajesh, K. Kaneto, *Current Applied Physics*, 5 (2005) 178-183.
- [174] M.A. McRipley, R.A. Linsenmeier, *Journal of Electroanalytical Chemistry*, 414 (1996) 235-246.
- [175] J.J. Gooding, D.B. Hibbert, *TrAC Trends in Analytical Chemistry*, 18 (1999) 525-533.
- [176] C.D. Gwenin, M. Kalaji, P.A. Williams, R.M. Jones, *Biosensors and Bioelectronics*, 22 (2007) 2869-2875.

- [177] K. Hernandez, R. Fernandez-Lafuente, *Enzyme and Microbial Technology*, 48 (2011) 107-122.
- [178] Y. Yonemori, E. Takahashi, H. Ren, T. Hayashi, H. Endo, *Analytica Chimica Acta*, 633 (2009) 90-96.
- [179] D. MacAodha, P. Ó Conghaile, B. Egan, P. Kavanagh, C. Sygmund, R. Ludwig, D. Leech, *Electroanalysis*, 25 (2013) 94-100.
- [180] S.R. Mikkelsen, G.A. Rechnitz, *Analytical Chemistry*, 61 (1989) 1737-1742.
- [181] L. Su, X. Qiu, L. Guo, F. Zhang, C. Tung, *Sensors and Actuators B: Chemical*, 99 (2004) 499-504.
- [182] T.J. Ohara, R. Rajagopalan, A. Heller, *Analytical Chemistry*, 65 (1993) 3512-3517.
- [183] M.E. Fischer, *Amine Coupling Through EDC/NHS: A Practical Approach*, in: N.J. Mol, M.J.E. Fischer (Eds.) *Surface Plasmon Resonance*, vol. 627, Humana Press, 2010, pp. 55-73.
- [184] T. Lai, Q. Hou, H. Yang, X. Luo, M. Xi, *Acta Biochimica et Biophysica Sinica*, 42 (2010) 787-792.
- [185] S. Nandini, S. Nalini, J. Sanetuntikul, S. Shanmugam, P. Niranjana, J.S. Melo, G.S. Suresh, *Analyst*, 139 (2014) 5800-5812.
- [186] M. Moyo, J.O. Okonkwo, N.M. Agyei, *Sensors (Basel, Switzerland)*, 12 (2012) 923-953.
- [187] K. Yang, B. El-Haik, *Design for Six Sigma: Roadmap to product development*, 2nd ed., McGraw-Hill, 2003.
- [188] M. Anderson, *The Industrial Physicist*, (1997) pp. 24-27.
- [189] J. Antony, *Design of Experiments for Engineers and Scientists* Elsevier, 2003.
- [190] L. Eriksson, E. Johansson, N.K. Wold, C. Wikstrom, S. Wold, *Design of Experiments: Principles and Applications* Umetrics Academy, 2008.
- [191] B. Qi, X. Chen, F. Shen, Y. Su, Y. Wan, *Industrial & Engineering Chemistry Research*, 48 (2009) 7346-7353.
- [192] E.C. Catalkaya, F. Kargi, *Chemosphere*, 69 (2007) 485-492.
- [193] R. Kumar, R. Singh, N. Kumar, K. Bishnoi, N.R. Bishnoi, *Chemical Engineering Journal*, 146 (2009) 401-407.
- [194] S. Babanova, K. Artyushkova, Y. Ulyanova, S. Singhal, P. Atanassov, *Journal of Power Sources*, 245 (2014) 389-397.
- [195] R.S. Nicholson, *Analytical Chemistry*, 37 (1965) 1351-1355.
- [196] G.A. Mabbott, *Journal of Chemical Education*, 60 (1983) 697.
- [197] A.J. Bard, L.R. Faulkner, *Electrochemical Methods: Fundamentals and Applications*, 2 ed., Wiley & Sons, New York, 2001.

- [198] E. Gileadi, *Physical Electrochemistry: Fundamental, Techniques and Applications*, WILEY-VCH Verlag GmbH & Co. KGaA, 2011.
- [199] J. Wang, *Analytical Electrochemistry 2ed.*, Wiley-VCH, 2000.
- [200] D.A. Skoog, D.M. West, *Principles of Instrumental Analysis 2ed.*, Saunders College Philadelphia 1980.
- [201] D.A. Skoog, D.M. West, F.J. Holler, S.R. Crouch, *Fundamentals of Analytical Chemistry 8ed.*, Thomson Brooks/Cole 2004.
- [202] P.G. Bruce, *Solid State Electrochemistry*, Cambridge University Press, 1995.
- [203] C.M.A. Brett, A.M.O. Brett, *Electrochemistry: Principles, Methods and Applications*, Oxford University Press, 1993.
- [204] F.-L. Mi, S.-S. Shyu, C.-K. Peng, *Journal of Polymer Science Part A: Polymer Chemistry*, 43 (2005) 1985-2000.
- [205] J. Ma, Y. Sahai, *Carbohydrate Polymers*, 92 (2013) 955-975.

Chapter 2:

Published as:

Immobilisation of Alkylamine-Functionalised Osmium Redox Complex on Glassy Carbon using Electrochemical Oxidation

Published as:

Rakesh Kumar and Dónal Leech. *Electrochimica Acta*, Vol. 140, pp. 209-216, 2014

DOI: 10.1016/j.electacta.2014.03.090

Co-author contributions:

I synthesised the osmium redox complexes, and performed the laboratory work, the analysis and wrote the first draft of the publication.

Dónal Leech, as the project supervisor, contributed through guidance and advice throughout and wrote the final draft of the publication.

Copyright License number: 3714851489955

Immobilisation of Alkylamine-Functionalised Osmium Redox Complex on Glassy Carbon using Electrochemical Oxidation

2.1 ABSTRACT

The electrochemical oxidation of alkylamines provides a method for modification of carbon, and other surfaces via formation of a radical amine that reacts with the surface. Direct electrochemical oxidation of an alkylamine functional group of a redox complex provides a simple route to preparation of a redox active layer on carbon surfaces. Here we report on oxidation of an osmium redox complex, containing an alkylamine ligand distal to the metal co-ordination site, on carbon electrodes to directly produce a redox active film on the surface. The presence of the redox-active layer of osmium complexes is confirmed by cyclic voltammetry and X-Ray photoelectron spectroscopy. The average surface coverage of the attached film upon electrolysis of an $[\text{Os}(2,2'\text{-bipyridine})_2(4\text{-aminomethylpyridine})\text{Cl}]\cdot\text{PF}_6$ complex is $0.84 (\pm 0.3) \times 10^{-10}$ moles cm^{-2} , demonstrating that coverages close to that predicted for a close-packed monolayer of complex is attained. The bioelectrocatalytic activity of the modified electrode was evaluated for oxidation of glucose in presence of glucose oxidase in solution. Hence, electrochemical coupling of alkylamine functionalised osmium redox complexes provides a simple and efficient methodology for obtaining redox active monolayers on carbon surfaces with potential applications to biosensor and biofuel cell device development.

2.2 Introduction

Modification of carbon electrode surfaces with redox layers is of interest to many application areas, such as biosensors, molecular electronics, biofuel cell devices and electrocatalysis [1, 2]. Modification of surfaces can provide new properties to a surface while maintaining the bulk properties [3] with potential use for both analytical and chemical sensing [4]. The ability to form strongly-bonded, stable, monolayers on carbon surfaces is attractive for molecular device and sensor applications [5, 6]. In addition, surface immobilised molecules which are capable of

heterogeneous electron transfer between redox centre and surface can have high impact on the rapidly emerging field of high speed molecular electronics applications [7, 8].

Various methods have been described for modification of carbon surfaces through a free radical grafting mechanism. For example, covalent modification of surfaces *via* reduction of aryldiazonium salts can lead to functionalised electrodes with high stability [2, 9, 10]. A major disadvantage to this approach is that synthesis and isolation of the diazonium salt is not always straightforward [11]. Apart from free radical grafting, formation of self-assembled monolayers (SAMs) using thiol chemistry on gold electrodes provides another way for introduction of chemical functionality to surfaces. However, the Au-thiol chemistry has several drawbacks such as thermal instability, prone to UV photo-oxidation [12] and mobility of layer results in a decreased electrochemical signal for many possible applications [10, 13, 14].

The covalent attachment of alkylamines to carbon and metallic surfaces using an electro-oxidation method has been reviewed in detail by Pinson and colleagues in recent years [15, 16] and proven to be an excellent method for surface modification [17]. The extent of surface derivatisation depends upon the degree of substitution at the amine functionality [18], as tertiary amines show no evident surface coverage, compared to primary and secondary amines, proposed to be because of the steric hindrance which blocks the accessibility of amine radicals to surfaces [6, 19].

Osmium and ruthenium based polypyridyl complexes are broadly explored for a range of applications as redox catalysts and mediators, due to the ease of synthetic variation of structure and therefore properties of these complexes [20]. For example, the redox potential of osmium based complexes can be tuned across a wide potential window by altering the ligand of a complex [21, 22]. The favourable relatively low redox potential of osmium complexes and their relative stability in both oxidation states (II/III) is advantageous over the iron and ruthenium based systems [23]. Surface confined osmium based complexes are capable of mediating electron transfer to/from enzymatic [24, 25] as well as microbial systems [26, 27] on electrodes.

Here, we report on direct grafting of an osmium complex, $[\text{Os}(2,2'\text{-bipyridine})_2(4\text{-aminomethylpyridine})\text{Cl}]\cdot\text{PF}_6$ (Os bpy4AMP), to glassy carbon and pyrolysed photoresist (PPF) surfaces by the simple methodology of electrochemical oxidation of the alkylamine functional group of the complex. Previously Buriez *et al.* [28] grafted a redox layer of amino-ferrocifen to carbon and metal surfaces based on electro-oxidation of the aryl-amine group of the organometallic complex, yielding strong attachment of the redox complex to surfaces [28]. Aramata *et al.* [29] grafted ligands of redox complexes onto carbon electrodes, using electro-oxidation of amine-containing ligands, to provide a platform for preparation of redox layers on carbon electrodes. Direct electro-oxidation of an osmium metal complex containing an aryl-amine ligand (4-aminopyridine) for grafting to carbon was also briefly described [29]. More recently, osmium polypyridyl complexes have been grafted to carbon surfaces to provide redox layers capable of mediating electron transfer to a glucose-oxidising enzyme in solution [30]. Details of the simple direct grafting of Os bpy4AMP to carbon surfaces by simple electro-oxidation of the alkylamine group is reported on here. The resulting modified surface is characterised by cyclic voltammetry (CV) and X-ray Photoelectron Spectroscopy (XPS). The experimental results demonstrate that a monolayer of redox complex is formed that is stable and can be used as a mediating surface for glucose oxidation by glucose oxidase in solution. Use of this chemical coupling methodology can provide a simple route for modification of a surface with a variety of osmium redox complexes for application to biosensor and biofuel cell device development.

2.3 Experimental

All chemicals were purchased from Sigma-Aldrich and used without any further purification. All solutions were prepared in Milli-Q (18.2 M Ω cm) water unless otherwise stated. Either glassy carbon disk (GC, 3 mm diameter) or glassy plate (25 \times 25 \times 1 mm) working electrodes were used along with a platinum wire counter electrode and an Ag/AgCl (3M KCl) reference electrode in a 10 mL single compartment electrochemical cell (all sourced from IJ Cambria). The pyrolysed photoresist (PPF) working electrodes (approximately 15 mm \times 15 mm) were a gift from Alison Downard, University of Canterbury. The PPF were fabricated using two

coats of photoresist which were spin coated onto silicon wafer followed by soft baked before pyrolyzing at 1050 °C [31, 32]. For the modification of PPF surface, the electrodes were mounted on an insulated metal stage with four springs. A hole in the bottom was positioned on top of a Viton O-ring that sealed the solution above the electrode. Phosphate buffered saline (PBS), pH 7.4, was prepared using 50 mM phosphate buffer with 0.1 M NaCl. Glucose oxidase type VII from *Aspergillus niger* (GOx, EC 1.1.3.4., average activity 180 unit/mg) was purchased from Sigma-Aldrich.

[Os(2,2'-bipyridine)₂(4-aminomethylpyridine)Cl].PF₆ was synthesised from (NH₄)₂OsCl₆ according to literature methods [33] and the 4-aminomethylpyridine (4-AMP) ligand substitution of a chloride achieved by heating an ethylene glycol solution of a 1.1 mole equivalent ligand and Os(2,2'-bipyridyl)₂Cl₂ complex at reflux, with precipitation of the resulting complex by addition of an aqueous NH₄PF₆ solution [34]. Final product was filtered and allowed to dry overnight at 50°C. Microanalysis for [Os(2,2'-bipyridine)₂(4-AMP)Cl].PF₆: C, 39.86%; H, 3.25%; N, 10.23% compared to theoretical values: C, 39.47%; H, 3.06%; N, 10.62%.

Prior to modification, GC disk electrodes were polished with 1 µm, 0.3 µm, and 0.05 µm of alumina slurry on microcloth pads (Buehler) followed by rinsing with Milli-Q-water and drying with nitrogen gas stream. The glassy carbon plate and PPF electrode were cleaned by sonicating in acetonitrile for 15 minutes. All experiments were carried out at room temperature unless otherwise stated.

2.3.1 Apparatus

All electrochemical measurements were performed using a CHI 620 potentiostat in a conventional three electrode cell. XPS was carried out using a Kratos AXIS 165 spectrometer with the following parameters: Sample Temperature: 20-30 °C, X-Ray Gun: mono Al K α 1486.58 eV; 150 W (10 mA, 15kV), Pass Energy: 160 eV for survey spectra and 20 eV for narrow regions. Step: 1 eV (survey), 0.05 eV (regions), Dwell: 50ms (survey), 100 ms (regions), Sweeps: survey (4), narrow regions (5-20). For calibration the C 1s line at 284.8 eV was used as charge reference for determining binding energies. Other spectra were collected in the normal to the

surface direction. XPS detection limit is estimated to be ~0.1 at%. Quantitative survey spectra were obtained on high resolution spectra of elements acquired. The measurements were taken at take-off angle of 30° (sample tilt 60°) for better surface sensitivity.

2.4 Results and discussion

2.4.1 Electrochemically induced attachment of alkylamine functionalised redox complex to carbon surface.

Prior to surface confinement, solution phase cyclic voltammetry (CV) is used to evaluate the redox potential for the Os(II/III) transition of the Osbpy4AMP complex. Characteristic oxidation and reduction peaks are observed centred at 0.34 V (vs. Ag/AgCl), Figure 1a, for 0.1 mM Osbpy4AMP in acetonitrile solution containing 0.1 M tetraethylammonium tetrafluoroborate as electrolyte. A formal potential of 0.30 V vs. Ag/AgCl can be estimated for the Os(II/III) transition from CV in aqueous phosphate buffer (pH 7.4); a value that is similar to that observed by others for the complex in buffer solution [35]. The electrochemically induced attachment of Osbpy4AMP to carbon surfaces was performed via oxidation of the alkylamine functional group of the complex, in acetonitrile solution containing 0.1 M of tetraethylammonium tetrafluoroborate as electrolyte. The consecutive cyclic voltammograms of 0.1 mM Osbpy4AMP show a broad electrochemically irreversible peak appearing at around 1.9 V vs. Ag/AgCl in the potential window from 1.5 to 2.1 V. The peak current decreases with multiple voltammetric scans recorded at 0.1 Vs⁻¹. This peak is attributed to the one electron electrochemical oxidation of the alkylamine with formation of an amine radical that can covalently couple to glassy carbon and pyrolysed photoresist (PPF) surfaces, as depicted in scheme 1. Under continuous cycling the magnitude of peak current decreases, as observed by others [6, 18], and as shown in figure 1(b). This is proposed to be as a result of a decrease in availability of surface area for coupling once the first scan, and coupling process, is undertaken [6, 18], thus indicating coupling reaction at electrode surfaces [15, 17, 36]. The redox potential for the oxidation is in agreement

with data for oxidation of alkylamines and mono-Boc-protected diamine compounds at glassy carbon electrodes [6, 17, 37].

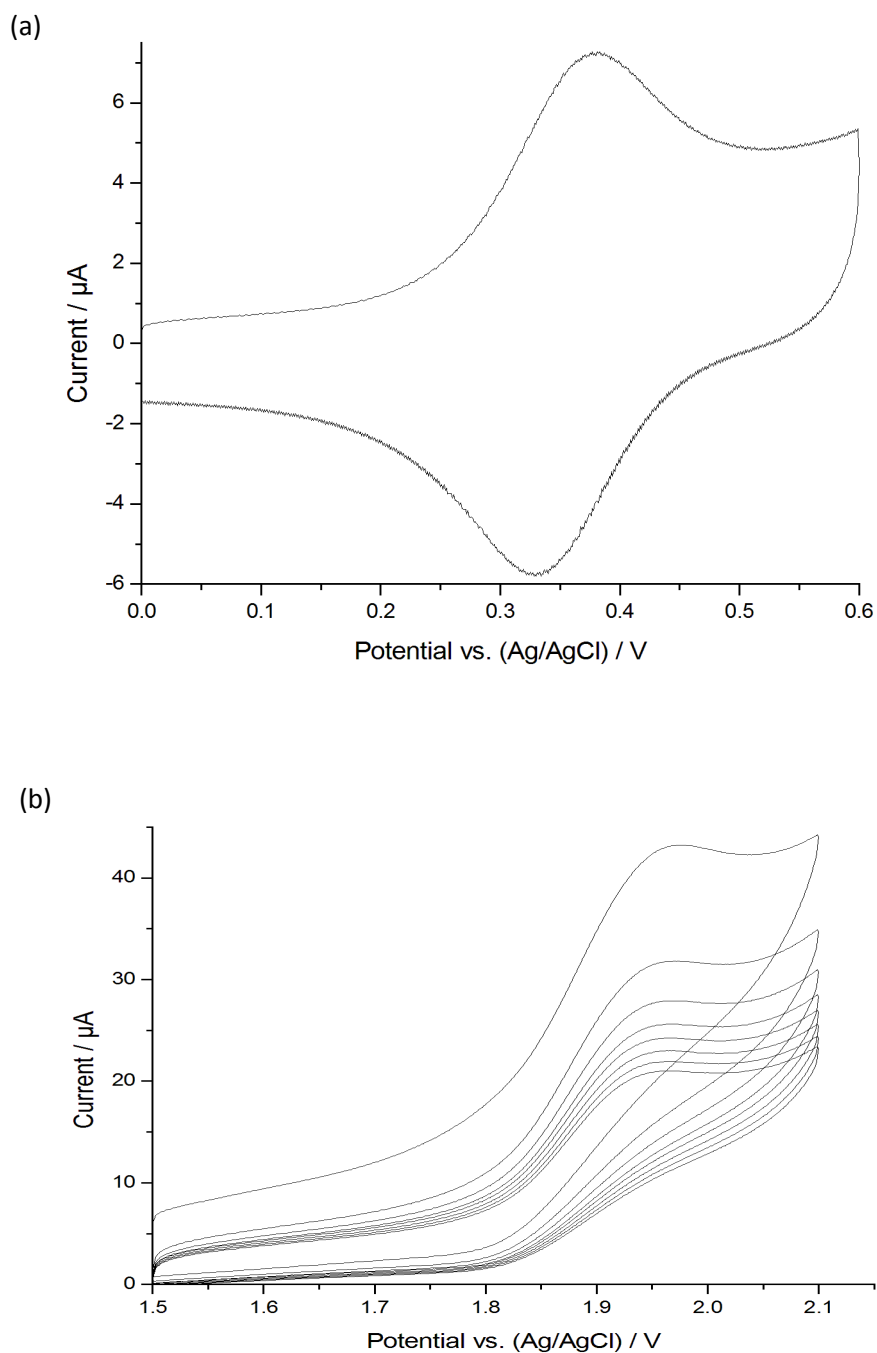
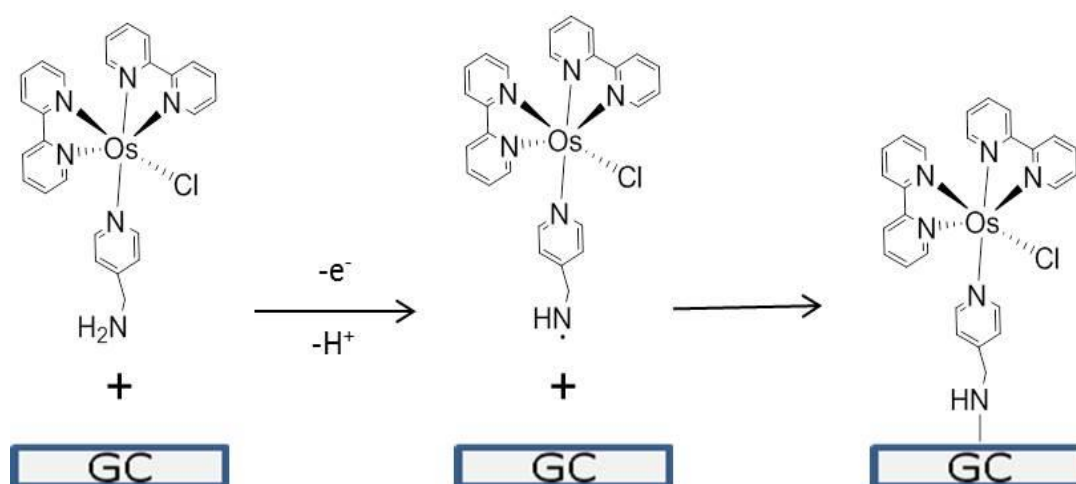


Fig. 1 Cyclic voltammograms of solution of 0.1 mM $[\text{Os}(\text{2,2}'\text{-bipyridine})_2(4\text{-aminomethylpyridine})\text{Cl}]\cdot\text{PF}_6$ in 0.1 M TEATFB in acetonitrile at a scan rate 0.1 V s^{-1} (a) with a potential window selected to show the Os(II/III) transition and (b) the electrochemical oxidation of the alkylamine (8 repeated cycles).



Scheme 1: Scheme depicting the proposed mechanism for electrochemically induced coupling of Osbpy4AMP to a glassy carbon surface.

2.4.2 Characterization of redox complex modified surface

Cyclic voltammetry can be used to evaluate if the redox complex is surface confined. The modified surface was cleaned with ultrapure millipore water, sonicated for 2 minutes and then voltammograms recorded in 0.05 M of phosphate buffer saline (pH 7.4), figure 2a. The redox potential for the Os(II/III) transition is 0.3 V vs Ag/AgCl similar to that for the complex in solution and coupled to adsorbed electrode films or to graphite electrodes [35, 38, 39], indicating that the redox potential of the Os(II/III) transition is generally not affected by immobilisation [21]. The anodic and cathodic peak currents increase linearly with scan rate, as expected for a surface-confined redox species, figure 2b [40].

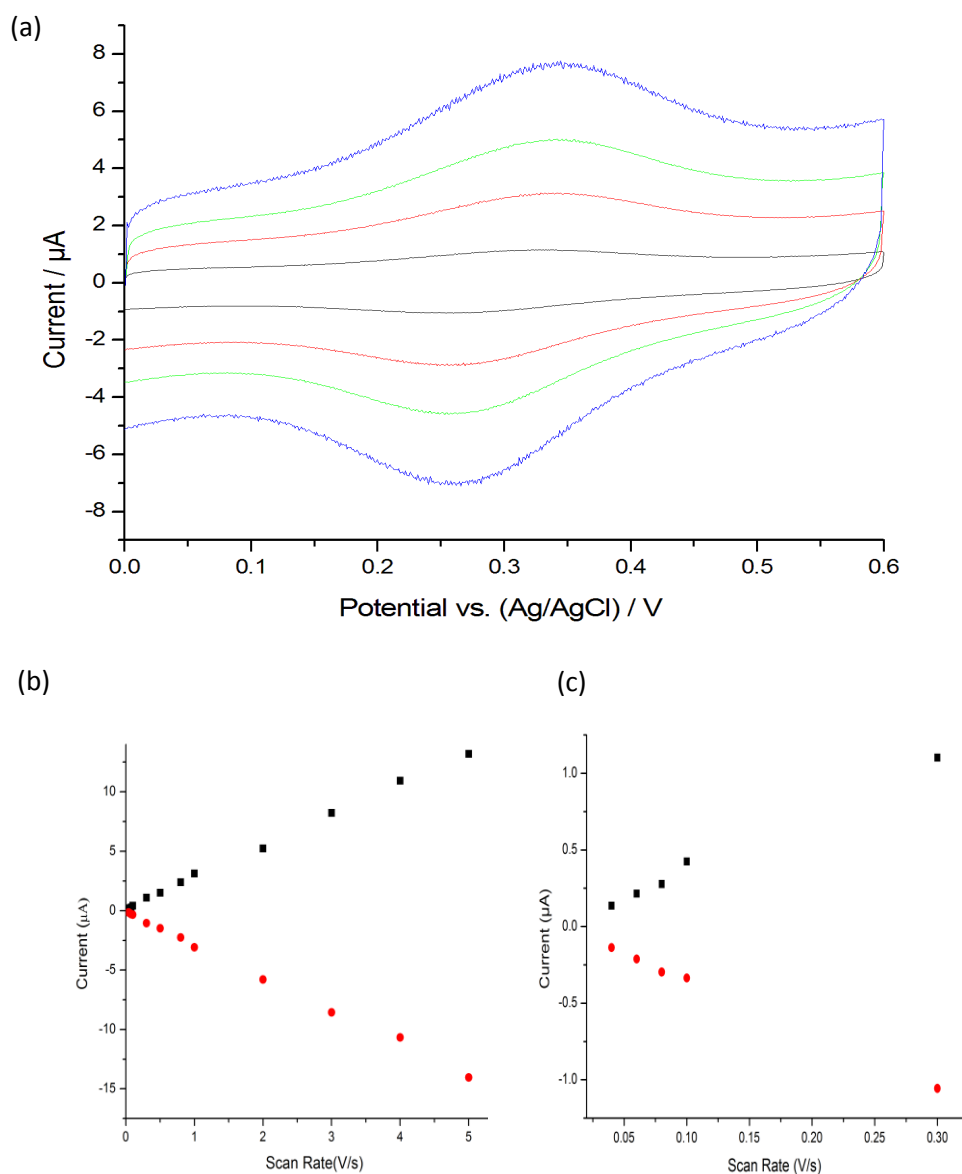


Fig. 2 (a) Cyclic voltammograms of a modified glassy carbon electrode in 0.05 M PBS (pH 7.4) at scan rates of 10 (black), 30 (red), 50 (green) and 80 (blue) mVs⁻¹. (b) Plot of anodic and cathodic peak current, extracted from cyclic voltammograms of a modified glassy carbon electrode, versus scan rate (Vs⁻¹). (c) Sub-section of Fig. 2 (b) of anodic and cathodic peak current versus scan rate plot.

The CVs of the surface bound complex at pH 7.4 in PBS shows non-ideal peak separation, greater than zero, particularly at higher scan rates, and a full-width at half-maximum of 160 mV, greater than the value for an ideal monolayer of a redox complex on an electrode surface [40]. This deviation may be attributed to a

combination of lateral interactions within the films [41]. The surfaces coverage (Γ_{Os}) of osmium can be calculated by integration of the charge passed under the oxidation peak (after baseline correction):

$$\Gamma_{Os} = Q/nFA \quad (1)$$

Where Q is the charge, F is the Faraday constant, n is number of electrons transferred, and A is area of the electrode.

The average Γ_{Os} value obtained from modified electrodes, prepared by cycling for one, three, or five cycles at 0.1 Vs^{-1} from 1.5 to 2 V, is $0.75 (\pm 0.2) \times 10^{-10}$ moles cm^{-2} . No trend in Γ_{Os} as a function of the number of CV cycles used in the preparation method is apparent. Electrochemical grafting under these conditions is thus independent of the number of cycles used. This is in agreement with a report that electrografting of primary alkyl amines to carbon surfaces through repetitive cycling or scanning to more positive potential ranges does not increase the surface coverage, as calculated from the N/C value using XPS [18]. Moreover, the final surface coverage of osmium complex does not scale with scan rate, in the range 0.06 Vs^{-1} to 0.5 Vs^{-1} when three CV cycles are used for electrochemically induced coupling of the complex to carbon electrodes, with an average Γ_{Os} of $0.84 (\pm 0.3) \times 10^{-10}$ moles cm^{-2} .

Integration of the charge for amine oxidation, for the lowest charge passed for one cycle at 0.5 Vs^{-1} gives an estimate of $2.0 \times 10^{-6} \text{ C}$ the equivalent of 2.1×10^{-11} moles of amine electrolysed in a one-electron oxidation, that results in formation of a layer on the electrode surface comprised of 6.7×10^{-12} moles of the osmium complex corresponding to surface coverage of 0.9×10^{-10} moles cm^{-2} . The primary amine radical cations formed after electro-oxidation are reportedly more unstable [17], thus more reactive, compared to secondary or tertiary amines, thus suggesting that passage of lower charge in the electro-oxidation may be necessary to probe for an effect on final surface coverage of the osmium complex.

From the average osmium complex surface coverage of $0.84 (\pm 0.3) \times 10^{-10}$ moles cm^{-2} an area per molecule of osmium complex of approximately 197 \AA^2 can be estimated, presuming complete monolayer coverage on a smooth surface. This is in reasonably good agreement with a projected area of 180 \AA^2 estimated from

crystallographic data, considering a radius of osmium polypyridyl complexes of 7.5 Å [42]. For comparison, an area per molecule of osmium polypyridyl complexes self-assembled as a monolayer on platinum electrode surfaces of approximately 240 Å² was reported, with a redox complex surface coverage of 1×10^{-10} moles cm⁻² [43]. Thus, the proposed electrochemical coupling procedure produces a relatively compact redox active layer, at close to monolayer coverage. Multilayer formation may be possible, but given the surface coverage is not likely, as reported on by others for surface grafting via electro-reduction of aryl diazonium salts [9, 38, 44]. The osmium surface coverages reported here are in good agreement with surface coverages reported for monolayers of osmium complexes self-assembled on platinum and gold [10, 37, 38, 43] and a surface coverage of 3.5×10^{-10} moles cm⁻² for attachment of a ferrocene complex to a bromophenyl-modified carbon electrode [45] and to a surface coverage of 2.1×10^{-10} moles cm⁻² for attachment of a copper complex to a gold surface using an aryldiazonium salt reduction method [46], while Boland *et al.* reported that attachment of the Osbpy4AMP osmium complex to a carboxylic acid-terminated carbon electrode using carbodiimide coupling yielded a surface coverage of 2.9×10^{-10} moles cm⁻² [10]. For comparison, Buriez *et al.* [28] reported the surface coverage of 2.7×10^{-10} moles cm⁻² for amino-ferrocifen complexes while Aramata *et al.* [29] reported a surface coverage of 1.7×10^{-10} moles cm⁻² for grafting of an arylamine osmium complex on carbon surfaces.

The short term stability of the osmium complex at the surface is tested by undertaking repetitive CV cycles (Figure 3a) at 0.1 Vs⁻¹ scan rate in 0.05 M PBS buffer, with no change in the osmium surface coverage over the 10 cycle testing period. Longer-term stability to storage conditions is estimated from cyclic voltammograms recorded in buffer with storage intervals in buffer solution under room temperature, Figure 3b. In this case, initially there is a loss in redox signal of immobilised complex of approximately 27% over a 4 hour period. This may be attributed to the loss of physisorbed molecules, as the decay profile does not follow a simple single-exponential fit, indicating that more than one process, or population of redox complex, may be responsible for the change in surface coverage as a function of storage time. Following this initial change, the surface coverage signal remains

steadily, losing only an average of 17% of the signal at 4 hours over the next 70 hours of storage.

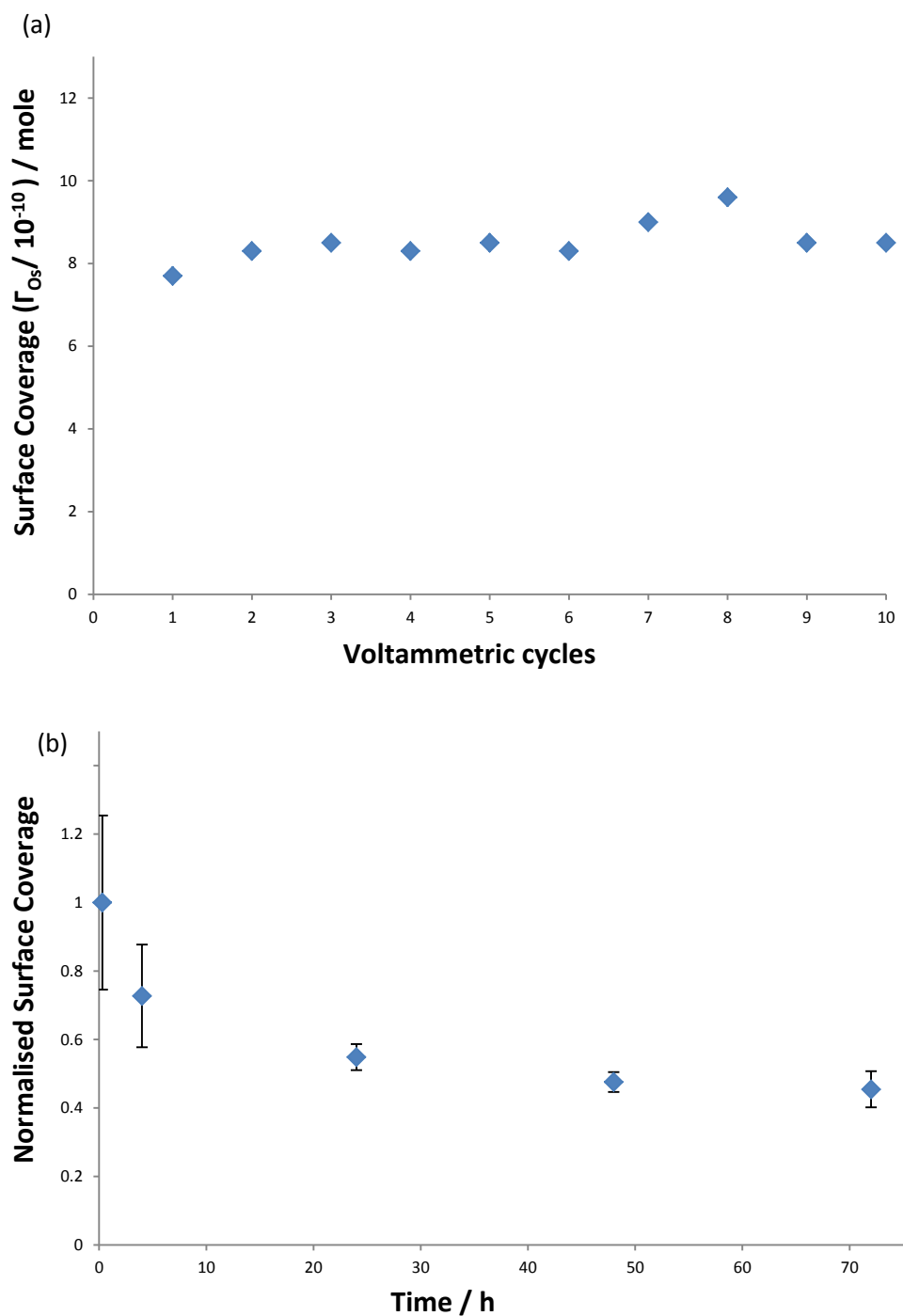


Fig. 3 Surface coverage of osmium complexes calculated from cyclic voltammetric peaks of modified glassy carbon electrodes at 0.1 Vs^{-1} scan rate in 0.05 M PBS buffer (pH 7.4) as a function of (a) continuous voltammetric cycling and (b) a single voltammetric cycle with storage of electrode in buffer (pH 7.4) at room temperature between scans ($n=3$).

The XPS results recorded after grafting of the osmium complex to glassy carbon plates confirms the presence of the complex on the surface. The survey scan of the modified glassy carbon surface, prepared by cycling for 3 cycles over a potential range from 1.5 to 2.0 V vs. Ag/AgCl in 1 mM Osbpy4AMP dissolved in ACN at 0.1 V s⁻¹ is shown in figure 4a. The spectrum exhibits the characteristic peaks for C 1s, N 1s and O 1s at 284.21, 400.5 and 532.21 eV, respectively. The presence of N, Os, and Cl XPS peaks for the modified surface is a clear indication that the Os complex is present on the carbon substrate. The peak F 1s at 685 eV corresponds to the fluoride (PF₆) present in the osmium complex salt. The Si 2p peak at 102 eV is assigned to adventitious substrate impurities, as reported on previously for XPS of carbon surfaces [47, 48]. The origin of the S 2p peak at 167 eV is not as yet identified, but may also likely have arisen by adventitious substrate contamination. The high resolution XPS scan of the N 1s region, Figure 4b, for the modified electrode surface shows a peak at 399.6 eV, has been attributed to the N in bipyridine [49, 50], while the component close to 400.5 eV is reported to correspond to an amine functional group. The higher energy peak around 402.0 eV may be due to protonation of the amine during the grafting process [17]. The atomic % ratio of N 1s / C 1s, after correction for instrumental sensitivity is 0.044, compared to a reported ratio for bare glassy carbon of 0.014 [6] once again providing evidence of the presence of the complex at the surface.

2.4.3 Bioelectrocatalysis for glucose oxidation

Osmium redox complexes are commonly used as mediators in research and development of glucose biosensors [12, 51] and glucose oxidising enzymatic biofuel cells [35, 52]. Clark *et al* developed the first enzyme based amperometric electrode in 1961 [42], and since then enzyme based electrode sensors have received great attention for application to glucose detection. As the redox active site of glucose oxidase is buried inside the insulating protein shell it is difficult to capture electron flow from the active site of enzyme as a result of glucose oxidation, to deliver them to the electrode, in so-called third generation biosensors devices [52]. The redox mediator is used, in second generation glucose biosensors, to shuttle electrons from the enzyme active site to the electrode surface. Redox mediator utilisation in

enzyme-based electrodes allows for increased sensitivity, selectivity, and detection of analyte at lower overpotentials in many applications ranging from industry, environmental, energy to clinical applications [12, 24, 52].

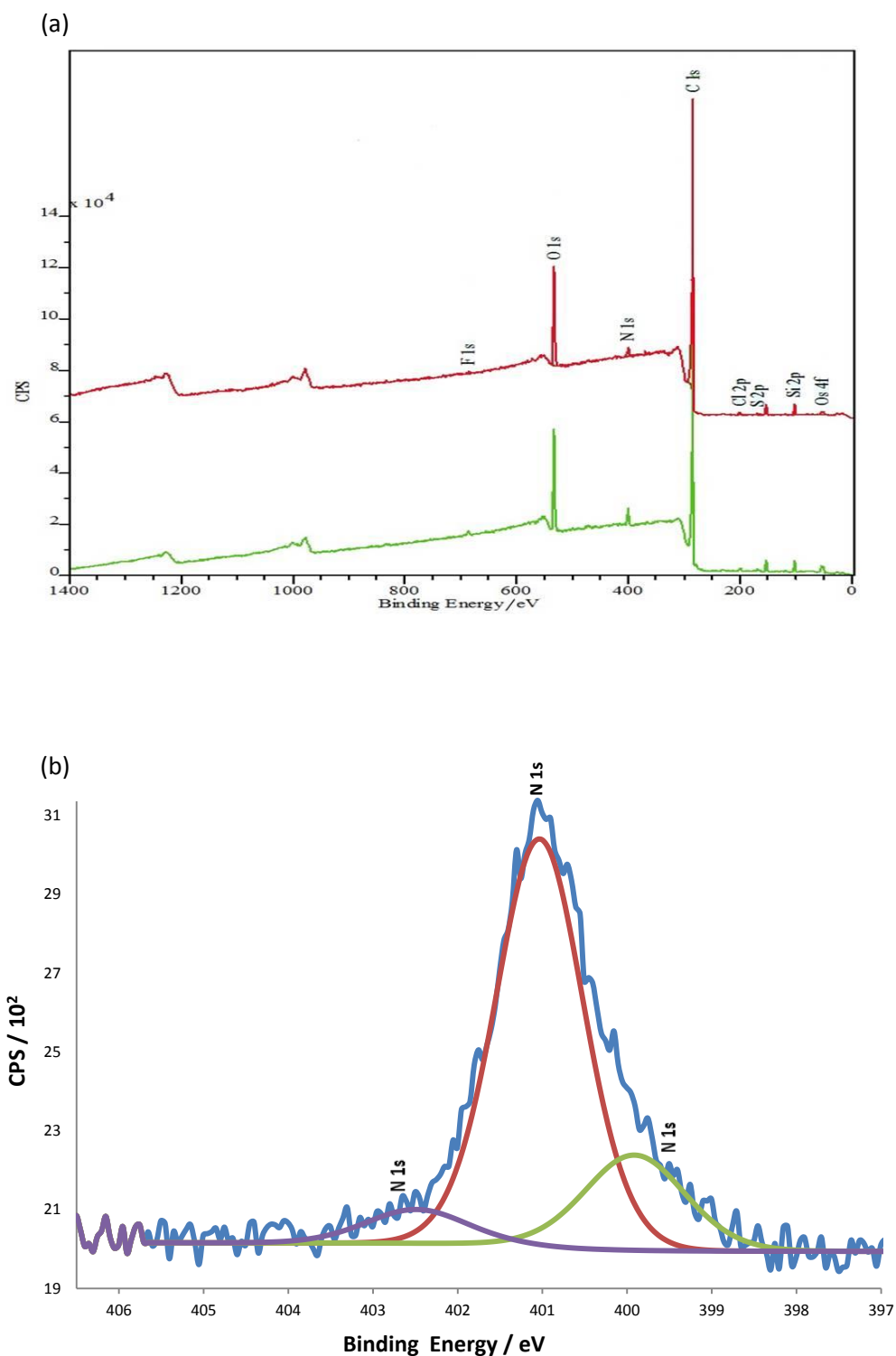


Fig. 4 XPS survey scans (a) at 30° (red) and 60° (green) and (b) N1s core fitting peak of a glassy carbon plate surface modified electrode by grafting of Osby4AMP.

The electrode surface modified by electrografting of an osmium complex was therefore examined in a preliminary test for its ability to mediate electron transfer from glucose oxidase, in solution, as a result of glucose oxidation. The response of the osmium complex modified electrode was evaluated using slow scan cyclic voltammetry in phosphate buffer solution (pH 7.4, 37 °C), figure 5. The modified electrode exhibited in absence substrate a CV signal with a pair of redox peaks centred at 0.3 V vs Ag/AgCl, indicating the presence of the osmium complex on the surface. Upon addition of glucose at saturation levels (0.1 M in the electrochemical cell), the cyclic voltammetric response altered with an increase in the oxidation current accompanied by a decrease in the reduction current, corresponding to a catalytic response [20, 40], demonstrating the possibility of using the electrografting methodology to prepare, and compare, a range of redox complex modified electrodes for screening for application to biosensor or biofuel cell device development.

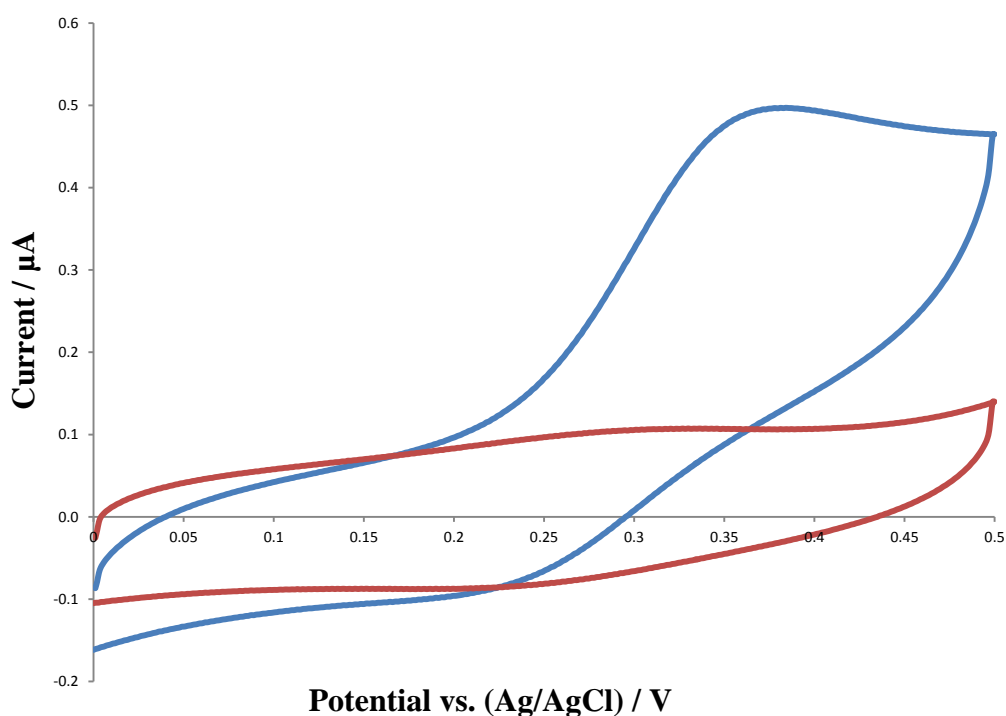


Fig. 5 CV recorded at modified, by electrografting Osbpy4AMP, glassy carbon electrode in 0.5 ml PBS buffer (0.05 M, pH 7.4, 37 °C) containing glucose oxidase (9 U) in the absence (red curve) and in the presence (blue curve) of 0.1 M glucose, at a scan rate of 5 mV s⁻¹.

2.5 Conclusion

Carbon electrode surfaces are modified via electrochemical coupling of an alkylamine functional group of an osmium-based redox complex in a simple procedure. Cyclic voltammetry and XPS data indicates the presence of the osmium complex at the surface. The modified electrode showed electrocatalytic activity for oxidation of glucose in presence of glucose oxidase. The same modification strategy may be extended to provide a simple route for immobilisation of a range of redox complexes that possess an alkylamine functional group distal to the central metal atom to explore the effect of structure and complex redox potential on the surface coverage of complex and electrocatalytic applications of the resulting redox layers. For example, the modified surfaces could have application in a wide range of biosensor and biofuel cell electrochemical devices, as well as exploring the use of redox layers for light-harvesting or water-splitting applications.

2.6 Acknowledgements

We acknowledge funding from the Earth and Natural Science Doctoral Studies Programme, of the Higher Education Authority (HEA) through the Programme for Research at Third-Level Institutions, Cycle 5 (PRTL-5), co-funded by the European Regional Development Fund (ERDF). We are grateful to Dr. Fathima Laffir of MSSSI, University of Limerick for recording XPS spectra.

2.7 References

- [1] A.J. Downard, *Electroanalysis*, 12 (2000) 1085-1096.
- [2] X. Li, Y. Wan, C. Sun, *Journal of Electroanalytical Chemistry*, 569 (2004) 79-87.
- [3] K.H. Vase, A.H. Holm, S.U. Pedersen, K. Daasbjerg, *Langmuir*, 21 (2005) 8085-8089.
- [4] B.D. Bath, H.B. Martin, R.M. Wightman, M.R. Anderson, *Langmuir*, 17 (2001) 7032-7039.
- [5] S. Ababou-Girard, H. Sabbah, B. Fabre, K. Zellama, F. Solal, C. Godet, *The Journal of Physical Chemistry C*, 111 (2007) 3099-3108.
- [6] M.A. Ghanem, J.-M. Chretien, A. Pinczewska, J.D. Kilburn, P.N. Bartlett, *Journal of Materials Chemistry*, 18 (2008) 4917-4927.
- [7] R.J. Forster, E. Figgemeier, P. Loughman, A. Lees, J. Hjelm, J.G. Vos, *Langmuir*, 16 (2000) 7871-7875.
- [8] J.F. Smalley, H.O. Finklea, C.E.D. Chidsey, M.R. Linford, S.E. Creager, J.P. Ferraris, K. Chalfant, T. Zawodzinsk, S.W. Feldberg, M.D. Newton, *Journal of the American Chemical Society*, 125 (2003) 2004-2013.
- [9] D.J. Garrett, P. Jenkins, M.I.J. Polson, D. Leech, K.H.R. Baronian, A.J. Downard, *Electrochimica Acta*, 56 (2011) 8-8.
- [10] S. Boland, F. Barriere, D. Leech, *Langmuir*, 24 (2008) 6351-6358.
- [11] S. Baranton, D. Bélanger, *The Journal of Physical Chemistry B*, 109 (2005) 24401-24410.
- [12] M.H. Schoenfisch, J.E. Pemberton, *Journal of the American Chemical Society*, 120 (1998) 4502-4513.
- [13] C.D. Bain, E.B. Troughton, Y.T. Tao, J. Evall, G.M. Whitesides, R.G. Nuzzo, *Journal of the American Chemical Society*, 111 (1989) 321-335.
- [14] C.D. Bain, J. Evall, G.M. Whitesides, *Journal of the American Chemical Society*, 111 (1989) 7155-7164.
- [15] J. Pinson, F. Podvorica, *Chemical Society Reviews*, 34 (2005) 429-439.
- [16] D. Belanger, J. Pinson, *Chemical Society Reviews*, 40 (2011) 3995-4048.
- [17] A. Adenier, M.M. Chehimi, I. Gallardo, J. Pinson, N. Vilà, *Langmuir*, 20 (2004) 8243-8253.
- [18] R.S. Deinhammer, M. Ho, J.W. Anderegg, M.D. Porter, *Langmuir*, 10 (1994) 1306-1313.
- [19] C. Combellas, F. Kanoufi, J. Pinson, F.I. Podvorica, *Journal of the American Chemical Society*, 130 (2008) 8576-8577.
- [20] D. Leech, P. Kavanagh, W. Schuhmann, *Electrochimica Acta*, 84 (2012) 223-234.

- [21] P. Ó Conghaile, D. MacAodha, B. Egan, P. Kavanagh, D. Leech, *Journal of The Electrochemical Society*, 160 (2013) G3165-G3170.
- [22] A.B.P. Lever, *Inorganic Chemistry*, 29 (1990) 1271-1285.
- [23] R.J. Forster, J.G. Vos, *Macromolecules*, 23 (1990) 4372-4377.
- [24] K. Habermüller, A. Ramanavicius, V. Laurinavicius, W. Schuhmann, *Electroanalysis*, 12 (2000) 1383-1389.
- [25] P. Kavanagh, S. Boland, P. Jenkins, D. Leech, *Fuel Cells*, 9 (2009) 79-84.
- [26] S. Timur, U. Anik, D. Odaci, L. Gorton, *Electrochemistry Communications*, 9 (2007) 1810-1815.
- [27] I. Vostiar, E.E. Ferapontova, L. Gorton, *Electrochemistry Communications*, 6 (2004) 621-626.
- [28] O. Buriez, E. Labbé, P. Pigeon, G. Jaouen, C. Amatore, *Journal of Electroanalytical Chemistry*, 619–620 (2008) 169-175.
- [29] A. Aramata, S. Takahashi, G. Yin, Y. Gao, Y. Inose, H. Mihara, A. Tadjeddine, W.Q. Zheng, O. Pluchery, A. Bittner, A. Yamagishi, *Thin Solid Films*, 424 (2003) 239-246.
- [30] S. Tsujimura, A. Katayama, K. Kano, *Chemistry Letters*, 35 (2006) 1244-1245.
- [31] S.S.C. Yu, A.J. Downard, *Langmuir*, 23 (2007) 4662-4668.
- [32] P.A. Brooksby, A.J. Downard, *Langmuir*, 20 (2004) 5038-5045.
- [33] E.M. Kober, J.V. Caspar, B.P. Sullivan, T.J. Meyer, *Inorganic Chemistry*, 27 (1988) 4587-4598.
- [34] C. Danilowicz, E. Cortón, F. Battaglini, *Journal of Electroanalytical Chemistry*, 445 (1998) 89-94.
- [35] S. Boland, P. Kavanagh, D. Leech, *ECS Transactions*, 13 (2008) 77-87.
- [36] J.K. Kariuki, M.T. McDermott, *Langmuir*, 15 (1999) 6534-6540.
- [37] M. Delamar, R. Hitmi, J. Pinson, J.M. Saveant, *Journal of the American Chemical Society*, 114 (1992) 5883-5884.
- [38] S. Boland, K. Foster, D. Leech, *Electrochimica Acta*, 54 (2009) 1986-1991.
- [39] P. Ó Conghaile, S. Kamireddy, D. MacAodha, P. Kavanagh, D. Leech, *Anal Bioanal Chem*, 405 (2013) 3807-3812.
- [40] Allen J. Bard, L.R. Faulkner, *Electrochemical Methods: Fundamentals and Applications*, 2 ed., JOHN WILEY & SON, INC., 2001.
- [41] E. Laviron, *Journal of Electroanalytical Chemistry and Interfacial Electrochemistry*, 100 (1979) 263-270.

- [42] H. Goodwin, D. Kepert, J. Patrick, B. keltn, A. White, *Australian Journal of Chemistry*, 37 (1984) 1817-1824.
- [43] R.J. Forster, L.R. Faulkner, *Journal of the American Chemical Society*, 116 (1994) 5444-5452.
- [44] J.K. Kariuki, M.T. McDermott, *Langmuir*, 17 (2001) 5947-5951.
- [45] O. Ghodbane, G. Chamoulaud, D. Bélanger, *Electrochemistry Communications*, 6 (2004) 254-258.
- [46] G. Liu, T. Böcking, J.J. Gooding, *Journal of Electroanalytical Chemistry*, 600 (2007) 335-344.
- [47] R.C. Engstrom, V.A. Strasser, *Analytical Chemistry*, 56 (1984) 136-141.
- [48] S.E. Creager, B. Liu, H. Mei, D. DesMarteau, *Langmuir*, 22 (2006) 10747-10753.
- [49] B.J. Lindberg, J. Hedman, *Chem. Scr.*, 7 (1975) 155.
- [50] C. Ferragina, M. Massucci, G. Mattogno, *J Incl Phenom Macrocycl Chem*, 7 (1989) 529-536.
- [51] W. Schuhmann, T.J. Ohara, H.L. Schmidt, A. Heller, *Journal of the American Chemical Society*, 113 (1991) 1394-1397.
- [52] P. Kavanagh, D. Leech, *Physical Chemistry Chemical Physics*, 15 (2013) 4859-4869.

Chapter 3:

Published as:

Coupling of Amine-Containing Osmium Complexes and Glucose Oxidase with Carboxylic Acid Polymer and Carbon Nanotube Matrix to Provide Enzyme Electrodes for Glucose Oxidation

Rakesh Kumar and Dónal Leech. Journal of the Electrochemical Society, Vol. 161, pp. H3005-H3010, 2014

DOI: 10.1149/2.0021413jes

Co-author contributions:

I synthesised the osmium redox complexes, and performed the laboratory work, the analysis and wrote the first draft of the publication.

Dónal Leech, as the project supervisor, contributed through guidance and advice throughout and wrote the final draft of the publication.

Coupling of Amine-Containing Osmium Complexes and Glucose Oxidase with Carboxylic Acid Polymer and Carbon Nanotube Matrix to Provide Enzyme Electrodes for Glucose Oxidation

3.1 ABSTRACT

The immobilisation methodology of enzyme and redox complex on electrode surfaces can have an impact on the magnitude and stability of amperometric current response, with implications for application as biosensor and fuel cell enzyme electrodes. Here we report on an investigation of carboxymethyl dextran (CMD) and polyacrylic acid polymers, bearing carboxylic functional groups, as chemical supports for immobilisation of amine-containing osmium redox complexes and enzymes at electrode surfaces. Cross-coupling using carbodiimide reagent of the CMD polymer support, [Os (2,2'-bipyridine)₂(4-aminomethyl pyridine)Cl].PF₆ redox complex, glucose oxidase (GOx) and multiwall carbon nanotubes (MWCNT), provides a 3-dimensional matrix for catalytic electro-oxidation of glucose yielding current density of $1.0 \pm 0.2 \text{ mA cm}^{-2}$ and $4.5 \pm 1.0 \text{ mA cm}^{-2}$ at 0.45 V vs. Ag/AgCl, in 50 mM phosphate buffer saline (pH 7.4, 37°C) containing 5 mM and saturated glucose amounts, respectively. Similar enzyme electrodes, but instead using [Os (4,4'-dimethoxy-2,2'-bipyridine)₂(4-aminomethyl pyridine)Cl].PF₆ of lower redox potential, produce current densities of $0.83 \pm 0.21 \text{ mA cm}^{-2}$ in 5 mM glucose and $3.4 \pm 0.7 \text{ mA cm}^{-2}$ in saturated glucose solution at 0.2 V vs. Ag/AgCl thus showing promise for application as low potential glucose oxidising biosensors and as anodes for *in-vivo* enzymatic fuel cells for power generation.

3.2 Introduction

Enzyme electrodes for glucose oxidation are of increasing interest due to their potential applications as biosensors and as anodes in membrane-less fuel cells operating on sugar as a fuel. Such enzymatic fuel cells (EFC) can use enzymes as specific catalysts to oxidise glucose at the anode and reduce oxygen at the cathode, that when combined as a fuel cell convert chemical energy into electrical power [1-3]. The advantages to the use of enzyme-based catalysts are substrate specificity, which can eliminate the need for casings and ion exchange membranes in assembled fuel cells, and of being capable of operating under moderate ambient conditions, compared to metal catalysts [1, 2].

A substantial body of research exists on approaches for maximising catalytic current capture as a result of enzyme redox reactions in enzyme electrodes through the co-immobilisation of enzymes and electron-shuttling mediators within redox-conducting hydrogels on solid electrodes. For example, over the past two decades, Heller and co-workers [3] have pioneered use of epoxy cross-linking of electrostatic adducts of redox enzyme and osmium redox polymers, using poly-vinylimidazole (PVI) as the polymer backbone, at electrode surfaces to provide “wired” enzyme electrodes capable of producing glucose oxidation current. Mediated electron transfer by electron-hopping self-exchange within these hydrogels allows connection between redox active sites of enzymes and electrode surfaces thus generating bio-electrocatalytic current [4-6]. As mediators, osmium based polypyridyl complexes are broadly explored [6-8], as these complexes possess advantages over iron and ruthenium based systems due to the low redox potential of the Os(II/III) redox transition and the relative stability of complexes in both oxidation states [1, 9].

Recent approaches to glucose enzyme electrode preparation have focused on improving the current signal and stability by co-immobilisation and crosslinking of a range mediator within polymer matrices at electrode surfaces [12-14]. Addition of multi-walled carbon nanotubes (MWCNT) to the enzyme electrode preparation step results in improved operational output and stability under pseudo-physiological conditions [10-12]. These nanostructures provide a support which acts as a scaffold for improved retention of enzymes and redox complexes.[10, 13, 14] A difficulty with use of PVI as the polymer backbone for preparation of redox polymers is the

lack of commercial availability of PVI, and laboratory-scale synthesis of PVI by bulk free radical polymerisation [15] results in wide molecular weight distribution which affects the physical properties of polymers such as solubility, density etc. In addition, osmium complex loading on the PVI backbone by ligand substitution is also difficult to control and replicate, leading to batch-to-batch variation in enzyme electrode performance using these redox polymers [2, 16, 17]. We, and others, have sought to use commercially available and well characterised polymer supports for preparation of enzyme electrodes. Danilowicz *et al.*[7] reported on coupling of osmium complexes that contain an aldehyde functional group distal to the metal co-ordinating site to amine-based polymers and enzymes in films on electrode to provide enzyme electrodes. We have reported [18] on coupling of osmium complexes that contain an amine functional group distal to the metal co-ordinating site, and glucose oxidase (GOx), to carboxymethyl dextran (CMD) polymers previously anchored to amine-functionalised electrode surfaces. More recently, Ó Conghaile *et al.*[19] reported on immobilisation of amine-functionalised osmium complexes and enzymes to a polyallylamine support using a di-epoxide reagent.

Here, we report on the preparation and comparison of enzyme electrodes based on coupling of GOx and amine-functionalised osmium complexes to carboxymethyl dextran (CMD) or polyacrylic acid polymer supports. Acid treated MWCNTs are added to the drop-coating solutions to attempt to provide increased surface area and higher current response [15-17]. Furthermore, variation in osmium complex redox potential is investigated by synthesis of complexes with more electron donating ligands [19, 20] and the response of enzyme electrodes prepared using such osmium complexes immobilised with GOx, MWCNT and CMD as a support evaluated.

3.3 Experimental

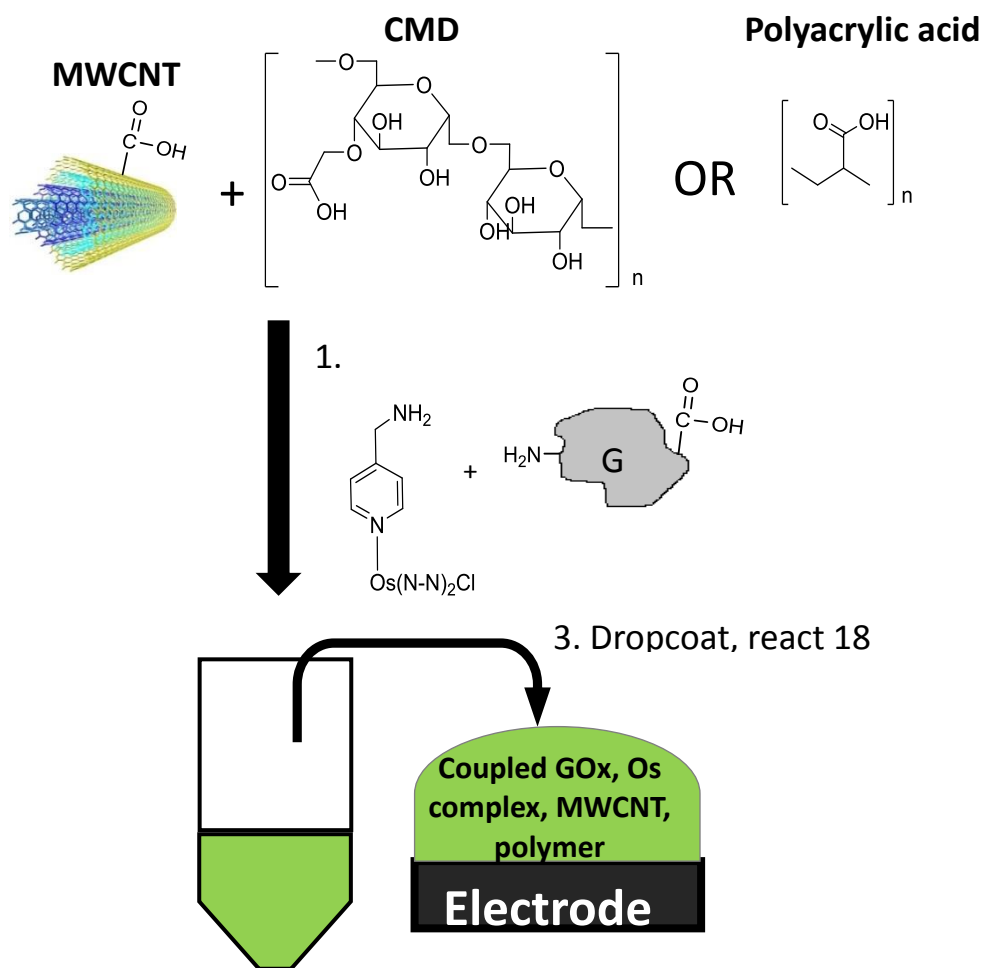
Materials. - All chemicals were purchased from Sigma-Aldrich (Dublin, Ireland) and used as received unless otherwise stated. All solutions were prepared from Milli-Q (18.2 MΩ cm) water. The complexes, [Os(N-N)₂(4-aminomethylpyridine)Cl].PF₆ and [Os(N-N)₂(4-aminoethylpyridine)Cl].PF₆, where N-N is either 2,2'-bipyridine or 4,4'-dimethoxy-2,2'-bipyridine, were synthesised by ligand substitution of one Cl ligand of [Os(N-N)₂Cl₂] with 4-aminomethylpyridine or 4-aminoethylpyridine by

heating of the complex in an ethylene glycol solution containing 1.1 mole equivalents of ligand at reflux, with ligand substitution monitored by cyclic voltammetry and differential pulse voltammetry, as reported on previously [9, 20]. The $[\text{Os}(\text{N-N})_2\text{Cl}_2]$ complexes were prepared from $(\text{NH}_4)_2\text{OsCl}_6$ according to literature methods.[20, 21] Glucose oxidase (EC 1.1.3.4., average activity 240 unit mg^{-1}), CMD (average molecular mass of 15,000 Da) and polyacrylic acid (average molecular mass of 450,000 Da) were purchased from Sigma-Aldrich. The MWCNTs (Sigma) were acid-treated by heating 20 mg mL^{-1} in HNO_3 at reflux for 6 hours at $\sim 150^\circ\text{C}$ [17].

Methods. - CH Instruments 600 series or 1030 multichannel potentiostat (IJ Cambria) coupled to a thermostated electrochemical cell was used to perform all electrochemical measurements. Custom built Ag/AgCl reference electrodes (3 M KCl) and platinum foil counter electrodes (Goodfellow) were used in the cell. Graphite disc electrodes (3 mm diameter) were prepared by shrouding graphite rods (Graphite store, part # NC001295) in heat-shrinkable tubing and polishing the exposed disk on 1200 grit silicon carbide paper (Buehler) followed by thorough rinsing with Milli-Q water. Working electrodes were sonicated in Milli-Q water for 10 min and dried under nitrogen gas prior to use. All electrochemical measurements were performed in phosphate buffer saline (PBS, 0.05 M phosphate, pH 7.4, 0.15 M NaCl) at 37°C . GOx activity was determined using the o-dianisidine and horseradish peroxidase-coupled spectrophotometric assay. The reaction was monitored on an Agilent 6453 UV/Vis spectrophotometer at 460 nm [22].

The enzyme electrode preparation protocol is illustrated in Scheme 1. Prior to enzyme electrode preparation, carboxylic acid functional groups of the polymer and the acid treated MWCNT were activated for coupling to amine functional groups by incubation of 5 μL of polymer (5 mg ml^{-1}) and 5 μL aqueous suspension (0.23 mg) of acid treated MWCNT with 4 μL of an aqueous solution of 40 mM *N*-[3-dimethylaminopropyl]-*N'*-ethylcarbodiimide (EDC) and 10 mM *N*-hydroxysuccinimide (NHS) in an eppendorf for 12 minutes. This was followed by addition of GOx (5 μL of 10 mg ml^{-1}) and redox complex (5 μL of 4.5 mM aqueous solution) to the eppendorf. Enzyme electrodes were prepared by drop coating 20 μL of the resulting solution onto the graphite disk, with the dropcoat dried for 18 hours

at room temperature to allow crosslinking, followed by rinsing of the enzyme electrode in PBS for ~ 5 seconds before testing commenced.

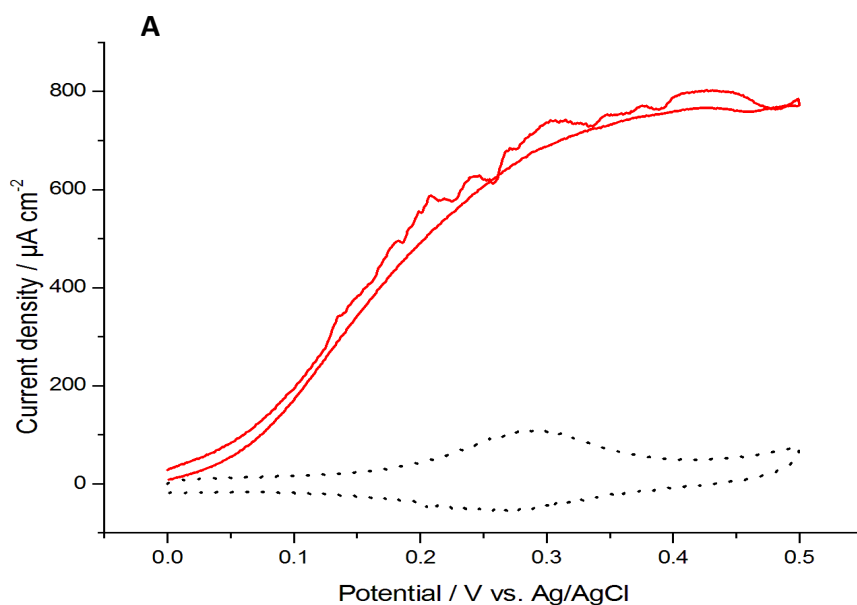


Scheme 1. Scheme depicting the enzyme electrode preparation method where *N-N* is bpy or dmbpy (see experimental section for more details).

3.4 Results and Discussion

Cyclic voltammetry (CV) is used to characterise the redox complexes within polymer supported and cross-linked films on graphite electrodes. For example, the redox complex $[\text{Os}(2,2'\text{-bipyridine})_2(4\text{-aminomethylpyridine})\text{Cl}]\cdot\text{PF}_6$ ($\text{Os}(\text{bpy})_2\text{4AMP}$) co-immobilised with GOx, MWCNT and CMD or polyacrylic acid as a polymer support on an electrode surface exhibits oxidation and reduction peaks corresponding to the osmium(II/III) transition at 0.30 V (versus Ag/AgCl), which is

similar to the redox potential observed for Os(bpy)₂4AMP in phosphate buffer [2, 23]. This redox potential is also close to that reported on for the complex immobilised by coupling either directly to a carbon electrode using electrochemical oxidation of the alkylamine functional group [24], or by reaction of the alkylamine with carboxylic acid groups introduced to carbon [25] or boron-doped diamond [26] electrodes, and for the complex immobilised within CMD films coupled to a carbon electrode [18]. The similarity of redox potential between solution-phase and immobilised complex indicates that the Os(II/III) redox transition is generally not affected by the immobilisation procedure.



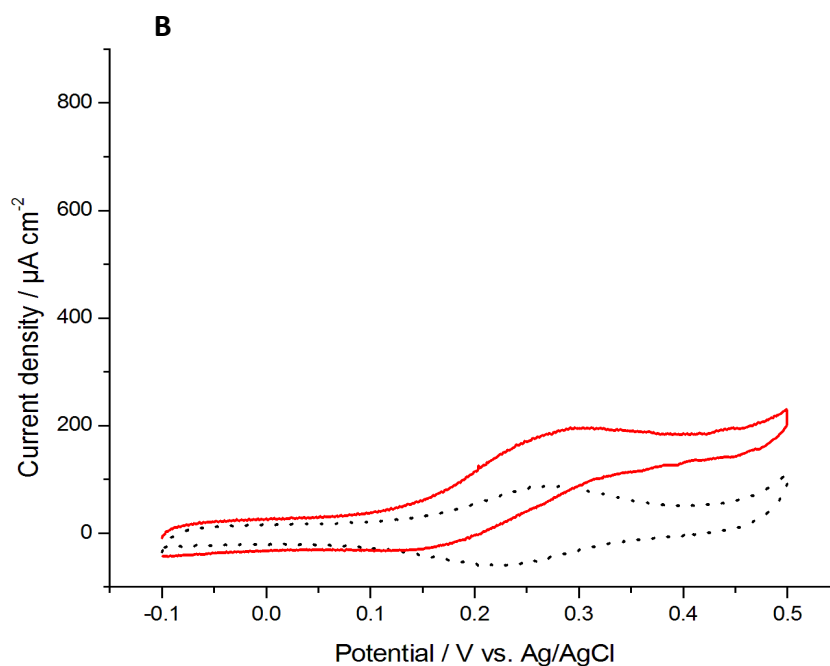


Figure 1. CVs recorded at 1 mV s^{-1} in the presence (red, solid) and absence (black, dashed) of 5 mM glucose in PBS (pH 7.4, 37°C) for enzyme electrodes prepared from $\text{Os}(\text{bpy})_24\text{AMP}$, MWCNT, GOx and either (A) CMD or (B) polyacrylic acid.

All enzyme electrodes display CV response in PBS, in the absence of glucose substrate, where the $\text{Os}(\text{II}/\text{III})$ peak currents vary linearly with scan rate, at slow scan rates ($<20 \text{ mVs}^{-1}$), indicative of a surface-controlled response [27]. At higher scan rates the peak currents scale linearly with the square root of scan rate, indicative of semi-infinite diffusion control of the response [8, 28, 29]. An estimation of redox complex surface coverage (Γ_{Os}) on the electrode can be obtained by integration of the charge passed during electrolysis of the complexes within films on the electrode using slow scan rate voltammetry in PBS solution [29]. For example, enzyme electrodes prepared using CMD, MWCNT and GOx result in redox complex surface coverage of $90 \pm 14 \text{ nmoles cm}^{-2}$, comparable to the value obtained previously for enzyme electrodes prepared by co-immobilisation of osmium redox polymers and enzymes [17, 30], and approximately one thousand-fold that expected for monolayer coverage of osmium pyridyl complexes [31] on electrode surfaces. Upon addition of glucose, sigmoidal-shaped cyclic voltammograms, characteristic of catalytic oxidation of glucose by the enzyme, with electron transfer mediated by the redox

complex from the enzyme active site to the electrode are obtained for all enzyme electrodes [29], as shown for example in Figure 1 for the enzyme electrode prepared using Os(bpy)₂4AMP, MWCNT, GOx and either CMD or polyacrylic acid as support.

Enzyme electrodes are prepared using Os(bpy)₂4AMP, GOx and either CMD or polyacrylic acid as polymer support in order to compare electrode performance as a function of polymer selection, and MWCNT addition. Performance of enzyme electrodes is compared using either CV or constant potential amperometry at an applied potential of 0.45 V vs Ag/AgCl, selected to be 150 mV positive of the Os(II/III) oxidation to ensure mediated glucose oxidation. The amperometric responses show glucose oxidation currents that are similar to the catalytic current observed in slow scan CVs, with slight increases in current density for amperometry over CV due to use of convection (150 rpm) of solutions in amperometry to avoid substrate depletion over the course of the experimental timescale. For example, the 1 mV s⁻¹ CV current density of $0.72 \pm 0.09 \text{ mA cm}^{-2}$, extracted at 0.45 V, for oxidation of 5 mM glucose at enzyme electrodes prepared from Os(bpy)₂4AMP co-immobilised with GOx, MWCNT and CMD as a polymer support compares well with the amperometric $1.0 \pm 0.2 \text{ mA cm}^{-2}$ current density obtained at 0.45 V applied potential, Figure 1A and Figure 2. In the initial comparison of the effect of polymer support on enzyme electrode response, increased glucose oxidation current density is obtained from CVs in 5 mM glucose in PBS for enzyme electrodes prepared using CMD as support, $0.72 \pm 0.09 \text{ mA cm}^{-2}$, over that obtained using polyacrylic acid as support, $0.23 \pm 0.04 \text{ mA cm}^{-2}$.

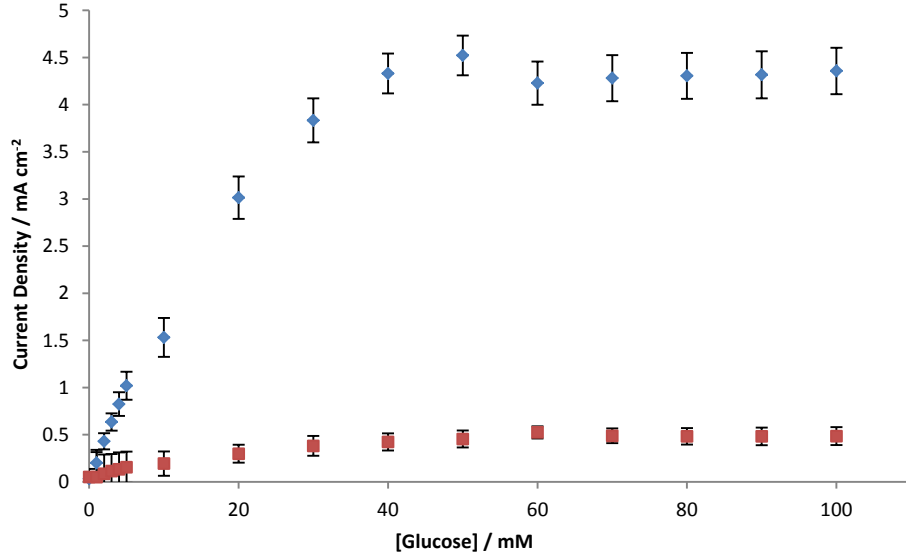


Figure 2. Current density in the presence of increasing concentrations of glucose recorded at an applied potential of 0.45 V, for films prepared using Os(bpy)₂4AMP co-immobilised with GOx, MWCNT and either CMD (◆) or polyacrylic acid(■) polymer support in pH 7.4 PBS at 37°C, solution stirred at 150 rpm. Error bars represent standard deviation (n=3).

A comparison of glucose oxidation current density, extracted from amperometric measurements at 0.45 V vs. Ag/AgCl, as function of glucose concentration for CMD-based and polyacrylic acid-based enzyme electrodes is shown in Figure 2. Substrate saturation is observed, in all cases, for concentrations of greater than 50 mM glucose. The characteristic apparent Michaelis-Menten constant, K_M^{app} , and the maximum current, I_{max} , can be estimated from non-linear least-squares curve fitting of these plots to the Michaelis-Menten equation (1) [32],

$$I = \frac{I_{max}[Glucose]}{K_M^{app} + [Glucose]} \quad (1)$$

Where, I is the current observed at a given [Glucose].

The average K_M^{app} , Table 1, for all enzyme electrodes is 9.3 ± 1.7 mM which compares well with the reported K_M value of 10 ± 5 mM for other GOx-based enzyme electrodes [19, 33]. The CMD and polyacrylic acid-based enzyme electrodes display maximum current densities, j_{max} , of 4.5 ± 0.9 mA cm⁻² and 0.34 ± 0.1 mA cm⁻², respectively, Table 1, confirming the improved performance of enzyme

electrodes using CMD over those prepared with polyacrylic acid. The inclusion of MWCNTs was undertaken based on results from previous studies using polyvinylimidazole-based osmium redox polymers that demonstrated an increase in glucose oxidation current density upon MWCNT addition to enzyme electrodes [17, 34]. The current densities of all enzyme electrodes increase after inclusion of MWCNT in the preparation steps, Table 1, even when no polymer support matrix is included. Enzyme electrodes without CMD, but with added MWCNT produce a j_{\max} of $0.85 \pm 0.08 \text{ mA cm}^{-2}$ at 0.45 V vs. Ag/AgCl, higher than the current density for enzyme electrodes with CMD only as support (no MWCNT), and for any of the polyacrylic acid-based enzyme electrodes, with or without MWCNT. The main contributing factor for higher current at enzyme electrodes based on MWCNT and CMD is the higher retained enzymatic activity, as presented in the data in Table 1. For example, enzyme electrodes based on GOx co-immobilised with CMD with 12 U of enzyme activity deposited in the electrode preparation step show 9.0 ± 0.1 U retained activity, using the peroxidase-coupled activity assay, compared to 2 ± 1 units for GOx co-immobilised with polyacrylic acid, perhaps because of lower reactivity of the polyacrylic acid carboxylate to EDC/NHS activation [35] or decreased access of the GOx for immobilisation to the activated carboxylate within the polyacrylic acid film. This results in the ten-fold increase in glucose oxidation current density for the CMD-based enzyme electrodes over the polyacrylic acid-based electrodes.

Comparison of this performance with other glucose-oxidising enzyme electrodes is rendered difficult due to different methodologies used for film preparation, and different test conditions. As examples, Danilowicz *et al.* [7] report glucose oxidation current density of $60 \mu\text{A cm}^{-2}$ extracted from 5 mV s^{-1} CV for enzyme electrodes using an osmium complex attached to a poly(allylamine) support, co-immobilised with GOx in the presence of 50 mM glucose compared to a current density of $4.3 \pm 0.9 \text{ mA cm}^{-2}$ from amperometry in 50 mM glucose for the CMD-based enzyme electrodes co-immobilised with Os(bpy)₂4AMP, MWCNT and GOx here. The response of these electrodes of $4.5 \pm 1.0 \text{ mA cm}^{-2}$ in 100 mM glucose and $1.0 \pm 0.2 \text{ mA cm}^{-2}$ in 5 mM glucose also compares well with reported glucose oxidation current density of 0.29 mA cm^{-2} in 100 mM glucose or 0.12 mA cm^{-2} in 5 mM glucose for enzyme electrodes of Os(bpy)₂4AMP co-immobilised by crosslinking

with GOx and a poly(allylamine) support [19]. From the results obtained, co-immobilisation of redox complex and GOx with the CMD polymer and MWCNT is selected for subsequent studies on the basis of higher glucose oxidation current density compared to other polymer supported enzyme electrodes.

Table 1 Enzyme electrode performance for electrodes prepared using redox complex, GOx and CMD or polyacrylic acid as a polymer support, in the presence or absence of MWCNT.

Film Component with GOx	$j_{max, app}$ (mA cm ⁻²)	K_M^{app} (mM)	Surface Coverage (Γ_{Os} nmole cm ⁻²)	Enzymatic Activity (U) ^a
CMD, Os(bpy)₂4AMP	0.53 ± 0.03	10 ± 1	47 ± 8	2.0 ± 1.0
CMD, Os(bpy)₂4AMP and MWCNT	4.5 ± 0.9	11 ± 1	90 ± 14	9.0 ± 0.1
Polyacrylic acid, Os(bpy)₂4AMP	0.11 ± 0.02	7 ± 1	63 ± 2	1.0 ± 0.1
Polyacrylic acid, Os(bpy)₂4AMP and MWCNT	0.34 ± 0.10	9 ± 1	60 ± 1	2.0 ± 1.0
MWCNT, Os(bpy)₂4AMP	0.85 ± 0.08		38 ± 17	
CMD, Os(dmoby)₂4AMP and MWCNT	3.4 ± 0.5	14 ± 2	67 ± 6	5.2 ± 2.1

^a Maximum enzyme activity, if all added enzyme activity is retained, is 12 U.

The enzyme electrodes prepared using the Os(bpy)₂4AMP redox complex require relatively high potentials to oxidise glucose and therefore may not be the most suitable electrodes for application to glucose biosensors or enzymatic biofuel cell anodes [1]. Synthesis of osmium redox complexes having lower redox potential can be achieved by alteration in the co-ordinating ligands of the complex [19, 33]. For example, replacement of the 4,4'-H on both bipyridines, by a more electron-donating methoxy-functional group can shift the redox potential of the osmium oxidation by ~ -0.25 V [10, 21, 36]. Thus synthesis of [Os(4,4'-dimethoxy-2,2'-bipyridine)₂(4-aminoethylpyridine)Cl].PF₆ (Os(dmoby)₂4AEP) and [Os(4,4'-dimethoxy-2,2'-bipyridine)₂(4-aminomethylpyridine)Cl].PF₆ (Os(dmoby)₂4AMP) redox complexes is targeted to provide enzyme electrodes for mediated oxidation of glucose at lower potentials. For enzyme electrodes prepared by co-immobilisation of these redox complexes with GOx, MWCNT and CMD polymer as support on electrode surfaces, oxidation and reduction peaks for the Os(II/III) transition at 0.05 V (vs. Ag/AgCl)

are obtained, Figure 3A, similar to the redox potential previously observed for an Os(dmobpy)₂4AMP complex in solution [19, 37]. As before, slow scan CVs (< 20 mV s⁻¹) in the absence of glucose display peak currents that vary linearly with scan rate, permitting estimation of Γ_{Os} of 67 ± 6 nmoles cm⁻² and 57 ± 18 nmoles cm⁻² for the enzyme electrodes containing GOx, MWCNT, CMD and Os(dmobpy)₂4AMP or Os(dmobpy)₂4AEP complexes, respectively. These values are comparable to those seen for the Os(bpy)₂4AMP complex, and for those reported previously for osmium redox polymers and enzyme based electrodes [17, 30].

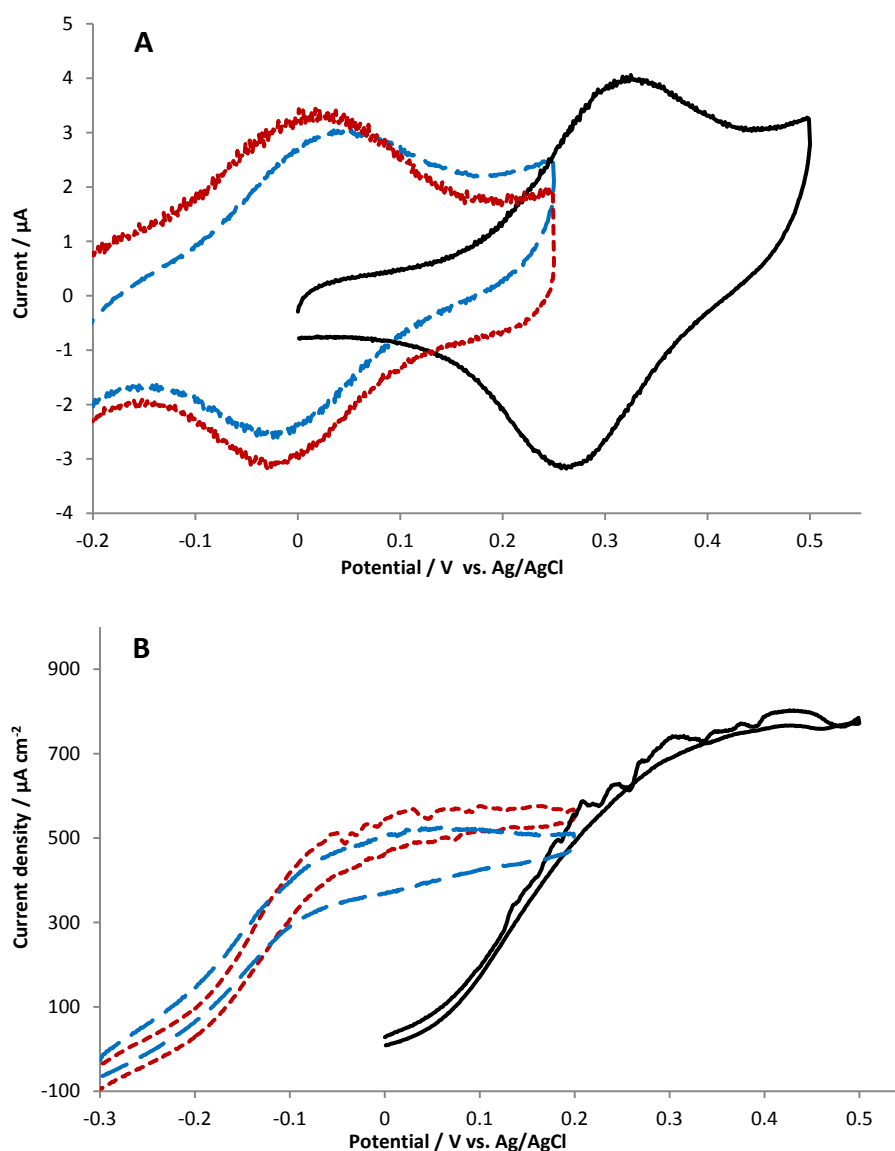


Figure 3. CVs recorded at 1 mVs^{-1} in PBS (pH 7.4, 37°C) for enzyme electrodes prepared from GOx, MWCNT and CMD co-immobilised with Os(dmobpy)₂4AEP (red, dotted), Os(dmobpy)₂4AMP (blue, dashed), or Os(bpy)₂4AMP (black, solid) in the absence (A) and the presence (B) of 5 mM glucose.

Upon addition of 5 mM glucose, sigmoidal shaped cyclic voltammograms are obtained, Figure 3B, characteristic of electrocatalytic oxidation of glucose [29]. The comparison of glucose oxidation currents for CMD based enzyme electrodes as a function of glucose concentration was extracted from amperometric measurements at 0.2 V vs. Ag/AgCl, again 150 mV more positive of the Os(II/III) oxidation to ensure mediated glucose oxidation. The characteristic apparent Michaelis-Menten constant, K_M^{app} , and the maximum current, I_{max} , can be estimated from non-linear least-squares curve fitting of these plots to the Michaelis-Menten equation [32]. The average K_M^{app} , for enzyme electrodes is 14 ± 2 mM which compares well with the value determined for enzyme electrodes based on the Os(bpy)₂4AMP complex above, and with the reported K_M value of 10 ± 5 mM for other GOx-based enzyme electrodes [19, 33]. From calibration curve which follow the trend expected for steady-state approximation, the maximum current density assuming Michaelis-Menten equation are on the order of 3.4 mA cm^{-2} for Os(dmobpy)₂4AMP enzyme electrodes can be estimated compared to higher j_{max} of 4.5 mA cm^{-2} for Os(bpy)₂4AMP enzyme electrodes. The enzyme electrodes prepared with Os(dmobpy)₂4AMP produce lower maximum glucose oxidation current density, j_{max} , of 3.4 mA cm^{-2} compared to 4.5 mA cm^{-2} for Os(bpy)₂4AMP. This lower glucose current density may be as result of the lower thermodynamic driving force for current generation, as observed previously for such systems in solution phase [1, 2], and/or a difference in physical properties such as swelling of films [16, 38, 39]. Nonetheless, substantial glucose oxidation current densities are obtained under pseudo-physiological conditions, with an amperometric current density of $0.83 \pm 0.21 \text{ mA cm}^{-2}$ at 0.2 V applied potential in 5 mM glucose in PBS for Os(dmobpy)₂4AMP enzyme electrodes, compared to the $1.0 \pm 0.2 \text{ mA cm}^{-2}$ current density obtained at 0.45 V applied potential for the Os(bpy)₂4AMP based enzyme electrodes under the same conditions. For comparison to other glucose-oxidising enzyme electrodes, a current density of 0.9 mA cm^{-2} is reported by amperometry at 0.25 V vs Ag/AgCl at enzyme electrodes prepared using [Os(4,4'-dimethyl-2,2'-bipyridine)₂(poly-vinyl imidazole)₁₀Cl]⁺ redox polymer crosslinked with GOx and MWCNT operating in 5 mM glucose [10]. A current density of 0.21 mA cm^{-2} is reported for enzyme electrodes based on a redox polymer [P20-Os(4,4'-dimethyl-2,2'-bipyridine)₂(4-aminomethyl pyridine)Cl].PF₆ co-immobilised with an FAD-

dependent GDH operating in 5 mM glucose at applied potential of 0.2 V vs. Ag/AgCl [39]. Carbon fibre enzyme electrodes prepared by co-immobilisation of an $[\text{Os}(4,4'\text{-dimethoxyl-2,2'}\text{-bipyridine})_2(\text{poly-vinylimidazole})\text{Cl}]^+$ redox polymer with GOx achieve a current density of only 0.6 mA cm^{-2} at 0 V vs. Ag/AgCl in 15 mM glucose [40]. A higher current density of 1.15 mA cm^{-2} is reported for a tethered redox polymer, $(\text{poly-vinylpyridine}[\text{Os}(N,N'\text{-dialkylated-2,2'}\text{-bi-imidazole})_3]^{2+/3+})$ modified carbon fibre electrode at a potential of -0.1 V vs. Ag/AgCl in 15 mM glucose [41]. More recently, tethered redox polymer-based enzyme electrodes co-immobilised with pyrroloquinoline quinone-dependent glucose dehydrogenase (PQQGDH) produced a current density of 1.3 mA cm^{-2} at a scan rate of 5 mV s^{-1} in 20 mM glucose solution stirred at 1000 rpm [42]. There remains however some difficulties with the use of polyvinylimidazole (PVI) based redox polymers, as these systems rely upon synthesis of PVI by bulk free radical polymerisation [15] that results in a wide molecular weight distribution that then affects the physical properties of polymers such as solubility, density etc. In addition, control of osmium complex loading, by ligand substitution, on PVI- based polymers is difficult and leads to batch-to-batch variations in redox polymer and hence enzyme electrode performance [2]. We, here and previously [14, 27], adopt the approach of using commercially available and water soluble polymer supports with suitable functional groups to permit coupling of osmium redox complexes instead of by ligand substitution reactions. For example, enzyme electrodes prepared by coupling of $\text{Os}(\text{dmobpy})_2\text{4AMP}$ and GOx to CMD brushes, anchored to diazonium salt-derivatised surfaces, yielded a current density of 0.22 mA cm^{-2} in 10 mM glucose, lower than reported here, as the polymer films were of the dimension of the polymer support only [18]. Enzyme electrodes based on co-immobilisation of PQQGDH and MWCNT with $\text{Os}(\text{dmobpy})_2\text{4AMP}$, but without incorporation of a polymer support, yielded glucose oxidation current density of 0.30 mA cm^{-2} in 5 mM glucose solutions [23]. The substantial glucose oxidation current density of $0.83 \pm 0.21 \text{ mA cm}^{-2}$ at 0.2 V applied potential achieved with $\text{Os}(\text{dmobpy})_2\text{4AMP}$ coupled within films of the water soluble CMD polymer matrix via EDC/NHS, is perhaps due to improved enzyme loading, and retention of enzyme activity within these CMD hydrogels. In any event, the performance of these enzyme electrodes shows promise

for their application as biosensors or as anodes in enzymatic biofuel cells for power generation.

Operational stability of glucose oxidation current generation for selected enzyme electrodes was evaluated from constant potential amperometry at 0.2 V vs. Ag/AgCl for 24 hr in saturated glucose (100 mM) solution whilst gently stirring to avoid localised substrate depletion. Approximately 68% of initial current density response remains after the 24 hr period for enzyme electrodes prepared from Os(dmobpy)₂4AMP, GOx, MWCNT and CMD compared to ~45% remaining for the Os(bpy)₂4AMP based enzyme electrodes. Interestingly, redox site surface coverage is retained to the same extent for Os(bpy)₂4AMP and Os(dmobpy)₂4AMP based enzyme electrodes, with 43% and 36% coverage retained, respectively, after 24 hrs. The improved operational stability of Os(dmobpy)₂4AMP based enzyme electrodes may be as a result of improved retention of glucose oxidase activity over time, as these electrodes retained 60% of initial enzyme activity compared to only 44% for the Os(bpy)₂4AMP based enzyme electrodes after 24 hrs. Interestingly, higher currents (rate constants) were previously reported for glucose oxidation at enzyme electrodes based on co-adsorption of redox complexes and GOX on graphite when redox complexes containing dmobpy ligands were used, supporting the results obtained here [33].

3.5 Conclusions

The use of CMD and polyacrylic acid has been investigated as support for co-immobilisation of components to provide glucose-oxidising enzyme electrodes. Overall, CMD based enzyme electrodes exhibit higher glucose oxidation current densities, of $1.0 \pm 0.2 \text{ mA cm}^{-2}$ in 5 mM glucose and of $4.5 \pm 1.0 \text{ mA cm}^{-2}$ in saturated glucose solutions in PBS (pH 7.4, 37 °C), over electrodes prepared using polyacrylic acid. This substantial current density is, however, achieved at the relatively high applied potential of +0.45 V vs Ag/AgCl. Variation in osmium complex structure to provide a redox complex of lower formal potential results in CMD-based enzyme electrodes producing current densities of $0.83 \pm 0.21 \text{ mA cm}^{-2}$ in 5 mM glucose and of $3.4 \pm 0.7 \text{ mA cm}^{-2}$ in saturated glucose solutions in PBS at an applied potential of +0.2 V vs. Ag/AgCl showing promise for application as

glucose oxidising biosensors, and as anodes for *in-vivo* enzymatic fuel cells. Future work is focused on variation in enzyme selection in the proposed matrix of CMD, Os(dmobpy)₂4AMP, and MWCNT to further improve the current output signal of such enzyme electrodes.

3.6 Acknowledgements

RK acknowledges support from the Earth and Natural Science Doctoral Studies Programme funded by the Higher Education Authority (HEA) through the Programme for Research at Third-Level Institutions, Cycle 5 (PRTL-5) and co-funded by the European Regional Development Fund (ERDF).

3.7 References

- [1] D. Leech, P. Kavanagh, W. Schuhmann, *Electrochimica Acta*, 84 (2012) 223-234.
- [2] P. Kavanagh, D. Leech, *Physical Chemistry Chemical Physics*, 15 (2013) 4859-4869.
- [3] A. Heller, B. Feldman, *Chemical Reviews*, 108 (2008) 2482-2505.
- [4] A. Heller, B. Feldman, *Accounts of Chemical Research*, 43 (2010) 963-973.
- [5] D. MacAodha, P.Ó. Conghaile, B. Egan, P. Kavanagh, D. Leech, *ChemPhysChem*, 14 (2013) 2302-2307.
- [6] N. Mano, F. Mao, A. Heller, *Journal of the American Chemical Society*, 124 (2002) 12962-12963.
- [7] C. Danilowicz, E. Cortón, F. Battaglini, E.J. Calvo, *Electrochimica Acta*, 43 (1998) 3525-3531.
- [8] E.J. Calvo, C. Danilowicz, L. Diaz, *Journal of the Chemical Society, Faraday Transactions*, 89 (1993) 377-384.
- [9] R.J. Forster, J.G. Vos, *Macromolecules*, 23 (1990) 4372-4377.
- [10] D. MacAodha, P. Ó Conghaile, B. Egan, P. Kavanagh, C. Sygmund, R. Ludwig, D. Leech, *Electroanalysis*, 25 (2013) 94-100.
- [11] D. Wen, L. Deng, M. Zhou, S. Guo, L. Shang, G. Xu, S. Dong, *Biosensors and Bioelectronics*, 25 (2010) 1544-1547.
- [12] C.-M. Yu, M.-J. Yen, L.-C. Chen, *Biosensors and Bioelectronics*, 25 (2010) 2515-2521.
- [13] M. Holzinger, A. Le Goff, S. Cosnier, *Electrochimica Acta*, 82 (2012) 179-190.
- [14] I. Osadebe, D. Leech, *ChemElectroChem*, 1 (2014) 1988-1993.
- [15] B.B. Dambatta, J.R. Ebdon, *European Polymer Journal*, 22 (1986) 783-786.
- [16] J.W. Gallaway, S.A. Calabrese Barton, *Journal of Electroanalytical Chemistry*, 626 (2009) 149-155.
- [17] D. MacAodha, M.L. Ferrer, P.O. Conghaile, P. Kavanagh, D. Leech, *Physical Chemistry Chemical Physics*, 14 (2012) 14667-14672.
- [18] S. Boland, P. Kavanagh, D. Leech, *ECS Transactions*, 13 (2008) 77-87.
- [19] P. Ó Conghaile, S. Kamireddy, D. MacAodha, P. Kavanagh, D. Leech, *Anal Bioanal Chem*, 405 (2013) 3807-3812.
- [20] E.M. Kober, J.V. Caspar, B.P. Sullivan, T.J. Meyer, *Inorganic Chemistry*, 27 (1988) 4587-4598.
- [21] A.B.P. Lever, *Inorganic Chemistry*, 29 (1990) 1271-1285.

- [22] H.U. Bergmeyer, *Methods of Enzymatic Analysis*, 2nd edition ed., 2nd edition, Academic Press, New York & London, 1974.
- [23] P. Ó Conghaile, D. MacAodha, B. Egan, P. Kavanagh, D. Leech, *Journal of The Electrochemical Society*, 160 (2013) G3165-G3170.
- [24] R. Kumar, D. Leech, *Electrochimica Acta*, 140 (2014) 209-216.
- [25] S. Boland, F. Barrière, D. Leech, *Langmuir*, 24 (2008) 6351-6358.
- [26] J. Niedziółka-Jönsson, S. Boland, D. Leech, R. Boukherroub, S. Szunerits, *Electrochimica Acta*, 55 (2010) 959-964.
- [27] E. Laviron, *Journal of Electroanalytical Chemistry and Interfacial Electrochemistry*, 52 (1974) 395-402.
- [28] R.J. Forster, J.G. Vos, *Langmuir*, 10 (1994) 4330-4338.
- [29] A.J. Bard, L.R. Faulkner, *Electrochemical Methods: Fundamentals and Applications*, 2 ed., Wiley & Sons, New York, 2001.
- [30] T.J. Ohara, R. Rajagopalan, A. Heller, *Analytical Chemistry*, 65 (1993) 3512-3517.
- [31] R.J. Forster, L.R. Faulkner, *Journal of the American Chemical Society*, 116 (1994) 5444-5452.
- [32] D.L. Nelson, M.M. Cox, *Lehninger principles of biochemistry*, New York: W.H. Freeman, 2004.
- [33] S.M. Zakeeruddin, D.M. Fraser, M.K. Nazeeruddin, M. Grätzel, *Journal of Electroanalytical Chemistry*, 337 (1992) 253-283.
- [34] N. Liu, Q. Zhang, M. Chan-Park, C. Li, P. Chen, *Carbon Nanotubes for Electrochemical and Electronic Biosensing Applications*, in: D. Shi (Ed.) *NanoScience in Biomedicine*, Springer Berlin Heidelberg, 2009, pp. 205-246.
- [35] C. Wang, Q. Yan, H.-B. Liu, X.-H. Zhou, S.-J. Xiao, *Langmuir*, 27 (2011) 12058-12068.
- [36] S. Rengaraj, P. Kavanagh, D. Leech, *Biosensors and Bioelectronics*, 30 (2011) 294-299.
- [37] S. Boland, K. Foster, D. Leech, *Electrochimica Acta*, 54 (2009) 1986-1991.
- [38] M.N. Zafar, X. Wang, C. Sygmond, R. Ludwig, D. Leech, L. Gorton, *Analytical Chemistry*, 84 (2011) 334-341.
- [39] P. Ó Conghaile, S. Pöller, D. MacAodha, W. Schuhmann, D. Leech, *Biosensors and Bioelectronics*, 43 (2013) 30-37.
- [40] N. Mano, A. Heller, *Journal of The Electrochemical Society*, 150 (2003) A1136-A1138.
- [41] F. Mao, N. Mano, A. Heller, *Journal of the American Chemical Society*, 125 (2003) 4951-4957.
- [42] V. Flexer, N. Mano, *Analytical Chemistry*, 86 (2014) 2465-2473.

Chapter 4

Published as:

A glucose anode for enzymatic fuel cells optimized for current production under physiological conditions using a design of experiment approach

Rakesh Kumar and Dónal Leech. Bioelectrochemistry, Vol. 106, pp. 41-46, 2015

DOI: 10.1016/j.bioelechem.2015.06.005

Co-author contributions:

I synthesised the osmium redox complexes, design the experiment and performed the laboratory work, the analysis, and wrote the first draft of the publication.

Dónal Leech, as the project supervisor, contributed through guidance and advice throughout and wrote the final draft of the publication.

Copyright License number: 3741860290211

A glucose anode for enzymatic fuel cells optimised for current production under physiological conditions using a design of experiment approach

4.1 ABSTRACT

This study reports a design of experiment methodology to investigate and improve the performance of glucose oxidizing enzyme electrodes. Enzyme electrodes were constructed by co-immobilization of amine-containing osmium redox complexes, multiwalled carbon nanotubes and glucose oxidase in a carboxymethyl dextran matrix at graphite electrode surfaces to provide a 3-dimensional matrix for electrocatalytic oxidation of glucose. Optimisation of the amount of the enzyme electrode components to produce the highest current density under pseudo-physiological conditions of 5 mM glucose in saline buffer at 37°C was performed using response surface methodology. A statistical analysis showed that the proposed model had a good fit with the experimental results. From the validated model, the addition of multiwalled carbon nanotubes and carboxymethyl dextran components was identified as major contributing factors to the improved performance. Based on the optimised amount of components, enzyme electrodes display current densities of $1.2 \pm 0.1 \text{ mA cm}^{-2}$ and $5.2 \pm 0.2 \text{ mA cm}^{-2}$ at 0.2 V vs. Ag/AgCl in buffer containing 5 mM and 100 mM glucose, respectively, largely consistent with the predicted values. This demonstrates that use of a design of experiment approach can be applied effectively and efficiently to improve the performance of enzyme electrodes as anodes for biofuel cell device development.

4.2 Introduction

Enzymatic biofuel cells (EFCs) are bioelectrochemical devices capable of converting chemical energy into electrical energy using enzymes as catalysts [1, 2]. Use of an enzyme as biocatalyst rather than conventional noble metal catalysts can render the catalytic reaction more specific towards fuel or oxidant [3, 4]. Enzymes immobilised at electrodes provide therefore the possibility for a membrane-less configuration of fuel cell, opening up opportunities for development of miniaturised systems for powering electronic devices [2, 5]. Much interest in recent years has focused on the development of potentially implantable, miniaturised membrane-less EFCs that can deliver power using oxidation of fuel such as glucose present in the bloodstream at an anode and oxygen reduction at a cathode [6, 7].

Various anode compositions, utilising glucose oxidising enzymes as a catalyst, have been investigated for EFC applications [8, 9]. For example, a series of studies focused on improving the current signal and stability for glucose oxidation by co-immobilisation of enzymes inside redox-conducting hydrogels at electrode surfaces [10]. Hydrogels based on osmium polypyridyl complexes co-ordinatively bound to polymers are widely used as mediators in EFCs, as they can “wire” enzymes by electron-hopping self-exchange within the hydrogels for connection between redox active sites of enzymes and electrode surface [5]. Osmium based systems possess advantages over iron and ruthenium based systems due to the low redox potential of Os(II/III) redox transition and relative stability of complexes in both oxidation states [11, 12]. The inclusion of multiwalled carbon nanotubes (MWCNTs) in enzyme electrode films results in improved catalytic current and operational stability of the enzyme electrodes [13]. These nanostructures provide a conductive support which acts as scaffold for retention of enzyme activity, as a function of the amount deposited [3, 14, 15].

As an alternate approach to immobilising redox complexes, Danilowicz et al. reported on coupling of aldehyde functional groups, distal to the osmium metal center of complexes, to amine-based polymer and enzymes to form films on electrode surfaces [12]. Boland et al. reported on coupling of osmium complexes, that contain an amine functional group distal to the metal centre, and glucose oxidase (GOx) to a carboxymethylated dextran (CMD) polymer previously anchored to

functionalised electrode surfaces [16]. Similarly amine functionalised osmium complexes and enzymes have been coupled to a polyallylamine support using a diepoxide reagent, to produce enzyme electrodes [17]. More recently, co-immobilisation of amine functionalised osmium complexes and enzymes to a CMD polymer and MWCNTs on graphite electrodes using a carbodiimide coupling approach has been used to prepare enzyme electrodes [18]. Given the number of different components, and the range of amounts and methods used to prepare these enzyme electrodes, a comprehensive study is required on optimisation of each component used in enzyme electrode preparation to identify the interaction or dependency of these components on the performance of enzyme electrodes. Rather than adopt an optimisation approach based on alteration of one factor at a time, a design-of-experiment (DoE) approach can be used to determine optimal enzyme electrode performance. For example, Babanova et al. recently reported on a DoE approach for optimisation of performance of an air-breathing bilirubin oxidase-based EFC cathode [19].

Here we report on use of a response surface methodology (RSM) technique for optimisation of EFCs component amounts to produce glucose-oxidising enzyme electrodes. This DoE model is developed and validated for enzyme electrode performance in pseudo-physiological conditions (5 mM glucose, 50 mM phosphate buffered saline, PBS, pH 7.4, 37 °C). The enzyme electrodes are prepared by co-immobilising $[\text{Os}(4,4'\text{-dimethoxy-}2,2'\text{-bipyridine})_2(4\text{-aminomethylpyridine})\text{Cl}]\cdot\text{PF}_6$, GOx, MWCNTs and CMD using carbodiimide coupling, as described previously [17]. The DoE-optimised enzyme electrodes display a 32 % improved glucose oxidation current density compared to previously reported values for the system optimised by variation of one factor at a time [18].

4.3 Experimental

4.3.1. Materials

The mediator redox complex $[\text{Os}(4,4'\text{-dimethoxy-}2,2'\text{-bipyridine})_2(4\text{-aminomethylpyridine})\text{Cl}]\cdot\text{PF}_6$ ($\text{Os}(\text{dmobpy})_2\text{4AMP}$) was synthesised by ligand substitution of $\text{Os}(4,4'\text{-dimethoxy-}2,2'\text{-bipyridine})_2\text{Cl}_2$ in ethylene glycol at reflux,

upon addition of 1.1 mol equivalents of 4-aminomethylpyridine, as reported previously [17, 20, 21]. The $\text{Os}(4,4'\text{-dimethoxy-2,2'-bipyridine})_2\text{Cl}_2$ was prepared from $(\text{NH}_4)_2\text{OsCl}_6$ according to literature methods [20, 22]. All other chemicals were purchased from Sigma-Aldrich (Dublin, Ireland) and used as received unless otherwise stated. The CMD has an average molecular mass of 15,000 Da, glucose oxidase (EC 1.1.3.4) average activity ($240 \text{ units mg}^{-1}$) was determined using the o-dianisidine and horseradish peroxidase-coupled spectrophotometric assay. The reaction was monitored on an Agilent 6453 UV/Vis spectrophotometer at 460 nm [23] and the MWCNTs were acid-treated by heating 20 mg mL^{-1} in concentrated HNO_3 at reflux for 6 h at $\sim 150 \text{ }^\circ\text{C}$ [13]. All solutions were prepared from Milli-Q ($18.2 \text{ M}\Omega \text{ cm}$) water.

Methods: A CH Instruments 1030 multichannel potentiostat (IJ Cambria) coupled to a thermostated electrochemical cell was used to perform all electrochemical measurements. Custom built Ag/AgCl reference electrode (3 M KCl) and platinum foil counter electrode (Goodfellow) were used in the cell. Graphite disk electrodes (3 mm diameter) were prepared by shrouding graphite rods (Graphite store, part # NC001295) in heat-shrinkable tubing and polishing the exposed disk on 1200 grit silicon carbide paper (Buehler) followed by thorough rinsing with Milli-Q water. Working electrodes were sonicated in Milli-Q water for 10 min and dried under nitrogen gas prior to use. All electrochemical measurements were performed in phosphate buffer saline (PBS, 0.05 M phosphate, pH 7.4, 0.15 M NaCl) at $37 \text{ }^\circ\text{C}$. Currents are normalised to the two-dimensional projected area of the graphite disk electrodes to provide current density data.

The procedure for the enzyme electrode preparation involves activation of carboxylic acid functional groups of solutions of CMD (5 mg mL^{-1}) and acid treated MWCNTs (46 mg mL^{-1}), by addition of $4 \text{ }\mu\text{L}$ aqueous solution of 40 mM *N*-[3-dimethylaminopropyl]-*N'*-ethylcarbodiimide (EDC) and 10 mM *N*-hydroxysuccinimide (NHS) in an eppendorf for 12 min, for coupling to amine functional groups of GOx (10 mg mL^{-1}) and redox complex (4.5 mM aqueous solution). Enzyme electrodes are prepared by drop coating a volume of the resulting solutions onto graphite disks and drying the electrodes for 18 h at room temperature. The amount of different components of CMD, MWCNTs, $\text{Os}(\text{dmobpy})_2\text{4AMP}$ and

GOx added in the enzyme electrode preparation step is determined by the Design Expert software (version 9, STAT-EASE Inc. Minneapolis, USA), as described in the Results and discussion section.

4.4 Results and discussion

4.4.1. Enzyme electrode electrochemistry

Cyclic voltammetry (CV) is initially used to evaluate the redox potential of the Os(II/III) transition for the Os(dmobpy)₂4AMP complex in the enzyme electrodes. All prepared enzyme electrodes, in the absence of glucose substrate, exhibit oxidation and reduction peaks at 0.07 ± 0.01 V (vs. Ag/AgCl), Fig. 1, which is similar to the redox potential observed for the osmium complexes in solution and also close to that previously reported for the complex immobilised within CMD films or directly coupled to a carbon electrode [16, 18]. Redox peak currents vary linearly with scan rate for scan rates less than 20 mVs^{-1} , indicative of a surface-controlled response [22]. At higher scan rates, the peak currents scale linearly with the square root of scan rate, indicative of semi-infinite diffusion control of the response, as expected for multi-layered films on electrodes [24, 25]. Osmium complex surface coverage (Γ_{Os}), calculated by integration of the charged passed under the redox complex oxidation peak using slow scan rate voltammetry in PBS solution [25], is comparable to values obtained previously [18] and approximately one thousand-fold that expected for monolayer coverage of osmium polypyridyl complexes [26, 27]. Upon addition of glucose substrate to the PBS electrolyte, a sigmoidal-shaped slow-scan rate cyclic voltammogram characteristic of electrocatalytic oxidation of glucose is obtained for all enzyme electrodes, Fig.1. However, a difference in potential of ~ 80 mV is observed between the formal potential of the immobilised redox complex in the absence of glucose and the half-wave potential, $E_{1/2}$, of the catalytic sigmoidal-shaped CV in the presence of glucose. It has been reported that a shift in $E_{1/2}$ occurs in the catalytic sigmoidal-shaped CV of mediated enzyme electrode reactions when the boundary between a mediator-limited case and a substrate-limited case is crossed [28, 29], indicating that glucose substrate

transport may limit the current flow under these conditions for the enzyme electrodes.

A comparison of glucose oxidation current for enzyme electrodes as a function of glucose concentration is extracted from amperometric measurements at 0.2 V vs. Ag/AgCl applied potential, selected to be 150 mV more positive of the redox potential of the osmium complex to ensure sufficient mediated glucose oxidation. Amperometric response of enzyme electrodes displays slightly higher glucose oxidation current density over the current density observed in slow scan CVs, due to use of convection (150 rpm) of solutions in amperometry to avoid substrate depletion over the experiment duration.

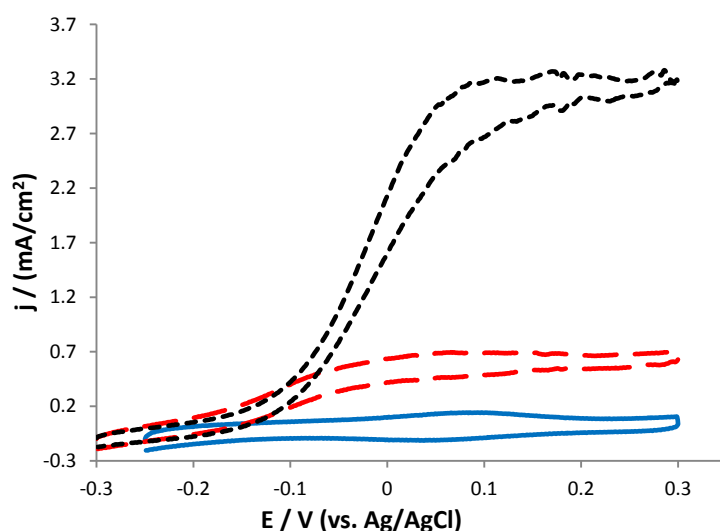


Fig. 1. CVs recorded at 1 mV s^{-1} in the presence of 100 mM (black dot), 5 mM (red, dashed) and 0 mM (blue solid) glucose in PBS (37 °C) for enzyme electrodes prepared by co-immobilising $\text{Os}(\text{dmobpy})_2\text{4AMP}$ (30 μg), MWCNTs (400 μg), GOx (50 μg) and CMD (50 μg) on graphite electrodes.

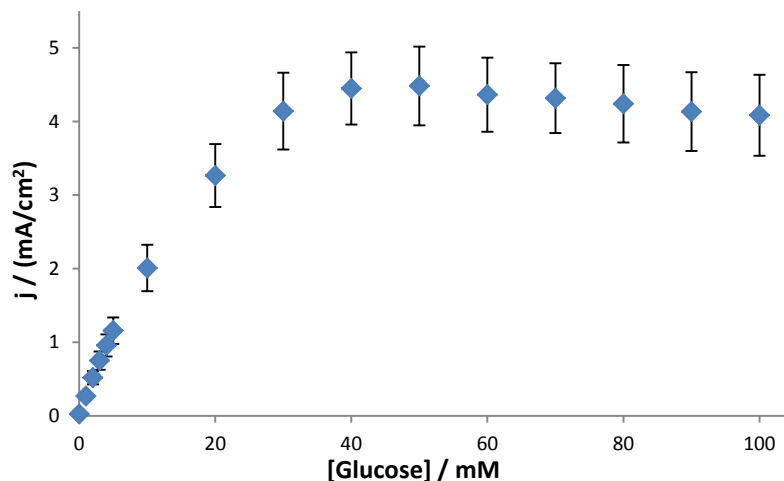


Fig. 2. Current density recorded in PBS (37 °C) at 150 rpm at an applied potential of 0.2 V, as a function of glucose concentration, for enzyme electrodes (n=4) prepared by co-immobilising Os(dmobpy)₂4AMP (30 µg), MWCNTs (400 µg), GOx (50 µg) and CMD (50 µg) on graphite electrodes.

Substrate saturation is observed for concentrations greater than 50 mM glucose for all enzyme electrodes. Apparent Michaelis-Menten constants, K_M^{app} , and maximum current densities, j_{max} can be estimated from non-linear least squares fitting of these plots to the Michaelis-Menten equation [30]. Whilst the shape of the current density curves versus glucose concentration may be fit to the Michaelis-Menten equation, it should be noted that substrate limitation of the current can also result in Michaelis-Menten dependence of the curves [31]. Nonetheless, average K_M^{app} for enzyme electrodes prepared using Os(dmobpy)₂4AMP, MWCNTs, GOx and CMD of 14.5 ± 0.5 mM, is similar to previously obtained values [17, 32] and indicates the response range to glucose for these enzyme electrodes. As one potential application for enzyme electrodes is to deliver power to implanted or semi-implanted medical devices using glucose as a fuel available *in vivo*, the amperometric response in pseudo-physiological conditions (5 mM glucose in PBS, 37 °C, 150 rpm) is set to be the standard output parameter for all enzyme electrodes prepared.

4.4.2. Response surface factorial design for the optimisation of EFC anode

A typical approach for the optimisation of enzyme electrode preparation involves changing variables one factor at a time based on a trial-and-error method. Whilst this

technique is very informative it involves a lengthy process for incremental system improvement. A DoE approach can provide information about interaction and response of interconnected factors over a wide range of values [33]. Here, a DoE based on response surface factorial Box-Behnken Design (BBD) with a three-level factorial design is used to evaluate the main effect and interaction between the CMD, MWCNTs, osmium complex and GOx components required to prepare glucose-oxidising enzyme electrodes, optimised to produce the highest current density in pseudo-physiological conditions. In a 3-level DoE design, three values for each component are used. The range and level of components investigated are given in Table 1 and 2.

Symbols	Factor	Low level (-1)	Central Point (0)	High level (+1)
x_1	CMD (μg)	0	25	50
x_2	MWCNTs (μg)	0	230	460
x_3	Os(dmobpy) ₂ 4AMP (μg)	10	25	50
x_4	GOx (μg)	20	50	100

Table 1. The selected factors and the corresponding 3 levels for the amounts deposited for each factor in the enzyme electrode preparation step.

For the 3-level four factorial BBD experimental designs, a total of 29 experimental runs were undertaken, defined as $N = 2k(k-1) + C_0$, [34] where k is the number of factors and C_0 is the number of central points, with design arrangement and response shown in Table 2. The mathematical relationship between the enzyme electrode response and variables can be presented by a second degree quadratic equation [34]

$$\begin{aligned}
 y = & b_0 + b_1x_1 + b_2x_2 + b_3x_3 + b_4x_4 + b_{11}x_1^2 + b_{22}x_2^2 + b_{33}x_3^2 + b_{44}x_4^2 + \\
 & b_{12}x_1x_2 + b_{13}x_1x_3 + b_{14}x_1x_4 + b_{23}x_2x_3 + b_{24}x_2x_4 + \\
 & b_{34}x_3x_4
 \end{aligned} \tag{1}$$

where y is the predicted value, x_1 , x_2 , x_3 and x_4 are the CMD, MWCNTs, Os(dmobpy)₂4AMP and GOx amounts used in the enzyme electrode preparation, b_0

is the constant coefficient (intercept), b_1, b_2, b_3, b_4 and $b_{12}, b_{13}, b_{14}, b_{23}, b_{24}, b_{34}$ are linear and cross product coefficients, respectively, and the quadratic coefficients are b_{11}, b_{22}, b_{33} and b_{44} . On the basis of this equation, the design model provides a tool for improvement of experimental outcome by finding the best combination of component levels within the test set. Further, the model generated can be validated using confirmatory experiments.

Run no.	Variables				Response / y
	x_1	x_2	x_3	x_4	Current density / mA cm ⁻² (5 mM)
1	-1	0	1	0	0.33
2	0	0	-1	-1	0.70
3	0	0	0	0	0.73
4	1	0	-1	0	1.06
5	1	1	0	0	1.00
6	0	1	0	1	1.02
7	-1	0	0	-1	0.52
8	0	0	0	0	0.70
9	1	0	1	0	0.72
10	0	-1	-1	0	0.24
11	0	0	-1	1	0.71
12	0	0	0	0	0.80
13	0	1	0	-1	0.74
14	0	1	1	0	0.84
15	-1	-1	0	0	0.11
16	-1	0	-1	0	0.59
17	0	0	0	0	0.69
18	-1	1	0	0	0.61

19	0	0	0	0	0.70
20	-1	0	0	1	0.56
21	0	0	1	-1	0.57
22	0	0	1	1	0.44
23	0	-1	0	1	0.18
24	1	-1	0	0	0.20
25	0	-1	1	0	0.14
26	0	1	-1	0	0.60
27	1	0	0	1	0.54
28	0	-1	0	-1	0.18
29	1	0	0	-1	0.70

Table 2. Box-Behnken design arrangement variables and measured amperometric current density response at 0.2 V vs Ag/AgCl for enzyme electrodes under pseudo-physiological conditions.

In this BBD design [34-36], the low level of GOx and Os(dmoby)₂4AMP complex is selected to be 20 µg and 10 µg, respectively, because of a requirement for a minimum level of each to produce a current density for glucose oxidation, as previously reported [1, 2, 5, 11, 12]. The high level of CMD, MWCNTs, Os(dmoby)₂4AMP and GOx is selected to be not more than 50 µg, 460 µg, 50 µg, and 100 µg respectively, because of the difficulty to control drop-casting of higher amounts to these on electrode surfaces. The response of each enzyme electrode is evaluated from constant potential amperometry at 0.2 V vs. Ag/AgCl in pseudo-physiological conditions, for each of the designed combinations in Table 2. Analysis of variance (ANOVA) is used for statistical testing of the response model, with results provided in Table 3. The coefficient of variation (R^2), Fisher's (F -test) test and probability (P -value) are used to evaluate the appropriateness of the model [37]. The model data demonstrates that the model was statically significant, as is evident from a calculated F -value of 33.64 with a low probability value (0.0001). The larger

the magnitude of the F -value, the more likely is rejection of the null hypothesis that the data show no variation. In addition, probability values of 0.0001 estimated for MWCNTs and CMD components imply that their effect is statistically significant to the variation in enzyme electrode performance. The sample coefficient of determination (R^2) value of 0.97 indicates that the model can explain 97% of the variation in response [38]. The adjusted R^2 (Adj R^2) value of 0.94, used to measure the amount of variation in model response adjusted for the number of predictors in the model, suggests significant correlation between predicted and observed responses [39, 40], [41]. Fig. 3 shows the observed glucose oxidation current density versus predicted values for the model. The predicted current densities of enzyme electrodes correlate well with the observed current densities. No irregularities of the DoE model were observed from the residual diagnostics.

Source	Sum of Squares	Degree of freedom	Mean Squares	F -value	$P^a > F$	R^{2b}
Model	10.28	14	0.73	33.64	< 0.0001	0.97
Residual	0.31	14	0.022			
Lack of fit	0.30	10	0.030	16.77	0.0076	
Pure error	7.1×10^{-3}	4	1.7×10^{-3}			
Total	10.59	28				

^a Probability values (P -values).

^b Coefficient of determination.

Table 3. Analysis of variance (ANOVA) of the quadratic model for the enzyme electrode response.

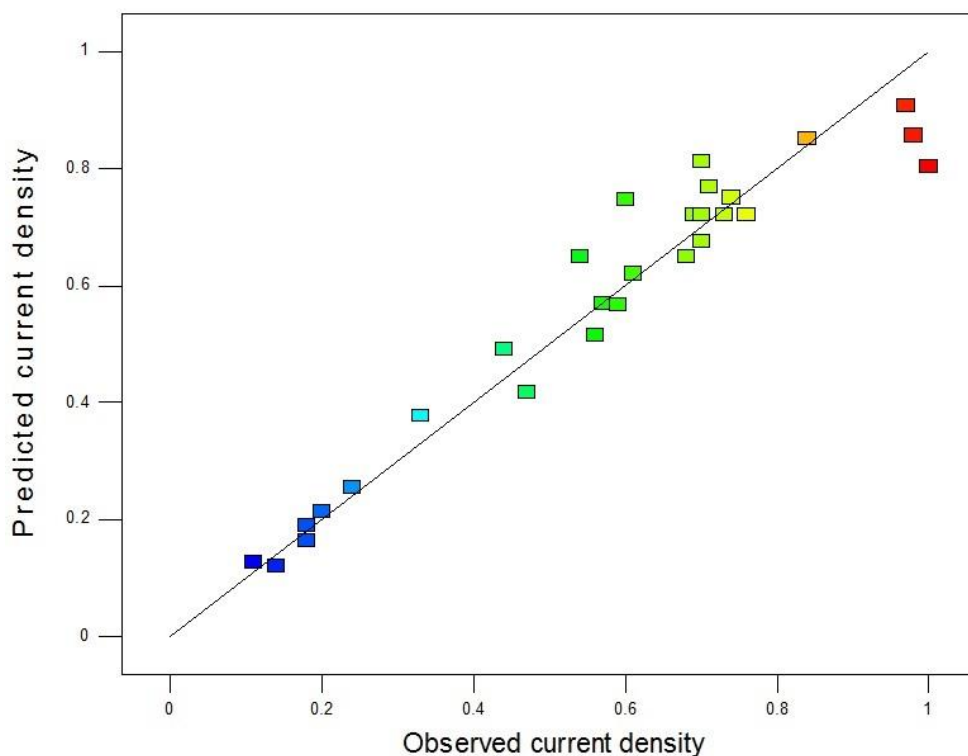


Fig. 3. Observed amperometric glucose oxidation current densities (mA cm^{-2}) vs. the predicted current densities (mA cm^{-2}) at 0.2 V vs. Ag/AgCl in 5 mM glucose solution.

4.4.3. Model validation

Based upon the model, enzyme electrodes prepared by co-immobilising CMD (50 μg), MWCNTs (236 μg), $\text{Os}(\text{dmbpy})_2\text{4AMP}$ (30 μg) and GOx (62 μg) are predicted to display a current density of $0.79 \pm 0.10 \text{ mA cm}^{-2}$ in pseudo-physiological conditions. Initial model validation was tested using such enzyme electrodes, with the CV response for enzyme electrodes at 1 mV s^{-1} scan rate in PBS (37 $^\circ\text{C}$) containing 0 mM, 5 mM and 100 mM glucose shown in Fig. 4. Amperometric response of enzyme electrodes at 0.2 V vs. Ag/AgCl, as shown in Fig. 5, produces glucose oxidation currents upon addition of glucose to the PBS solution (37 $^\circ\text{C}$). A current density of $0.78 \pm 0.10 \text{ mA cm}^{-2}$ ($n=4$) is obtained in 5 mM glucose in PBS, consistent with the predicted values of $0.79 \pm 0.10 \text{ mA cm}^{-2}$.

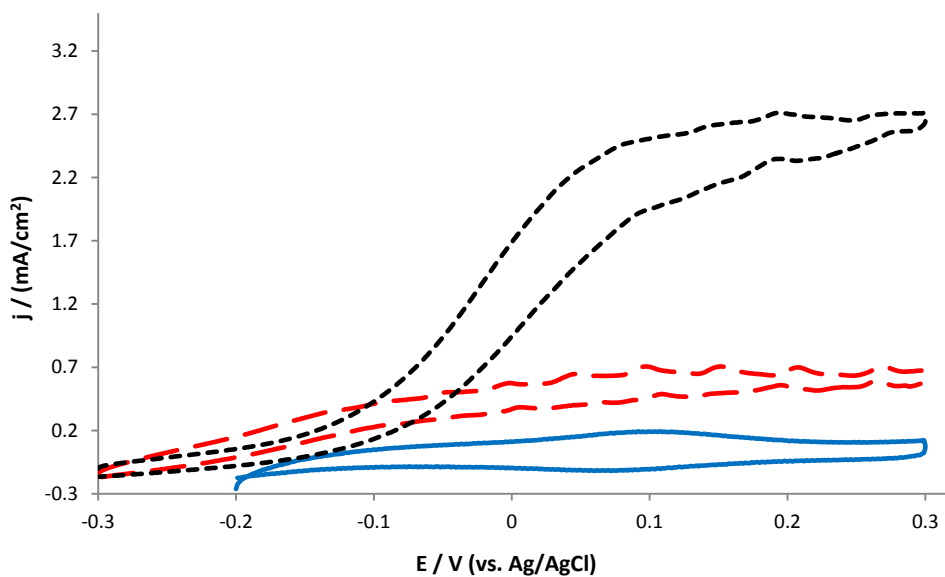


Fig. 4. CVs recorded at 1 mV s^{-1} in the presence of 100 mM (black dot), 5 mM (red, dashed) and 0 mM (blue solid) glucose in PBS ($37 \text{ }^\circ\text{C}$) for enzyme electrodes prepared by co-immobilising $\text{Os}(\text{dmbpy})_2\text{4AMP}$ ($30 \text{ }\mu\text{g}$), MWCNTs ($236 \text{ }\mu\text{g}$), GOx ($62 \text{ }\mu\text{g}$) and CMD ($50 \text{ }\mu\text{g}$) on graphite electrodes.

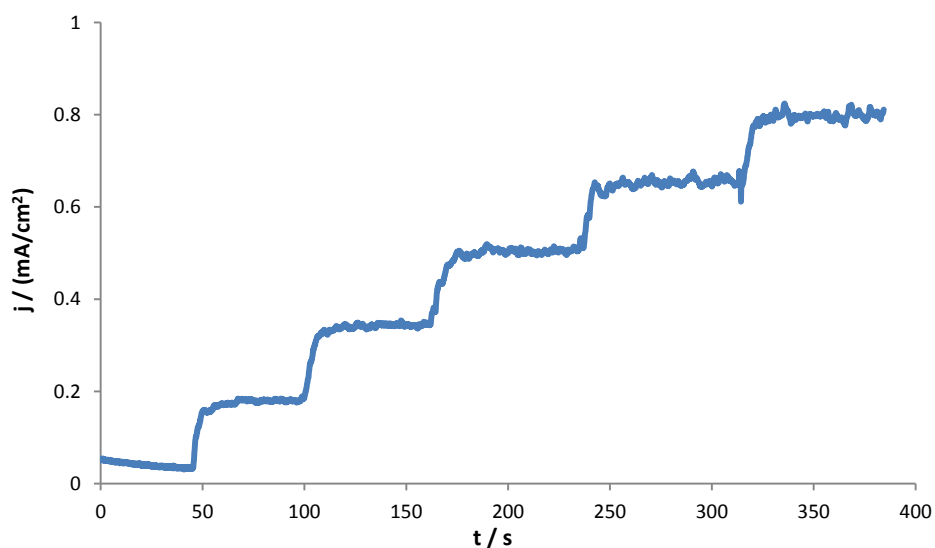


Fig. 5. Current density recorded in PBS ($37 \text{ }^\circ\text{C}$) at 150 rpm at an applied potential of 0.2 V vs. Ag/AgCl, as a function of a glucose concentration increment of 1 mM at each current density step, for enzyme electrode prepared by co-immobilising $\text{Os}(\text{dmbpy})_2\text{4AMP}$ ($30 \text{ }\mu\text{g}$), MWCNTs ($236 \text{ }\mu\text{g}$), GOx ($62 \text{ }\mu\text{g}$) and CMD ($50 \text{ }\mu\text{g}$) on graphite electrodes.

4.4.4. Optimisation of enzyme electrode components

A perturbation diagram for enzyme electrode performance with respect to the four different factors is shown in Fig. 6, where the influence of each factor around a specific point in the design range is plotted. In this method, the current density is plotted with respect to only one variable of the overall process, one at a time over its range, considering the other variables as constant at their centre point. A steep slope or curvature in a factor shows that current density response is sensitive to that factor and a flatter line therefore represents insensitivity to modification of that factor. A sharp curvature for MWCNTs (B) and CMD (A) is obtained compared to Os(dmobpy)₂4AMP (C) and GOx (D) factors, indicating that the MWCNTs and CMD factors have a larger impact on current density of enzyme electrodes, in the ranges tested.

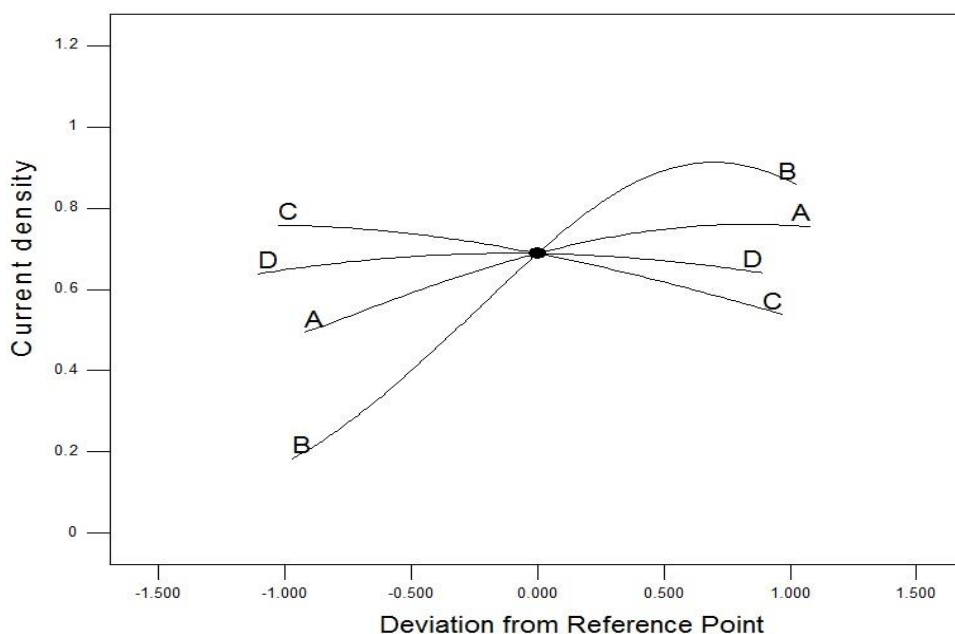


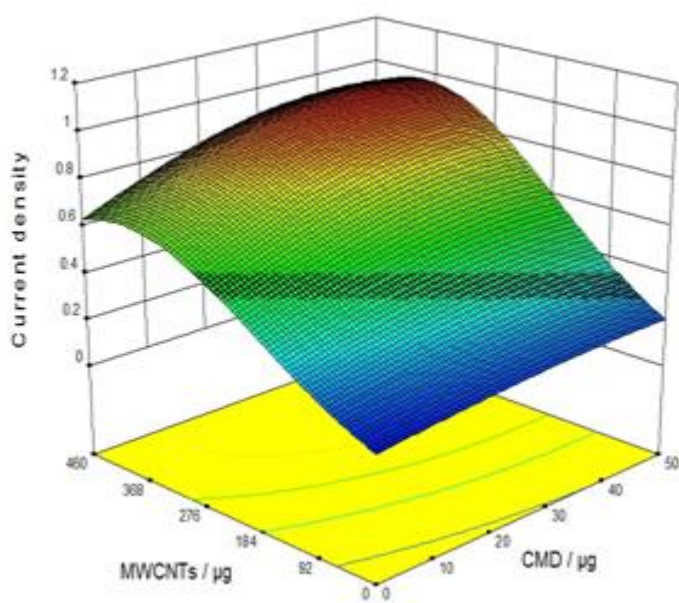
Fig. 6. Deviation graph of predicted current density (mA cm^{-2}) versus the deviation of process parameters (A: CMD, B: MWCNTs, C: Os(dmobpy)₂4AMP, D: GOx).

Three-dimensional response surface plots of the relationship between CMD and MWCNTs, on the current density response of enzyme electrodes are shown in Fig. 7. Fig. 7A shows that when the loading of MWCNTs increased from 0 μg to 400 μg , the current density significantly increased from 0.08 mA cm^{-2} to 0.56 mA cm^{-2} , at a

fixed center level value of GOx (60 μg) and Os(dmobpy)₂4AMP (30 μg). The MWCNTs scaffold has been shown to provide an increased surface area contributing to retention of enzyme activity which results in higher current density for enzyme electrodes [6, 13]. A decrease in glucose oxidation current is obtained upon addition of MWCNTs > 400 μg to enzyme electrodes, as previously reported [15]. Increasing CMD loading from 0 μg to 50 μg in the enzyme electrode preparation step also displays a positive effect on the observed current density. However, the combined effect of CMD and MWCNTs has a larger impact on current density response, as shown in Fig. 7, possibly because incorporation of CMD permits uniform dispersion and alignment of carbon nanotubes [42], perhaps leading to improved mass transport within the films as substrate availability is the factor that limits the current density.

An optimisation study was performed from the validated DoE model to evaluate the experimental parameters for enzyme electrode preparation to achieve the highest current density under the target conditions. The optimum of each enzyme electrode component based on the combination of the response surface and their contours is given in Table 4, with the experimentally determined response for the enzyme electrodes prepared and tested in pseudo-physiological conditions and shown in Fig. 1 and 2, also provided.

A



B

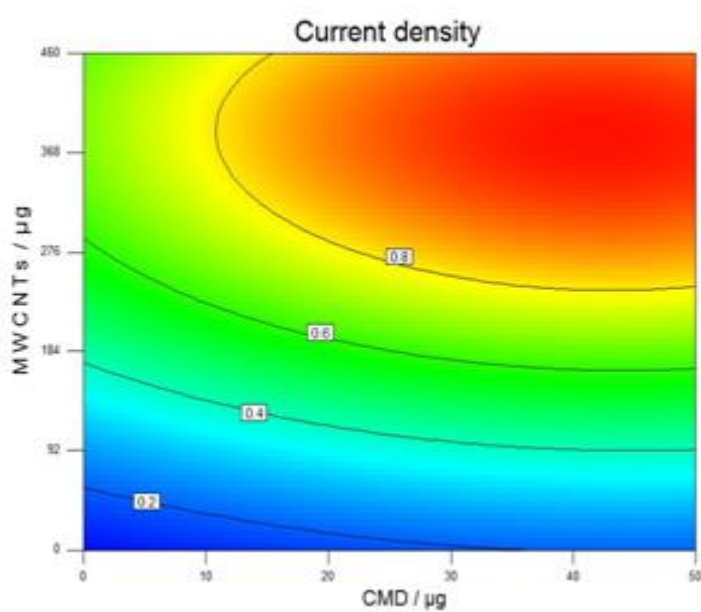


Fig. 7. Response surface (A) and contours (B) of CMD vs. MWCNTs amount on glucose oxidation current density (mA cm^{-2}) at center level for GOx and Os(dmobpy)₂4AMP.

Table 4. Predicted and experimental values of the enzyme electrode response at optimum conditions (n=4).

CMD (μg)	MWCNTs (μg)	Os(dmobpy) ₂ 4AMP (μg)	GOx (μg)	Current density (mA cm^{-2})	
				Predicted Values	Experimental Value
50	400	30	50	1.0 ± 0.1	1.2 ± 0.1

Substantial glucose oxidation current densities are obtained under pseudo-physiological conditions, with a current density of $1.2 \pm 0.1 \text{ mA cm}^{-2}$ at 0.2 V vs. Ag/AgCl in 5 mM glucose for the DoE optimised enzyme electrodes, compared to 0.83 mA cm^{-2} obtained previously for Os(dmobpy)₂4AMP based enzyme electrodes under similar conditions, optimised using a one-factor-at-a-time approach [18]. For comparison to other enzyme electrodes, a glucose-oxidising current density of 0.9 mA cm^{-2} was reported for enzyme electrodes based on co-immobilisation of a [Os(4,4'-dimethyl-2,2'-bipyridine)₂(poly-vinylimidazole)₁₀Cl]⁺ redox polymer and MWCNTs, operating in 5 mM glucose [14]. A current density of 0.21 mA cm^{-2} at an applied potential of 0.2 V vs. Ag/AgCl was reported for enzyme electrodes based on redox polymer [P20-Os(4,4'-dimethyl-2,2'-bipyridine)₂(4-aminomethylpyridine)Cl].PF₆ co-immobilised with a flavin adenine dinucleotide dependent glucose dehydrogenase operating in 5 mM glucose [6]. The optimised enzyme electrodes display maximum current density j_{max} , of $5.0 \pm 0.1 \text{ mA cm}^{-2}$ at 0.2 V vs. Ag/AgCl, compared to the maximum current density of 3.4 mA cm^{-2} previously reported for enzyme electrodes prepared by co-immobilising GOx, Os(dmobpy)₂4AMP, MWCNTs and CMD [18], confirming the improved performance of the DoE optimised enzyme electrodes and showing promise for application to bioelectricity generation.

4.5 Conclusions

Components used to construct enzyme electrodes were optimised and verified by response surface methodology coupled with a central composite design. The amperometric current generated in pseudo-physiological condition at 0.2 V vs. Ag/AgCl from the DoE improved enzyme electrode is 32% higher than that previously observed for enzyme electrodes optimised by varying of one factor at a

time [18]. The statistical model based on DoE methodology was developed and validated. Enzyme electrode components that contribute most to the improved performance are the amounts of MWCNTs and CMD added. The glucose oxidation current also displayed a dependency on the level of GOx and Os(dmobpy)₂4AMP used. DoE optimised enzyme electrodes result in glucose oxidation current density of $1.2 \pm 0.1 \text{ mA cm}^{-2}$ in pseudo-physiological conditions and $5.0 \pm 0.1 \text{ mA cm}^{-2}$ in saturated glucose solutions, at an applied potential of 0.2 V vs. Ag/AgCl, showing promise for application as glucose oxidising anodes in enzymatic fuel cells for in vivo or ex vivo power generation. Further studies involving screening of different glucose oxidising enzymes using a DoE approach are underway.

4.6 Acknowledgement

RK acknowledges support from the Earth and Natural Science Doctoral Studies Programme funded by the Higher Education Authority (HEA) through the Programme for Research at Third-Level Institutions, Cycle 5 (PRTL-5) and co-funded by the European Regional Development Fund (ERDF).

4.7 References

- [1] A. Heller, B. Feldman, *Chemical Reviews*, 108 (2008) 2482-2505.
- [2] A. Heller, *Physical Chemistry Chemical Physics*, 6 (2004) 209-216.
- [3] S.D. Minteer, B.Y. Liaw, M.J. Cooney, *Current Opinion in Biotechnology*, 18 (2007) 228-234.
- [4] N. Mano, A. Heller, *Journal of The Electrochemical Society*, 150 (2003) A1136-A1138.
- [5] N. Mano, F. Mao, A. Heller, *Journal of the American Chemical Society*, 124 (2002) 12962-12963.
- [6] P. Ó Conghaile, D. MacAodha, B. Egan, P. Kavanagh, D. Leech, *Journal of The Electrochemical Society*, 160 (2013) G3165-G3170.
- [7] J.A. Castorena-Gonzalez, C. Foote, K. MacVittie, J. Halánek, L. Halámková, L.A. Martinez-Lemus, E. Katz, *Electroanalysis*, 25 (2013) 1579-1584.
- [8] F. Davis, S.P.J. Higson, *Biosensors and Bioelectronics*, 22 (2007) 1224-1235.
- [9] P.A. Jelliss, S.S. Graham, A. Josipovic, S. Boyko, S.D. Minteer, V. Svoboda, *Polyhedron*, 50 (2013) 36-44.
- [10] B.A. Gregg, A. Heller, "Polymer and enzyme." U.S. Patent No. 5,262,035 (1993).
- [11] E.J. Calvo, C. Danilowicz, L. Diaz, *Journal of the Chemical Society, Faraday Transactions*, 89 (1993) 377-384.
- [12] C. Danilowicz, E. Cortón, F. Battaglini, E.J. Calvo, *Electrochimica Acta*, 43 (1998) 3525-3531.
- [13] D. MacAodha, M.L. Ferrer, P.O. Conghaile, P. Kavanagh, D. Leech, *Physical Chemistry Chemical Physics*, 14 (2012) 14667-14672.
- [14] S.D. Minteer, P. Atanassov, H.R. Luckarift, G.R. Johnson, *Materials Today*, 15 (2012) 166-173.
- [15] I. Osadebe, D. Leech, *ChemElectroChem*, 1 (2014) 1988-1993.
- [16] S. Boland, P. Kavanagh, D. Leech, *ECS Transactions*, 13 (2008) 77-87.
- [17] P. Ó Conghaile, S. Kamireddy, D. MacAodha, P. Kavanagh, D. Leech, *Anal Bioanal Chem*, 405 (2013) 3807-3812.
- [18] R. Kumar, D. Leech, *Journal of The Electrochemical Society*, 161 (2014) H3005-H3010.
- [19] S. Babanova, K. Artyushkova, Y. Ulyanova, S. Singhal, P. Atanassov, *Journal of Power Sources*, 245 (2014) 389-397.
- [20] E.M. Kober, J.V. Caspar, B.P. Sullivan, T.J. Meyer, *Inorganic Chemistry*, 27 (1988) 4587-4598.

- [21] R.J. Forster, J.G. Vos, *Macromolecules*, 23 (1990) 4372-4377.
- [22] A.B.P. Lever, *Inorganic Chemistry*, 29 (1990) 1271-1285.
- [23] H.U. Bergmeyer, *Methods of Enzymatic Analysis*, 2nd edition ed., 2nd edition, Academic Press, New York & London, 1974.
- [24] R.J. Forster, J.G. Vos, *Langmuir*, 10 (1994) 4330-4338.
- [25] A.J. Bard, L.R. Faulkner, *Electrochemical Methods: Fundamentals and Applications*, 2 ed., Wiley & Sons, New York, 2001.
- [26] R.J. Forster, L.R. Faulkner, *Journal of the American Chemical Society*, 116 (1994) 5444-5452.
- [27] R. Kumar, D. Leech, *Electrochimica Acta*, 140 (2014) 209-216.
- [28] P.N. Bartlett, K.F.E. Pratt, *Journal of Electroanalytical Chemistry*, 397 (1995) 61-78.
- [29] B.t. Limoges, J. Moiroux, J.-M. Savéant, *Journal of Electroanalytical Chemistry*, 521 (2002) 8-15.
- [30] D.L. Nelson, M.M. Cox, *Lehninger principles of biochemistry*, New York: W.H. Freeman, 2004.
- [31] P.N. Bartlett, K.F.E. Pratt, *Journal of Electroanalytical Chemistry*, 397 (1995) 53-60.
- [32] S.M. Zakeeruddin, D.M. Fraser, M.K. Nazeeruddin, M. Grätzel, *Journal of Electroanalytical Chemistry*, 337 (1992) 253-283.
- [33] L. Eriksson, E. Johansson, N. Kettaneh-Wold, C. Wikstrom, S. Wold, *Design of Experiments*, 3 ed., MKS Umetrics AB, 2008.
- [34] B. Qi, X. Chen, F. Shen, Y. Su, Y. Wan, *Industrial & Engineering Chemistry Research*, 48 (2009) 7346-7353.
- [35] E.C. Catalkaya, F. Kargi, *Chemosphere*, 69 (2007) 485-492.
- [36] R. Kumar, R. Singh, N. Kumar, K. Bishnoi, N.R. Bishnoi, *Chemical Engineering Journal*, 146 (2009) 401-407.
- [37] G. Chen, J. Chen, C. Srinivasakannan, J. Peng, *Applied Surface Science*, 258 (2012) 3068-3073.
- [38] P.D. Haaland, *Separating signals from the noise. In Experimental design in biotechnology*, Marcel Dekker Inc., p 61, 1989.
- [39] H.-Y. Fu, P.-C. Xu, G.-H. Huang, T. Chai, M. Hou, P.-F. Gao, *Desalination*, 302 (2012) 33-42.
- [40] J. Ren, M. Zhao, J. Shi, J. Wang, Y. Jiang, C. Cui, Y. Kakuda, S.J. Xue, *LWT - Food Science and Technology*, 41 (2008) 1624-1632.
- [41] K. Shabbiri, A. Adnan, B. Noor, S. Jamil, *Ann Microbiol*, 62 (2012) 523-532.

[42] P.-C. Ma, N.A. Siddiqui, G. Marom, J.-K. Kim, *Composites Part A: Applied Science and Manufacturing*, 41 (2010) 1345-1367.

Immobilisation of redox complexes on electrode surfaces for application to biofuel cells

5.1 Introduction

The immobilisation of redox enzymes and complexes, as electron transfer catalysts, on electrode surfaces contributes to increased amperometric current response for electrochemical sensing and electricity-generating devices [1-4]. For example, the co-immobilisation of glucose-oxidising enzyme and electron-shuttling mediators within redox-conductive hydrogels provided “wired” enzyme electrodes capable of producing glucose oxidation current, that are used in continuous glucose monitoring systems [1, 5-7]. Most studies on enzyme co-immobilisation within redox polymer hydrogels have been based on the use of a diepoxide crosslinker, poly(ethylene glycol)diglycidyl ether (PEGDGE) [7-10]. Application of such redox active hydrogel films on electrodes as biocatalytic fuel cells shows potential, if leaching of enzyme and redox mediator is avoided [2, 11, 12]. There have been many attempts to increase current output and active lifetime of enzyme electrodes. To increase the stability of biofilms on electrodes chemisorption and chemical attachment of different components to a polymer matrix can be used. Retaining enzyme electrode components through immobilisation on surfaces remains one of the key challenges to overcome for developing implantable bioelectrochemical devices. This chapter focuses on the immobilisation of enzyme electrode components using genipin as a crosslinker on a chitosan support at electrode surfaces, as an alternate to the PEGDGE used heretofore.

Genipin, a naturally occurring monoterpene derivative found in *Gardenia jasminoides* fruit extract, has attracted interest for biomedical applications because it can be used to efficiently cross-link cellular tissues and biomaterials (including chitosan, bovine serum albumin, collagen or gelatin) by coupling primary amino-residues, and it exhibits much lower cytotoxicity than conventional cross-linkers (i.e. 5000- to 10000-fold compared to glutaraldehyde) [13, 14]. Thus, there is a potential for incorporation of more biocompatible technology in bioelectrochemical devices aimed at *in vivo* applications. Furthermore, genipin acts as a solution phase crosslinker, unlike the diepoxide crosslinker, allowing for immobilisation in flow-

through devices. Recently, El Ichi *et. al.* [15] reported on the performance of genipin-crosslinked thin films of chitosan and laccase at multiwalled carbon nanotube (MWCNTs) electrodes as oxygen-reducing biocathodes for fuel cell applications. These chitosan-MWCNTs-laccase based biocathodes have shown stable *in vivo* electrical output for almost 6 months after implantation. The longevity of biocathode output is also attributed to a new fuel cell design that resists degradation of the biocathode from body fluid and improves the biocompatibility for longer term *in vivo* applications. Suitability of genipin as a crosslinker of redox active hydrogels consisting of mediators and enzymes could provide an alternate to present crosslinking approaches..

In this work, we explore the use of genipin to create redox hydrogels on electrodes based on the simultaneous crosslinking of an osmium redox complex [Os(2,2'-bipyridine)₂(4-aminomethylpyridine)Cl].PF₆ (Os(bpy)₂4AMP) containing an amino functional group distal to the metal centre and a glucose oxidising enzyme (GOx) using chitosan (CS) as an amino-functionalised platform to network between the complex and enzyme. The novel redox hydrogel electrodes are tested for glucose oxidation with a view to application as anodes in enzymatic fuel cells.

5.2 Experimental

5.2.1 Materials and reagents

All chemicals were purchased from Sigma-Aldrich unless otherwise stated. All solutions were made from Milli-Q (18.2 MΩ cm) unless otherwise indicated. GOx from *Aspergillus niger* (EC 1.1.3.4) was used as received. MWCNTs were acid-treated by heating in nitric acid at reflux for 6 hours at 150 °C. Chitosan (CS, Batch #06513AE, deacetylation degree (88 ± 2), Average $M_v = 617$ KDa) was purchased from Sigma-Aldrich. It was dissolved in 0.15 M aqueous acetic solution to give a polymer concentration of 1% w/w and then filtered.

The initial complexes of (Os (*N-N*)₂Cl₂) were synthesised from (NH₄)₂OsCl₆ where *N-N* is 2,2'-bipyridine according to literature methods [41, 42]. The ligand substitution of a chloride is achieved by heating an ethylene glycol solution of a 1.1 mole equivalent ligand (4-aminomethylpyridine) and Os (*N-N*)₂ Cl₂ complex at reflux, with precipitation of the resulting complex by addition of an aqueous NH₄PF₆

solution [43]. The ligand substitution is monitored by cyclic voltammetry and differential pulse voltammetry, as reported on previously [9, 41, 43, 44]. The precipitated product is filtered and allowed to dry overnight at 50°C. Graphite disc electrodes (3 mm diameter) were prepared by shrouding graphite rods (graphite store) in heat shrinkable tubing and polishing the exposed disk on 1200 grit silicon carbide paper (Buehler) followed by through rinsing with Milli-Q water. Working electrodes (CH Instrument Inc.) were sonicated in Milli-Q water for 10 min and dried under nitrogen gas prior to use. GOx activity was determined using the o-dianisidine and horseradish peroxidase-coupled spectrophotometric assay. The reaction was monitored on an Agilent 6453 UV/Vis spectrophotometer at 460 nm.

5.2.2 Methods

Enzyme electrode preparations: Genipin cross-linked redox hydrogels were formed on electrodes by mixing 5 μL of CS polymer (8 mg ml^{-1} in 40 mM acetic acid solution, adjusted to pH 5.5), 5 μL of 30 mM genipin aqueous solution, GOx (5 μL of 10 mg ml^{-1} aqueous solution), 5 μL acid treated MWCNTs (46 mg ml^{-1} aqueous dispersion) and redox complex (5 μL of 4.5 mM aqueous solution containing 1% DMSO) in an eppendorf, stirring for one hour and then drop-coating 25 μL of the resulting mixture onto the graphite disk electrode. The drop was dried for 18 hours at room temperature to allow crosslinking, followed by rinsing of the enzyme electrode in PBS for ~5 seconds before testing commenced. For comparison, control and PEGDGE-based enzyme electrodes were prepared by adding 5 μL of Milli-Q water or PEGDGE (28 mM aqueous solution) to the mixture instead of the corresponding amount of genipin. Electrochemical experiments were conducted using CH Instruments 1030a multichannel potentiostat or a CHI 620 potentiostat (IJ Cambria, UK) on a three electrode cell in 50 mM PBS (pH 7.4, 37 °C) using custom built Ag/AgCl (3 M) reference electrode and platinum mesh counter electrode (Goodfellow, UK).

5.3 Results and discussion

5.3.1 Genipin cross-linked enzyme electrode

Figure 1, displays a cyclic voltammogram for an enzyme electrode prepared by co-immobilisation using genipin of GOx, Os(bpy)₂4AMP redox complex and CS as a polymer support, recorded in 50 mM PBS (37 °C, pH 7.4) at 1 mV s⁻¹ in the absence and presence of 5 mM and 100 mM glucose. In the absence of substrate, the CV exhibits oxidation and reduction peaks associated with the Os(II/III) transition, centred at a formal potential of 0.31 ± 0.03 V (vs. Ag/AgCl), similar to that previously reported for the redox complex in solution or immobilised on electrode surfaces [9, 47, 48]. The similarity of the formal redox potential in solution and immobilised indicates that the Os(II/III) transition is generally not affected by the immobilisation procedure. Osmium surface coverages (Γ_{Os}) of 4.5 (±6) × 10⁻⁸ mol cm⁻² and 5.3 (±4) × 10⁻⁸ mol cm⁻² are obtained by integration of charge passed during electrolysis of complexes within films on the electrode surface using slow scan rate voltammetry in PBS solution for genipin and PEGDGE based enzyme electrodes, respectively. This Γ_{Os} value is approximately one thousand fold that expected for monolayer coverage of osmium polypyridyl complexes [49] on electrode surfaces, indicating that three-dimensional films are formed on the electrodes. All enzyme electrodes display similar CV response in PBS in the absence of glucose substrate, where the Os(II/III) peak current varies linearly with scan rates (<20 mVs⁻¹) indicative of a surface-controlled response [50]. At higher scan rates peak current scales linearly with the square root of scan rate indicative of semi-infinite diffusion control [2, 26, 51] again indicative of three-dimensional films formed on the electrodes. In the presence of 5 mM and 100 mM glucose in PBS (pH 7.4, 37°C), sigmoidal shaped cyclic voltammograms, characteristic of catalytic oxidation of glucose by the enzyme, are obtained as shown in Figure 1 (blue and black traces) for the genipin crosslinked enzyme electrode prepared using Os(bpy)₂4AMP, GOx and chitosan as support.

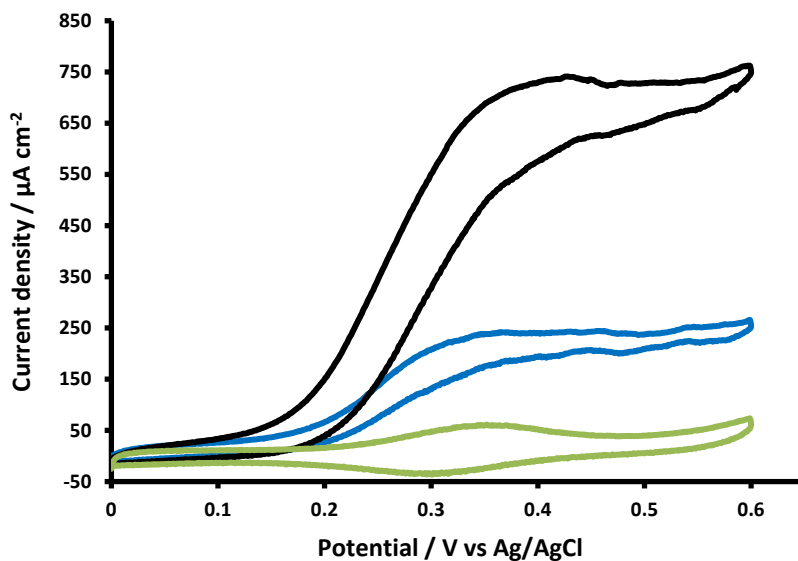


Figure 1: Cyclic voltammograms recorded in 50 mM PBS (37 °C, pH 7.4) at scan rate of 1 mV s^{-1} for an enzyme electrode prepared by co-immobilisation, using genipin, of GOx, Os(bpy)₂4AMP and CS in the absence (green), and presence of 5 mM (blue) and 100 mM (black) glucose.

A comparison of glucose oxidation current for enzyme electrodes prepared either with genipin or PEGDGE as a function of glucose concentration is extracted from amperometric measurements at 0.45 V (vs. Ag/AgCl) applied potential, 150 mV more positive of the redox potential of the complex to ensure sufficient overpotential for mediated bioelectrocatalysis. The amperometric response of enzyme electrodes prepared using genipin or PEGDGE as cross-linkers achieve current densities of 0.74 ± 0.08 or $0.44 \pm 0.06 \text{ mA cm}^{-2}$, respectively, at 0.45 V (vs. Ag/AgCl) in 50 mM PBS (pH 7.4, 37°C, 150 rpm) containing 100 mM glucose. The higher current response for genipin-based anodes compared to those crosslinked with PEGDGE point to it as a possible replacement for the PEGDGE cross-linker. It should be noted that the control enzyme electrode, prepared without addition of a cross-linker, displayed a higher current density compared to genipin or PEGDGE based enzyme electrodes. In this case the GOx on the control electrode does not undergo chemical modification via a chemical crosslinker or coupling technique to the polymer matrix and may therefore display initially higher current density (see Table 1) [26, 27, 52]. The control electrodes do however display lower current stability over 20 h of continuous testing using amperometry at 0.45 V (vs. Ag/AgCl). The use of genipin in the

electrode preparation step results in 18% of signal retained after 20 h continuous operation compared to 3% and 5% for control and PEGDGE based enzyme electrodes. The stability of initial glucose oxidation current density for genipin based enzyme electrodes is therefore increased by up to three and six fold when compared to either the PEGDGE or control enzyme electrodes, respectively, providing further evidence for the suitability of genipin as a crosslinker to construct enzymes electrode for power generation applications.

Glucose oxidation current density, extracted from amperometric measurement at 0.45 V vs. Ag/AgCl, as a function of glucose concentration for genipin and PEGDGE based enzyme electrodes is plotted in Figure 2. Substrate saturation is observed for concentrations higher than 50 mM glucose for all enzyme electrodes. Apparent Michaelis-Menten constants, K_m^{app} , and maximum current densities, j_{max} , can be calculated from non-linear least squares fitting of these plots to Michaelis-Menten equation [53] as shown in Figure 2, with values displayed in Table 1. Average K_m^{app} for genipin crosslinked enzyme electrodes prepared using Os(bpy)₂4AMP, GOx and CS is 14.6 ± 5.9 mM which is similar to previously reported values for other GOx based enzyme electrodes [1, 54].

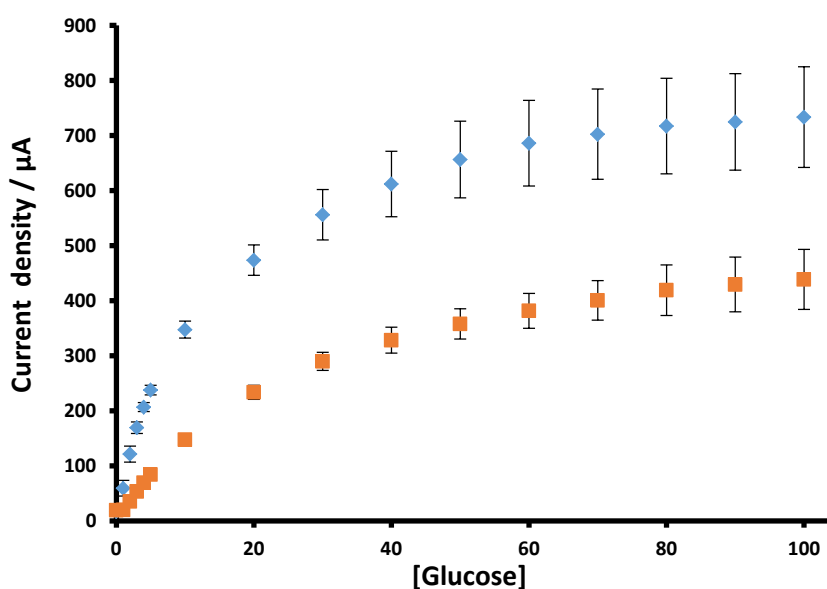


Figure 2: Glucose oxidation current densities extracted from steady-state amperometry at an applied potential of 0.45 V (vs. Ag/AgCl) as a function of glucose concentration, for genipin (♦) or PEGDGE (■) cross-linked films prepared using CS, GOx and the redox complex Os(bpy)₂4AMP in 50 mM PBS (pH 7.4, 37°C), solution stirred at 150 rpm.

Additions of MWCNTs into redox hydrogels results in increased biocatalytic current response as reported previously [44, 55-57]. The current density of genipin-based enzyme electrodes increases upon inclusion of MWCNTs in the preparation step (see Table 1). A current density of $4.90 \pm 0.33 \text{ mA cm}^{-2}$ is observed from steady-state amperometry at an applied potential of 0.45 V (vs. Ag/AgCl) in 50 mM PBS (pH 7.4, 37 °C, 150 rpm) containing 100 mM glucose. The main contributing factor to increased current density is the higher retention of the enzyme activity on the electrode surface, calculated by peroxidase-coupled based spectrophotometric assay [58]. Initially, an enzyme activity of 9 U is deposited in the electrode preparation step for all enzyme electrodes. The genipin-based electrodes retain activity of $2.0 \pm 0.2 \text{ U}$ compared to $1.0 \pm 0.1 \text{ U}$ retained for the PEGDGE-based electrodes, further highlighting the improved efficiency of genipin as a crosslinker. Upon addition of MWCNTs, an increase in retained enzyme activity was observed for genipin and PEGDGE-based enzymatic electrodes as shown in table 1. However, it is interesting to note that control enzyme electrodes (without crosslinker) showed considerably higher retained enzyme activity of $3.0 \pm 1.1 \text{ U}$ compared to genipin or PEGDGE based enzyme electrodes. This is possibly because enzymes are physisorbed directly on the electrode surface without a crosslinker and therefore leach into the testing solution.

Table 1. Genipin/PEGDGE based enzyme electrode performance for electrodes prepared using redox complex, GOx and chitosan. (n=4)

Enzyme Electrodes	Surface coverage (Γ_{Os} n mole cm^{-2})	Enzymatic Activity (U)	K_M^{app} [mM]	j ($mA\ cm^{-2}$)		% j_{max} in 100 mM glucose after 20 h
				5 mM	100 mM	
No Crosslinker	31 ± 6	3.0 ± 1.1	13.3 ± 3.0	0.37 ± 0.04	1.24 ± 0.11	3.0
PEGDGE	59 ± 4	1.0 ± 0.1	16.3 ± 1.2	0.08 ± 0.01	0.44 ± 0.15	5.0
Genipin	51 ± 7	2.0 ± 0.2	14.6 ± 5.9	0.24 ± 0.01	0.74 ± 0.08	18.0
Genipin + MWCNT	91 ± 7	4.2 ± 1.6	23.7 ± 1.4	0.85 ± 0.1	4.90 ± 0.33	0.4
PEGDGE + MWCNT	69 ± 11	4.0 ± 1.0	12.0 ± 1.0	0.14 ± 0.01	0.64 ± 0.1	8.0

Comparison of the genipin-based electrode with other glucose oxidising enzyme electrode is difficult due to different methodologies used for the film preparation and experimental conditions. A similar response to glucose as that obtained for the genipin-based enzyme electrodes was obtained from enzyme electrodes prepared by co-immobilising redox complexes, GOx and carboxymethyl dextran as a polymer support (described in chapter 3 and 4) using peptide, carbodiimide-based, coupling. As example, a current density of $60\ \mu A\ cm^{-2}$ is extracted from the slow scan at $5\ mV\ s^{-1}$ cyclic voltammogram for enzyme electrode in presence of 50 mM glucose using osmium complexes and GOx attached using PEG-400 crosslinker to a poly(allylamine) support [54]. A current density of $1.0 \pm 0.2\ mA\ cm^{-2}$ at 0.45 V in PBS (pH 7.4, 37°C) containing 5 mM glucose was reported for the enzyme electrodes prepared using carbodiimide-based coupling of the carboxymethyl dextran polymer support, Os(bpy)₂4AMP, glucose oxidase and MWCNTs [44]. Similarly, the obtained current density of enzyme electrodes under physiological conditions are comparable to $0.5\ mA\ cm^{-2}$ or $1\ mA\ cm^{-2}$, for those achieved with polyvinyl imidazole (PVI) based enzyme electrodes crosslinked with PEGDGE [59] or GA [60] indicating the suitability of genipin for the preparation of redox hydrogels for biofuel cell applications.

5.4 Conclusions

In conclusion, use of genipin as a cross-linker to immobilise glucose oxidase and an amine-containing redox complex to a chitosan matrix on electrodes with potential applications to *in vivo* and *in vitro* sensing or energy generation is demonstrated. Future experiments will involve optimisation of immobilisation parameters using a design of experiment approach. It would be interesting to investigate the interaction of amine-functionalized MWCNT with chitosan and amine-functionalised osmium complexes having low redox potential using genipin as a crosslinker, which could result in increased current density of the more stable (than PEGDGE) genipin-crosslinked enzyme electrodes.

5.5 References

- [1] E.J. Calvo, C. Danilowicz, L. Diaz, *Journal of the Chemical Society, Faraday Transactions*, 89 (1993) 377-384.
- [2] T.J. Ohara, R. Rajagopalan, A. Heller, *Analytical Chemistry*, 65 (1993) 3512-3517.
- [3] H.M. Wu, R. Olier, N. Jaffrezic-Renault, P. Clechet, A. Nyamsi, C. Martelet, *Electrochimica Acta*, 39 (1994) 327-331.
- [4] D. Rochefort, L. Kouisni, K. Gendron, *Journal of Electroanalytical Chemistry*, 617 (2008) 53-63.
- [5] N. Mano, A. Heller, *Journal of The Electrochemical Society*, 150 (2003) A1136-A1138.
- [6] A. Heller, *Physical Chemistry Chemical Physics*, 6 (2004) 209-216.
- [7] A. Heller, B. Feldman, *Accounts of Chemical Research*, 43 (2010) 963-973.
- [8] X.-L. Luo, J.-J. Xu, Y. Du, H.-Y. Chen, *Analytical Biochemistry*, 334 (2004) 284-289.
- [9] P. Ó Conghaile, S. Kamireddy, D. MacAodha, P. Kavanagh, D. Leech, *Anal Bioanal Chem*, 405 (2013) 3807-3812.
- [10] P. Ó Conghaile, S. Pöllner, D. MacAodha, W. Schuhmann, D. Leech, *Biosensors and Bioelectronics*, 43 (2013) 30-37.
- [11] A. Heller, *Current Opinion in Chemical Biology*, 10 (2006) 664-672.
- [12] B.A. Gregg, A. Heller, *The Journal of Physical Chemistry*, 95 (1991) 5970-5975.
- [13] H.-W. Sung, R.-N. Huang, L.L.H. Huang, C.-C. Tsai, *Journal of Biomaterials Science, Polymer Edition*, 10 (1999) 63-78.
- [14] F.-L. Mi, S.-S. Shyu, C.-K. Peng, *Journal of Polymer Science Part A: Polymer Chemistry*, 43 (2005) 1985-2000.
- [15] S. El Ichi, A. Zebda, J.P. Alcaraz, A. Laaroussi, F. Boucher, J. Boutonnat, N. Reverdy-Bruas, D. Chaussy, M.N. Belgacem, P. Cinquin, D.K. Martin, *Energy & Environmental Science*, 8 (2015) 1017-1026.
- [16] P. Kavanagh, D. Leech, *Analytical Chemistry*, 78 (2006) 2710-2716.
- [17] J. Hajdukiewicz, S. Boland, P. Kavanagh, D. Leech, *Biosensors and Bioelectronics*, 25 (2010) 1037-1042.
- [18] J.J. Fei, S.S. Hu, *Russ J Electrochem*, 41 (2005) 1296-1304.
- [19] T.G. Drummond, M.G. Hill, J.K. Barton, *Nat Biotech*, 21 (2003) 1192-1199.
- [20] J.J. Gooding, *Electroanalysis*, 14 (2002) 1149-1156.
- [21] E. Palek, M. Fojta, *Analytical Chemistry*, 73 (2001) 74 A-83 A.
- [22] H. Holden Thorp, *Trends in Biotechnology*, 21 (2003) 522-524.

- [23] P. Kavanagh, D. Leech, *Analytical Chemistry*, 78 (2006) 2710-2716.
- [24] B. Wang, I. Jansson, J.B. Schenkman, J.F. Rusling, *Analytical Chemistry*, 77 (2005) 1361-1367.
- [25] J.C. Forgie, S. El Khakani, D.D. MacNeil, D. Rochefort, *Physical Chemistry Chemical Physics*, 15 (2013) 7713-7721.
- [26] T. Ohara, *Platinum Metals Rev*, 39 (1995) 54-62.
- [27] A. Sinz, *Mass Spectrom Rev*, 25 (2006) 663-682.
- [28] J.Y. Lai, *Int J Mol Sci*, 13 (2012) 10970-10985.
- [29] D.E. Tallman, S.L. Petersen, *Electroanalysis*, 2 (1990) 499-510.
- [30] M.T. Carter, M. Rodriguez, A.J. Bard, *Journal of the American Chemical Society*, 111 (1989) 8901-8911.
- [31] A. Ghosh, A. Mandoli, D.K. Kumar, N.S. Yadav, T. Ghosh, B. Jha, J.A. Thomas, A. Das, *Dalton Transactions*, (2009) 9312-9321.
- [32] P.A. Norowski, S. Mishra, P.C. Adatrow, W.O. Haggard, J.D. Bumgardner, *Journal of Biomedical Materials Research Part A*, 100A (2012) 2890-2896.
- [33] G. Barone, A. Terenzi, A. Lauria, A.M. Almerico, J.M. Leal, N. Busto, B. García, *Coordination Chemistry Reviews*, 257 (2013) 2848-2862.
- [34] W. Kaim, J. Rall, *Angewandte Chemie International Edition in English*, 35 (1996) 43-60.
- [35] A. Silvestri, G. Barone, G. Ruisi, D. Anselmo, S. Riela, V.T. Liveri, *J Inorg Biochem*, 101 (2007) 841-848.
- [36] G. Shul, C.A.C. Ruiz, D. Rochefort, P.A. Brooksby, D. Bélanger, *Electrochimica Acta*, 106 (2013) 378-385.
- [37] U. Oesch, J. Janata, *Electrochimica Acta*, 28 (1983) 1237-1246.
- [38] Mudasir, K. Wijaya, N. Yoshioka, H. Inoue, *Journal of Inorganic Biochemistry*, 94 (2003) 263-271.
- [39] A. Robertazzi, A.V. Vargiu, A. Magistrato, P. Ruggerone, P. Carloni, P. de Hoog, J. Reedijk, *The Journal of Physical Chemistry B*, 113 (2009) 10881-10890.
- [40] T. Hirohama, Y. Kuranuki, E. Ebina, T. Sugizaki, H. Aarii, M. Chikira, P. Tamil Selvi, M. Palaniandavar, *J Inorg Biochem*, 99 (2005) 1205-1219.
- [41] R.J. Forster, J.G. Vos, *Macromolecules*, 23 (1990) 4372-4377.
- [42] E.M. Kober, J.V. Caspar, B.P. Sullivan, T.J. Meyer, *Inorganic Chemistry*, 27 (1988) 4587-4598.
- [43] A.B.P. Lever, *Inorganic Chemistry*, 29 (1990) 1271-1285.
- [44] R. Kumar, D. Leech, *Journal of The Electrochemical Society*, 161 (2014) H3005-H3010.

- [45] S. Trasatti, O.A. Petrii, *Journal of Electroanalytical Chemistry*, 327 (1992) 353-376.
- [46] S. Trasatti, O.A. Petrii, *Pure Appl. Chem.*, 63 (1991) 711-734.
- [47] R. Kumar, D. Leech, *Electrochimica Acta*, 140 (2014) 209-216.
- [48] S. Boland, P. Kavanagh, D. Leech, *ECS Transactions*, 13 (2008) 77-87.
- [49] R.J. Forster, L.R. Faulkner, *Journal of the American Chemical Society*, 116 (1994) 5444-5452.
- [50] E. Laviron, *Journal of Electroanalytical Chemistry and Interfacial Electrochemistry*, 52 (1974) 395-402.
- [51] D. Leech, P. Kavanagh, W. Schuhmann, *Electrochimica Acta*, 84 (2012) 223-234.
- [52] A.A. Yakovlev, *Neurochem. J.*, 3 (2009) 139-144.
- [53] A.J. Bard, L.R. Faulkner, *Electrochemical Methods: Fundamentals and Applications*, 2 ed., Wiley & Sons, New York, 2001.
- [54] C. Danilowicz, E. Cortón, F. Battaglini, E.J. Calvo, *Electrochimica Acta*, 43 (1998) 3525-3531.
- [55] P. Kavanagh, D. Leech, *Physical Chemistry Chemical Physics*, 15 (2013) 4859-4869.
- [56] D. MacAodha, P.Ó. Conghaile, B. Egan, P. Kavanagh, D. Leech, *ChemPhysChem*, 14 (2013) 2302-2307.
- [57] I. Osadebe, D. Leech, *ChemElectroChem*, 1 (2014) 1988-1993.
- [58] H.U. Bergmeyer., *Methods of Enzymatic Analysis*, Academic Press, Verlag Chemie, 1974.
- [59] S. Rengaraj, P. Kavanagh, D. Leech, *Biosensors and Bioelectronics*, 30 (2011) 294-299.
- [60] D. MacAodha, M.L. Ferrer, P.O. Conghaile, P. Kavanagh, D. Leech, *Physical Chemistry Chemical Physics*, 14 (2012) 14667-14672.

Chapter 6: Conclusions and future directions

6.1 Conclusions

The overall objective of this thesis was to investigate immobilisation strategies to couple redox complexes and biocatalysts within films on electrode surfaces capable of transferring electrons between enzyme and electrode, for applications to biosensing and energy generation. Biofuel cells have the potential to provide power to implanted devices therefore alternative strategies were used as described in this thesis for the assembly of mediated enzyme electrodes capable of operating in physiological conditions (37 °C, pH 7.4, 5 mM glucose) with the aim of producing improved current densities and stability. A design of experiment approach is used to probe the optimum combination of enzyme, mediator and support materials for glucose oxidising anodes. We have outlined some of the approaches we have taken in the effort towards fabrication of redox active monolayer or multilayer platforms envisaged to be of use in the implantable biofuel cell or biosensor research.

We have demonstrated the proof-of-principle that electrochemically-induced coupling of an alkylamine functionalised redox complex to an electrode provides a simple methodology to obtain redox active monolayers on electrode surfaces. The average surface coverage of the attached complex, upon electrolysis of [Os(2,2'-bipyridine)₂(4-aminomethylpyridine)Cl].PF₆, is $0.84 (\pm 0.3) \times 10^{-10}$ moles cm⁻², close to that predicted for a close-packed monolayer of this polypyridyl complex. The modified electrode shows electrocatalytic activity for oxidation of glucose in the presence of glucose oxidase. However, the small current response of 0.5 μA was obtained due to the lower surface coverage of electron shuttling osmium complexes. Hence, a methodology to prepare multilayer films of redox complexes and catalysts using polymer matrix at electrode surfaces was investigated. This was done to optimise the current density of enzyme electrodes as described in chapter 3 and 4.

We have explained the new approach to prepare multi-layered films by addition of nanostructured supports and by cross-linking a range of osmium complexes bearing alkyl-amine functional groups, distal to a ligand of the metal complex, to redox

enzyme and functionalised polymers, with concomitant adsorption to the electrode surface. The redox potential of these complexes can be altered by substitution of electron withdrawing or electron donating groups on the bipyridine ligand and the response of enzyme electrodes prepared using such osmium complexes immobilised with GOx, multiwalled carbon nanotubes and carboxymethylated dextran/polyacrylic acid as a support was evaluated. Substantial current densities of $0.8 \pm 0.21 \text{ mA cm}^{-2}$ in 5 mM glucose and $3.4 \pm 0.7 \text{ mA cm}^{-2}$ in saturated glucose solutions in PBS are obtained at an applied potential of 0.2 V vs. Ag/AgCl, showing promise for application as glucose oxidising biosensors and anodes for enzymatic fuel cells. The current response of these enzyme electrodes was further improved using design of experiment approach. Using this approach, we optimised the amount of each component used in enzyme electrode preparation and also recognised the interaction or dependency of these components on the performance of enzyme electrodes as anodes for biofuel cell device development as described in chapter 4. Components used to construct enzyme electrodes were optimised using surface response methodology coupled with a central composite design. The maximum current density obtained for the optimised enzyme electrode is $1.2 \pm 0.1 \text{ mA cm}^{-2}$ under pseudo-physiological conditions (37 °C, pH 7.4, 50 mM PBS containing 5 mM glucose) 32% higher than the enzyme electrode optimised by variation of one factor at a time.

Additionally, we have explored the use of genipin to create redox hydrogel based on the simultaneous crosslink of an osmium redox complex $[\text{Os}(2,2'\text{-bipyridine})_2(4\text{-aminomethylpyridine})\text{Cl}]\cdot\text{PF}_6$ containing an amino functional group distal to the metal centre and a glucose oxidising enzyme using chitosan as an amino-functionalised platform. These genipin-based enzyme electrodes display a glucose oxidation current density of 0.70 mA cm^{-2} for 100 mM glucose in 50 mM PBS (pH 7.4, 37°C, 150 rpm) at 0.45 V showing the ability of genipin to create suitable redox hydrogels for glucose oxidation. This initial study as described in chapter 5 demonstrates the application of genipin as a crosslinker to fabricate films of enzyme and redox complex on electrode surfaces for potential applications as a biosensor or in vivo EFC anode for energy generation.

6.2 Future directions

Future work could focus on screening of combinations of different sugar oxidising enzyme, redox complex and nanostructure materials as a matrix using the DoE approach, with the aim of improving power output for anodes, ideally sufficient to power implantable devices. For example, a combination of the method reported on in chapter 2 for simple formation of redox active monolayers could be extended to form multilayers, should conductive monolayers be produced, perhaps by addition of CNTs during electro-reduction, or should multi-valent alkylamine redox complexes be used to form the electrode attached layers and to crosslink to enzymes and redox complexes/supports. As in chapter 3, synthetic approaches to vary the redox potential of osmium-based complexes can be adopted. The approach of incorporating a MWCNT scaffold, GOx, redox complex and polymer support to enhance the performance of a glucose oxidase anode as described in chapter 3 and 4, could be used to screen a wide range of sugar oxidising enzymes and osmium based mediators in order to determine whether further improvement in current density/stability of anodes for EFC is possible.

Incorporation of conducting support (MWCNT) to the enzyme electrode has led to an increased current response, as described in chapter 3 and 4. The MWCNT acts as the conductive scaffold for immobilisation of redox complexes and enzymes [1-3]. It is, however, not completely clear that conductivity of support has a major role in increasing the current output of enzyme electrode. Therefore, it would be interesting to investigate whether use of conductive or non-conductive supports has a direct effect on current response or not. It could be tested by sampling the response of enzyme electrode prepared using different conductive and non-conductive nanoparticles of similar surface areas or mass as support.

The use of enzyme cascades is another promising approach for the improvement of the power output of EFCs [4-6]. Whereas one enzyme would oxidise, for example, glucose, a second enzyme could oxidise the resulting metabolite of the first enzyme. Utilisation of multiple enzyme cascades for full or partial oxidation of fuels has been demonstrated to improve power output in biofuel cell assemblies. Palmore *et al.*[7]

firstly reported the multiple stepped oxidations of a substrate by combining alcohol, aldehyde and formate dehydrogenase to oxidise methanol completely to carbon dioxide. Shao et al. [5] demonstrated the extraction of 6 electrons in the oxidation of glucose by enzyme electrodes based on a pyranose dehydrogenase and a cellobiose dehydrogenase. More recently, Zhu *et al.* [8] stated EFC based on 13 enzymes in an air-breathing fuel cell that exhibits a maximum power output of 0.8 mW cm^{-2} from complete oxidation of maltodextrin via the synthetic catabolic pathways. Enzyme electrode prepared using such a combination to mimic metabolic pathways and optimised using DoE approach may provide a promising route to increased power density of EFC.

The alternate immobilisation strategies to couple osmium complexes and enzymes presented in this thesis could be used to prepare an anode in EFC or biosensing devices. For example, the genipin based crosslinking method as described in Chapter 5, could be used to prepare enzyme electrodes. Recently, biocompatibility of genipin cross-linked electrodes were evaluated through in vivo implantation that displayed low toxicity compared to another cross-linked enzyme electrode [9-11] therefore, highlights further the suitability of genipin to construct enzyme electrode for particularly in vivo power generation applications. Also, it would be interesting to investigate the incorporation of amine functionalised MWCNT into genipin coupled biofilms containing redox complexes, enzymes and chitosan as support. The genipin based coupling approach to prepare enzyme electrode may possibly also be used to screen different osmium mediators having low redox potential and glucose oxidising enzyme in order to seek further improvement in current density or stability of enzyme electrodes. DoE method can be employed to obtain this objective.

Further promising applications of the modified electrode is in the area of deoxyribonucleic acid (DNA) diagnostics. This area has grown considerably in past 10 years due to their potential to detect nucleic acid binding events in more rapid, simplistic and cost effects manner as compared to conventional hybridization technology [12-14]. Electrochemical based DNA sensing reworded sensitivity, selectivity and low cost for the detection of selected DNA sequences associated with human disease [14-16]. The electrochemical detection of specific DNA sequences

permits the analysis of a complex mixture of nucleic acids without optical instrument [17]. Previously, Kavanagh *et al.* [12] demonstrated the detection of nucleic acids based upon the recognition surface formed by co-immobilisation of redox polymer mediator and DNA probe sequences crosslinked and tethered to a gold surface via anchoring self-assembled monolayer (SAM) of cysteamine. Earlier, the Heller group [18-20] demonstrated the enzyme linked immunosorbent assay by using redox mediated electro-reduction of peroxide by peroxidase-labelled target DNA. Nevertheless, the covalent or affinity labelling of an oligonucleotide with enzyme is time consuming and complicated [12, 14]. However, various drawbacks are associated with this DNA detection assay. These are the use of a solid phase reaction based on epoxide, PEGDGE, crosslinking and manual drop coating/drying methods to form the recognition layer that introduce variability in the assay result [12, 14, 20, 21].

The recognition capabilities of DNA through hybridisation reaction are well studied but adequate transducers are needed to generate the signal from hybridisation events. For this purpose, electroactive metal complexes of bidentate ligands such as 1,10-phenanthroline or 2,2'-bipyridyl were investigated due to their mode of interaction with DNA (intercalative or electrostatic) which leads to their potential application in the molecular recognition of nucleic acid hybridisation [22, 23]. Attachment of DNA directly to the electrode surface provides a controlled environment in which the kinetics and thermodynamic parameters of DNA hybridisation can be evaluated [15, 24]. Future work could focus on the synthesis and characterisation of dipyrindyl phenazine ligands based metal complexes which are capable of binding DNA through intercalation [25-27]. These metal complexes could be immobilised on electrode surface via thiol or covalent grafting. The attached redox active layer could acts as a reporter of the DNA hybridisation event. Therefore, the hypothesis can be tested by measuring the shift in redox potential of the metal complex due to the effect of DNA binding. This charging fingerprint could be very sensitively dependent on the redox probe environment. Also, it would be interesting to explore the interaction mechanism of osmium based redox complexes with DNA molecules on the microelectrode surface.

6.3 References

- [1] D. MacAodha, M.L. Ferrer, P.O. Conghaile, P. Kavanagh, D. Leech, *Physical Chemistry Chemical Physics*, 14 (2012) 14667-14672.
- [2] M. Holzinger, A. Le Goff, S. Cosnier, *Electrochimica Acta*, 82 (2012) 179-190.
- [3] I. Osadebe, D. Leech, *ChemElectroChem*, 1(2014) 1988-1993.
- [4] F. Tasca, L. Gorton, M. Kujawa, I. Patel, W. Harreither, C.K. Peterbauer, R. Ludwig, G. Nöll, *Biosensors and Bioelectronics*, 25 (2010) 1710-1716.
- [5] M. Shao, M. Nadeem Zafar, C. Sygmund, D.A. Guschin, R. Ludwig, C.K. Peterbauer, W. Schuhmann, L. Gorton, *Biosensors and Bioelectronics*, 40 (2013) 308-314.
- [6] P. Kavanagh, D. Leech, *Physical Chemistry Chemical Physics*, 15 (2013) 4859-4869.
- [7] G.T.R. Palmore, H. Bertschy, S.H. Bergens, G.M. Whitesides, *Journal of Electroanalytical Chemistry*, 443 (1998) 155-161.
- [8] Z. Zhu, T. Kin Tam, F. Sun, C. You, Y.H. Percival Zhang, *Nature Communication*, 5 (2014).
- [9] S. El Ichi, A. Zebda, J.P. Alcaraz, A. Laaroussi, F. Boucher, J. Boutonnat, N. Reverdy-Bruas, D. Chaussy, M.N. Belgacem, P. Cinquin, D.K. Martin, *Energy & Environmental Science*, 8 (2015) 1017-1026.
- [10] J.Y. Lai, *Int J Mol Sci*, 13 (2012) 10970-10985.
- [11] P.A. Norowski, S. Mishra, P.C. Adatrow, W.O. Haggard, J.D. Bumgardner, *Journal of Biomedical Materials Research Part A*, 100A (2012) 2890-2896.
- [12] P. Kavanagh, D. Leech, *Analytical Chemistry*, 78 (2006) 2710-2716.
- [13] J. Hajdukiewicz, S. Boland, P. Kavanagh, D. Leech, *Biosensors and Bioelectronics*, 25 (2010) 1037-1042.
- [14] T.G. Drummond, M.G. Hill, J.K. Barton, *Nature Biotechnology*, 21 (2003) 1192-1199.
- [15] J.J. Gooding, *Electroanalysis*, 14 (2002) 1149-1156.
- [16] E. Palek, M. Fojta, *Analytical Chemistry*, 73 (2001) 74 A-83 A.
- [17] H. Holden Thorp, *Trends in Biotechnology*, 21 (2003) 522-524.
- [18] C.N. Campbell, D. Gal, N. Cristler, C. Banditrat, A. Heller, *Analytical Chemistry*, 74 (2002) 158-162.
- [19] J. Cheng, E.L. Sheldon, L. Wu, A. Uribe, L.O. Gerrue, J. Carrino, M.J. Heller, J.P. O'Connell, *Nature Biotechnology*, 16 (1998) 541-546.
- [20] Y. Zhang, H.-H. Kim, A. Heller, *Analytical Chemistry*, 75 (2003) 3267-3269.
- [21] B. Wang, I. Jansson, J.B. Schenkman, J.F. Rusling, *Analytical Chemistry*, 77 (2005) 1361-1367.

- [22] G. Shul, C.A.C. Ruiz, D. Rochefort, P.A. Brooksby, D. Bélanger, *Electrochimica Acta*, 106 (2013) 378-385.
- [23] A. Ghosh, A. Mandoli, D.K. Kumar, N.S. Yadav, T. Ghosh, B. Jha, J.A. Thomas, A. Das, *Dalton Transactions*, (2009) 9312-9321.
- [24] A. Silvestri, G. Barone, G. Ruisi, D. Anselmo, S. Riela, V.T. Liveri, *Journal of Inorganic Biochemistry*, 101 (2007) 841-848.
- [25] Mudasir, K. Wijaya, N. Yoshioka, H. Inoue, *Journal of Inorganic Biochemistry*, 94 (2003) 263-271.
- [26] A. Robertazzi, A.V. Vargiu, A. Magistrato, P. Ruggerone, P. Carloni, P. de Hoog, J. Reedijk, *The Journal of Physical Chemistry B*, 113 (2009) 10881-10890.
- [27] T. Hirohama, Y. Kuranuki, E. Ebina, T. Sugizaki, H. Arii, M. Chikira, P. Tamil Selvi, M. Palaniandavar, *Journal of Inorganic Biochemistry*, 99 (2005) 1205-1219.

Appendix

Publications and presentations

Publications

- **R. Kumar**, D. Leech, “Immobilisation of Alkylamine-Functionalised Osmium Redox Complex on Glassy Carbon using Electrochemical Oxidation” *Electrochimica Acta*, 140 (2014) 209-216.
- **R. Kumar**, D. Leech, “Coupling of Amine-Containing Osmium Complexes and Glucose Oxidase with Carboxylic Acid Polymer and Carbon Nanotube Matrix to Provide Enzyme Electrodes for Glucose Oxidation” *Journal of The Electrochemical Society*, 161 (2014) H3005-H3010.
- **R. Kumar**, D. Leech, “A glucose anode for enzymatic fuel cells optimized for current production under physiological conditions using a design of experiments approach” *Bioelectrochemistry*, 106, Part A (2015) 41-46.
- **R. Kumar**, P. Ó‘Conghaile, M. L. Ferrer, D. Leech, “Genipin Assisted Crosslinking of Redox active Chitosan-based Enzyme hydrogels: Improving biocompatibility environment for Glucose Oxidation” in preparation.

Selected Presentations

Oral presentations

- **R. Kumar**, P. Kavanagh, D. Leech, “Tailoring carbon electrodes, redox complexes and polymer supports for glucose oxidase Bioelectrocatalysis of glucose” in *Electrochem 2013: University of Southampton, UK*.
- **R. Kumar**, D. Leech, “Glucose oxidation at enzyme electrodes under physiological conditions for application to biosensors and biofuel cells” in 64th

Irish Universities Chemistry Research Colloquium; June 2014: National University of Ireland, Galway.

- **R. Kumar**, I. Osadebe, P. Ó'Conghaile, P. Kavanagh, D. Leech, "Glucose oxidising anodes under physiological conditions: Using design of experiment to probe optimum combination of enzyme, mediator and support materials" in 16th Topical International Society of Electrochemistry (ISE) meeting, March 2015, Angra dos Reis, Brazil.

Poster presentations

- **R. Kumar**, I. Osadebe, P. Ó'Conghaile, D. Mac Aodha, P. Kavanagh, D. Leech, "Synthesis of Osmium based synthetic mediator for electron transfer" in Inorganic Symposium on Inorganic Chemistry in Ireland, 2012: Galway, Ireland.
- **R. Kumar**, I. Osadebe, P. Ó'Conghaile, P. Kavanagh, D. Leech, "Immobilisation of redox complexes and enzyme in the polymer supported films at electrode surface for biofuel cells application" in National University of Ireland, Ryan Institute Research Day, 2013: Galway, Ireland.
- **R. Kumar**, I. Osadebe, P. Ó'Conghaile, D. Mac Aodha, P. Kavanagh, D. Leech, "Redox complex and enzyme immobilisation in different polymers support at functionalised electrode surfaces for application to biosensors and biofuel cells" in CASi 2013: Cork.
- **R. Kumar**, I. Osadebe, P. Ó'Conghaile, P. Kavanagh, D. Leech, "Redox complex and enzyme immobilisation at functionalised electrode surfaces to sensing and energy generation" in Earth Gathering 2013: UCD, Dublin, Ireland.

- **R. Kumar**, I. Osadebe, P. Ó'Conghaile, P. Kavanagh, D. Leech, "Power from blood: towards an implantable enzyme catalysed glucose/Oxygen fuel cell" National University of Ireland, Ryan Institute Research showcase, 2014: Galway, Ireland.

Training/Workshops attended during the doctoral program

- QCM-D (Quartz Crystal Microbalance with Dissipation) "A Real time, label free technique for analyzing interactions/reactions at surfaces," at National Physical Laboratory, UK, January 2014.
- Effective Design of Experiment (DoE) implementation "Practical approaches to design experiments, understand the key parameters, identify optimal feasible operating condition and choose the best design" at PRISM training and consultancy ltd., St. John's Innovation Centre, Cambridge, UK, Sept.16-17th 2014.